Author:
Preston, Amy B

Title:
Characterisation of Alzheimer's disease risk genes and their behavioural phenotypes in Drosophila melanogaster

Characterisation of Alzheimer's disease risk genes and their behavioural phenotypes in *Drosophila melanogaster*

By:
Amy Preston

A dissertation submitted to the University of Bristol in accordance with the requirements for award of the degree of Physiology and Pharmacology (MSc by Research) in the Faculty of Life Sciences.

School of Physiology, Pharmacology and Neuroscience March 2023

Word Count: 23537

Abstract

Alzheimer's disease (AD) is the most prevalent form of dementia worldwide. The pathology of the disease is complex and difficult to target therapeutically. Genome-wide association studies (GWAS) and epigenome-wide association studies (EWAS) are being increasingly used to identify single nucleotide polymorphisms (SNPs) and differentially methylated positions (DMPs) respectively that occur more frequently in individuals with AD. However, translation of these findings to rodent models is challenging due to high costs and false positive rates. *Drosophila melanogaster*, commonly known as the fruit fly, is a highly genetically tractable model organism that allows quick and efficient screening of risk genes by identifying mutant phenotypes, including those relevant to AD. This project aimed to use *Drosophila* to screen fly orthologues of GWAS and EWAS hits for AD-associated phenotypes, to identify candidate genes that are potentially involved in AD pathogenesis. Firstly, bioinformatic analysis of GWAS and EWAS hits was performed, and *Drosophila* orthologues of human hits were identified. The *GAL4-UAS* system, which allows tissue-specific genetic manipulation in *Drosophila*, was used to express *RNAi* against 11 *Drosophila* orthologues of novel AD risk genes identified in GWAS and EWAS and screen for AD-associated behavioural phenotypes. Eye neurodegeneration, locomotor ability, lifespan, sleep and circadian rhythms and memory of flies with candidate gene knockdown was assessed. RT-qPCR was used to assess the efficacy of *RNAi*-mediated knockdown for selected candidate genes. Preliminary data from a courtship assay was used to assess the hearing of flies with knockdown of *Ctl2*, an Alzheimer's and Parkinson's disease risk gene also implicated in autoimmune hearing loss. Expression of *RNAi* against six *Drosophila* orthologues of novel AD genes screened induced AD-associated phenotypes in one or more assays, including *Ctl2* (*SLC44A2*), *Kuz* (*ADAM10*), *Frl* (*FMNL1*), *MTA1-like* (*MTA3*), *Ppt2* (*PPT2*) and *Kdm2* (*KDM2B*). This demonstrates that these genes may be involved in AD pathology and should be further validated in *Drosophila* and rodent models.

Acknowledgements

I would firstly like to thank my supervisor, Dr James Hodge, for his invaluable guidance, support, and encouragement throughout the project. I would also like to thank Dr Bangfu Zhu and Dr Edgar Buhl for teaching me the experimental methods and offering insightful feedback and suggestions for data analysis. Thank you to Nicola Hill for her help and advice in the lab. Finally, I am grateful to Dr Paul Dodson and Dr Shamik DasGupta for their co-supervision and support.

Author’s Declaration

I declare that the work in this dissertation was carried out in accordance with the requirements of the University's Regulations and Code of Practice for Research Degree Programmes and that it has not been submitted for any other academic award. Except where indicated by specific reference in the text, the work is the candidate's own work. Work done in collaboration with, or with the assistance of, others, is indicated as such. Any views expressed in the dissertation are those of the author.

Signed: AMY PRESTON Date: 26/03/2023

Table of Contents

Abstract 2

Acknowledgements 3

Author's Declaration 4

List of figures 7

List of tables 8

Abbreviations 9

1 Introduction 11

1.1 Alzheimer's disease prevalence, symptoms, and diagnosis 11

1.2 Alzheimer's disease pathogenesis 12

1.3 Genetic and epigenetic involvement in Alzheimer's disease pathogenesis 17

1.4 *Drosophila melanogaster* as a model to study Alzheimer's disease 21

1.5 Alzheimer's disease risk genes selected for characterisation have diverse functions 25

1.6 Aims 30

2 Methods 31

2.1 Bioinformatic analysis 31

2.2 Fly stocks and husbandry 32

2.3 RT-qPCR 34

2.4 Eye degeneration assay 36

2.5 Climbing assay 37

2.6 Longevity assay 37

2.7 Memory assay 38

2.8 Sleep and circadian rhythms assay 39

2.9 Courtship Assay 41

3. Results 42

3.1 Bioinformatic analysis and verification of fly lines 42

3.2 Knockdown of candidate genes in the eye did not cause a change in gross morphology or surface area 49

3.3 Knockdown of candidate genes in neurons and glia affected locomotor ability 52

3.4 Knockdown of candidate genes in neurons and glia affected lifespan 58

3.5 Knockdown of Ctl2 in mushroom body neurons reduced 1-hr memory 64

3.6 Knockdown of candidate genes in clock cells affected sleep and circadian activity 66

3.7 Knockdown of *Ctl2* in the Johnston's organ did not affect courtship behaviour 72

4 Discussion 75

4.1 Experimental methods and project limitations 76
4.1.1 Bioinformatics and RT-qPCR 76
4.1.2 Eye degeneration assay 77
4.1.3 Negative geotaxis assay 78
4.1.4 Longevity assay 79
4.1.5 Memory assay 81
4.1.6 Sleep and circadian rhythm assay 82
4.1.7 Hearing assay 83
4.2 Advantages of using *Drosophila* as a model organism to study Alzheimer's disease 84
4.3 Knockdown of *Ctl2* induced lethality and a learning defect in *Drosophila* 86
4.4 Knockdown of *Kuz* in neurons induced lethality in *Drosophila* 90
4.5 Expression of *Ppt2 RNAi* induced premature death in *Drosophila* 91
4.6 Expression of *Frl-RNAi* and *MTA1-like-RNAi* induced a locomotor defect in *Drosophila* 92
4.7 Expression of *Kdm2-RNAi* caused hyperactivity in *Drosophila* 94
4.8 Future perspectives 97
4.9 Conclusion 99
Appendix 100
References 103

List of figures

Figure 1: Amyloid beta and tau neurofibrillary tangle formation in Alzheimer's disease. 14
Figure 2: Key pathological events in AD. 16
Figure 3: Flow diagram demonstrating methods used in AD GWAS and EWAS and gene-sets identified by each. 21
Figure 4: Use of the GAL4-UAS system in Drosophila to induce tissue-specific expression of candidate genes. 22
Figure 5: Comparison of the structure and cleavage sites of human APP and dAPPL. 24
Figure 6: T maze set up for olfactory shock aversive assay for memory assessment. 39
Figure 7: Drosophila activity monitor (DAM) system set-up. 41
Figure 8: Mating wheel used for courtship assay and behaviours observed. 42
Figure 9: Protein-protein interaction network for risk genes and hallmark AD proteins in humans and Drosophila. 45
Figure 10: Drosophila orthologues of AD risk genes show differential expression across cell types in the Drosophila brain. 47
Figure 11: Pan-neuronal expression of Frl RNAi and Ctl2 RNAi caused a reduction in Frl and Ctl2 mRNA. 49
Figure 12: Overexpression of human tAB42 and tau-0N4R in the developing Drosophila eye caused a decrease in eye surface area and change in gross morphology. 51
Figure 13: Pan-neuronal knockdown of Scr and CG6984 rescued age-dependent decline in climbing performance. 53
Figure 14: Pan-neuronal knockdown of Klp31E, Kdm2, AdamTS-A, and cv-c did not cause a change in climbing performance of flies compared to Elav-GAL4/+ control. 55
Figure 15: Pan-neuronal knockdown of Frl and MTA1-like induced an age-dependent climbing defect. 56
Figure 16: Glial knockdown of Kuz reduced climbing performance at 7 days post-eclosion. 57
Figure 17: Glial knockdown of Frl and MTA1-like decreased climbing ability. 58
Figure 18: Pan-neuronal expression of Ppt2 RNAi significantly reduced lifespan. 60
Figure 19: Pan-neuronal expression of RNAi for Klp31E, AdamTS-A, cv-c and Frl affected the lifespan of flies. 60
Figure 20: Glial expression of RNAi for Kuz, Ppt2, and Scr affected lifespan. 62
Figure 21: Glial expression of Kdm2 RNAi caused a small reduction in lifespan. 63
Figure 22: Pan-neuronal knockdown of Ctl2 in adult flies significantly reduced lifespan. 64
Figure 23: Knockdown of Ctl2 in the mushroom body in Drosophila reduced 1-hour memory performance in the olfactory shock assay. 66
Figure 24: Overexpression of human Tau-0N4R and tAB42 increased total activity at night and decreased total sleep at night. 68
Figure 25: Expression of candidate gene RNAi affected activity, sleep and circadian rhythmicity and period length. 70

Figure 26: Knockdown of Ctl2 in PDF neurons, dopamine neurons, and DN1 neurons caused changed in sleep and circadian rhythmicity. 72
Figure 27: Expression of tetanus toxin in the Johnston's organ affected the rate of successful copulation and wing song-copulation latency. 74
Figure 28: Possible AD-relevant effects of SLC44A2/CTL2 knockdown in humans. 90

List of tables

Table 1: Summary of suggested functions of human AD risk genes and their Drosophila orthologues chosen for screening in this project. 29
Table 2: GAL4 fly lines used in this project, their cytology, expression patterns, and sources. 32
Table 3: UAS and control fly lines used in this project. 33
Table 4: Forward and reverse primers used for RT-qPCR experiments. 36
Table 5: Cycling mode used for qPCR in QuantStudio 3 Real-Time **PCR machine.** 36
Table 6: AD risk genes selected and relevant annotations from Kunkle et al's 2019 GWAS meta-analysis and their Drosophila orthologues screened in this project. 43
Table 7: AD risk genes selected and relevant annotations from Smith et al's 2021 EWAS meta-analysis and their Drosophila orthologues screened in this project. 43
Table 8: Expression of selected human risk genes in human tissues. 46
Table 9: Summary of candidate genes suggested for further study based on this project. 95

Abbreviations

Aβ - Amyloid β

ACh – Acetylcholine

AChE – Acetylcholinesterase

AD – Alzheimer's disease

AOSA – Aversive olfactory shock assay

APOE – Apolipoprotein E

APP – Amyloid precursor protein

APPsα - Secreted amyloid precursor protein α

BBB – Blood-brain barrier

BDNF – Brain-derived neurotrophic factor

ChAT – Choline acetyltransferase

CNS – Central nervous system

CPM – Counts per million

DAM – *Drosophila* activity monitor

DIOPT – DRSC integrative orthologue prediction tool

DMP – Differentially methylated position

DNMT – DNA methyltransferase

DN1 – Dorsal neurons 1

ECM – Extracellular matrix

EOAD – Early-onset Alzheimer's disease

ER – Endoplasmic reticulum

EWAS – Epigenome-wide association study

FAD – Familial AD

GFP – Green fluorescent protein

GWAS – Genome-wide association study

LNv – Lateral ventral neuron

LOAD – Late-onset Alzheimer's disease

MAPT – Microtubule associated protein tau

MBON – mushroom body output neuron

MMSE – Mini mental state examination

MoCA – Montreal cognitive assessment

NuRD - Nucleosome remodelling and deacetylase complex

PDF – Pigment dispersing factor

PHF – Paired helical filament

RhoGAP – Rho GTPase activating protein

ROS – Reactive oxygen species

RPKM - reads per kilobase of exon per million reads mapped

RT-qPCR – Reverse transcriptase quantitative polymerase chain reaction

SAD – Sporadic Alzheimer's disease

SEM – Standard error of the mean

SNP – Single nucleotide polymorphism

STRING – Search tool for the retrieval of interacting genes/proteins

TNF – Tumour necrosis factor

1 Introduction

1.1 Alzheimer's disease prevalence, symptoms, and diagnosis

Alzheimer's disease (AD) is a progressive neurodegenerative disease and the most prevalent form of dementia, which is identified as the seventh-leading cause of death in the US [1]. Currently, only one disease-modifying therapy is available for AD in the US [2]. AD is characterised by cognitive decline and memory loss, but other symptoms also contribute to disease burden including neuropsychiatric changes such as depression, anxiety and aggression [3], changes in sleep and circadian rhythms [4, 5], and in some cases, motor dysfunction [6, 7]. Progression of the disease leads to patients being unable to perform day-to-day activities due to these symptoms, resulting in transfer to full-time care and generation of significant economic burden [1]. Patients generally die due to complications 3-12 years after diagnosis [8].

AD usually occurs in people aged 65 or older [9], and is referred to as late-onset Alzheimer's disease (LOAD). In most LOAD cases, there is no known specific genetic cause, referred to as sporadic AD (SAD), although the APOE4-ε4 allele is the most significant risk factor for the development of LOAD [1]. AD occurring before 65 years of age is referred to as early-onset Alzheimer's disease (EOAD). EOAD can be sporadic (SAD) or have a genetic cause, termed familial AD (FAD), caused by autosomal dominant mutations in three causative genes: *APP, PSEN1* and PSEN2 [10]. Familial AD accounts for only 1-2% of AD cases, and early onset only occurs in 5% of AD cases [2], making LOAD the most common form of AD. The main risk factors for LOAD are age, APOE-ε4 allele status, sex, race, and lifestyle factors including smoking, education, and diet [11].

AD is diagnosed by assessing patient and family history, current symptoms, and use of cognition testing with either the mini mental state examination (MMSE) or the Montreal Cognitive Assessment (MoCA). Both assess cognitive function by testing memory, language and attention, but the MoCA is more sensitive for the detection of MCI and mild AD [12]. However, the diagnosis of AD is generally only confirmed after death, as one of the defining features of AD is the accumulation of two

important proteins in the brains of AD patients: neurofibrillary tangles of tau and extracellular plaques of amyloid β [11]. Intraneuronal tangles of tau protein and extracellular plaques of amyloid β oligomers are important diagnostic and pathogenic characteristics of AD. They were first discovered by Dr Alois Alzheimer in a post-mortem histological examination of the brain of a patient suffering from the first documented case of AD (then termed presenile dementia) in 1906 [13]. Dr Alzheimer observed significant neuronal loss, intra-neuronal thick 'fibrils' (tau tangles) and extracellular 'miliary foci' (amyloid plaques). Presenile and senile dementia were later recognised to include early and late-onset Alzheimer's disease. AD diagnosis based on symptoms and cognitive assessment is not always accurate, as approximately 15-30% of individuals diagnosed with AD do not have these related brain changes (plaques and tangles) when post-mortem histopathological examination is performed [1].

1.2 Alzheimer's disease pathogenesis

The pathogenesis of AD is complex and still not fully understood. However, accumulation of tau neurofibrillary tangles and amyloid β (Aβ) plaques in the brains of patients (Figure 1) are recognised as defining features of AD and are generally considered essential to its causation. Aβ protein derives from β secretase cleavage of the transmembrane amyloid precursor protein (APP). *APP* was first cloned and identified as a transmembrane protein in 1987 [14], and is cleaved into multiple peptides by α, β, and γ secretases [15]. Under normal physiological conditions, cleavage of *APP* by α secretases (primarily *ADAM10*) constitute the majority of *APP* processing and creates an α-secretase cleaved soluble *APP* (APPsα) fragment which is non-amyloidogenic, meaning it does not lead to AD pathology [16] (Figure 1). This fragment is believed to be involved in neuroprotection and growth [17]. Conversely, β-secretase cleavage produces Aβ peptides, which is a minor pathway under physiological conditions, and in low concentrations Aβ1-40 peptides were shown to promote proliferation and differentiation of undifferentiated rat hippocampal neurons, but have neurotoxic effects on mature rat hippocampal cells when present in high concentrations [18]. Therefore, increased production of Aβ in the brains of AD patients was suggested to cause neurodegeneration. In 1991, Hardy and Allsop first proposed that increased Aβ deposition and plaque formation due to increased β

secretase processing resulting from *APP* mutations initiates AD pathology [19]. They argued that Aβ peptide formation precedes tau tangle formation due to these *APP* mutations and plaque formation preceding tau tangle formation in the brains of Down's syndrome patients (which have triplication of chromosome 21, the location of the *APP* gene).

However, tau neurofibrillary tangle formation is also thought to be a major event in the pathogenesis of AD. Tau protein is a brain-specific protein with six isoforms and is encoded by the microtubule associated protein tau (*MAPT*) gene on chromosome 17 [20]. These six isoforms are produced by alternative splicing and can contain three or four C-terminal microtubule binding repeats (Rs), and one, two or three N-terminal amino inserts (Ns), 2N4R being the longest isoform [21]. Tau is essential to the formation and stabilisation of microtubules and is regulated by phosphorylation [22]. Abnormally hyperphosphorylated tau is found in the brains of AD patients and precedes the formation of paired helical filaments (PHFs) of tau in neurofibrillary tangles [23, 24]. Abnormally phosphorylated tau is caused by a change in kinase and phosphatase activity balance and leads to microtubule destabilisation and impaired axonal transport, as well as aggregation of tau into PHFs in neurofibrillary tangles [21] (Figure 1).

For many years the amyloid and tau hypotheses have been at the forefront of AD research, although how Aβ and tau cause neurodegeneration is still debated. Both proteins appear to be directly toxic to neurons in their soluble and aggregated forms causing loss of calcium homeostasis and synaptic dysfunction [25-29]. Tau and Aβ have also been shown to interact with each other to mediate AD progression. Long-term potentiation is a form of synaptic plasticity involved in memory formation that is inhibited by Aβ oligomers [30]. In mouse hippocampal slices, tau was required for Aβ1-42-mediated reduction of long-term potentiation [31], and in another study, reduction of tau prevented Aβ-induced axonal transport dysfunction in tau knockout mouse hippocampal slices [32]. Conversely, mice expressing *APP* and *PSEN1* with tau knockout had reduced amyloid plaque burden and synapse loss compared to mice expressing *APP, PSEN1* and tau [33]. It has been hypothesised that tau is downstream of Aβ in the initial pathogenesis of AD, but that the two engage in a

positive feedback loop which leads to progressive neurodegeneration, where the resulting neuronal dysfunction and loss leads to AD symptoms including cognitive decline [34]. This makes Aβ and tau obvious targets for the development of AD therapies. However, most clinical trials for agents targeted to reduce amyloid plaque and tau neurofibrillary tangle burden have failed [35], calling the validity of the Aβ cascade hypothesis into question.

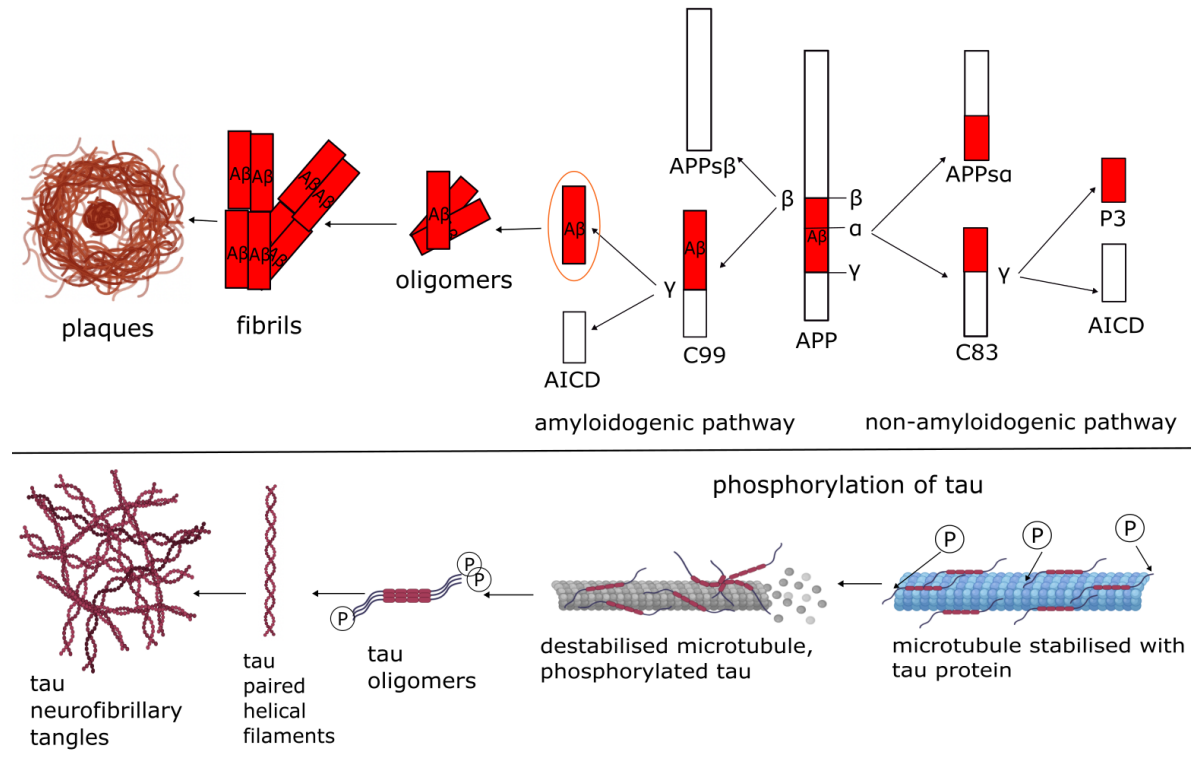

Figure 1: Amyloid beta and tau neurofibrillary tangle formation in Alzheimer's disease.

Amyloidogenic processing of *APP* by β-secretase (BACE1) initiates Aβ fibril formation and extracellular plaque deposition. Tau hyperphosphorylation at multiple sites causes microtubule destabilisation and leads to intracellular accumulation of tau tangles. These are considered the central events in AD pathogenesis and initiate other pathological events such as neuronal toxicity and microglial activation. Figure made in BioRender.com and Inkscape using information from [35, 36].

It has become increasingly clear, partially due to the failure of many drugs targeting tau and Aβ to modify or reverse the disease [35], that tau and Aβ dysregulation and aggregation are not the sole mediators of neurodegeneration. AD appears to be a

multifactorial disease, and other processes in aging including impaired lipid and glucose metabolism [37, 38], excitotoxicity [39] and neuroinflammation [40] can also contribute to the progression of the disease (Figure 2). Aβ activates Toll-like receptors [41] and multicomponent receptors comprising of scavenger receptors [42] on microglia, which leads to their activation. Under normal physiological conditions, brain microglia extend protrusions into the extracellular space for surveillance and can phagocytose neuronal debris following injury [43]. Microglia can also adhere to and phagocytose Aβ fibrils [44], understood to be a protective mechanism against Aβ toxicity. However, they can also undergo a process called priming during aging and neurodegeneration, where microglia take on an aberrant pro-inflammatory phenotype with increased reactive oxygen species (ROS) and reactive cytokine release and decreased phagocytic activity, due to a low level of exposure to inflammatory stimuli (including Aβ fibrils) over an extended period [45, 46]. IL-1α, tumour necrosis factor (TNF) and complement component 1q (C1q) cytokines released from activated microglia induce the A1 reactive phenotype of astrocytes [47]. These microglial and astrocytic states can promote axonal injury, neuronal dysfunction and apoptosis via blood-brain barrier (BBB) disruption, release of proinflammatory cytokines and release of ROS [40]. Other mediators of neurodegeneration include apolipoprotein E. The APOE ε4 allele is the most significant genetic risk factor for LOAD [11], and encodes for apolipoprotein E, a cholesterol carrier involved in lipid homeostasis (important in axonal growth and synaptic function), facilitation of Aβ uptake by microglia, and glucose metabolism [48]. The APOE locus therefore links multiple pathways implicated in AD pathogenesis. Ultimately, there are many pathological events alongside Aβ and tau that contribute to neurodegeneration and can modify Aβ and tau pathology.

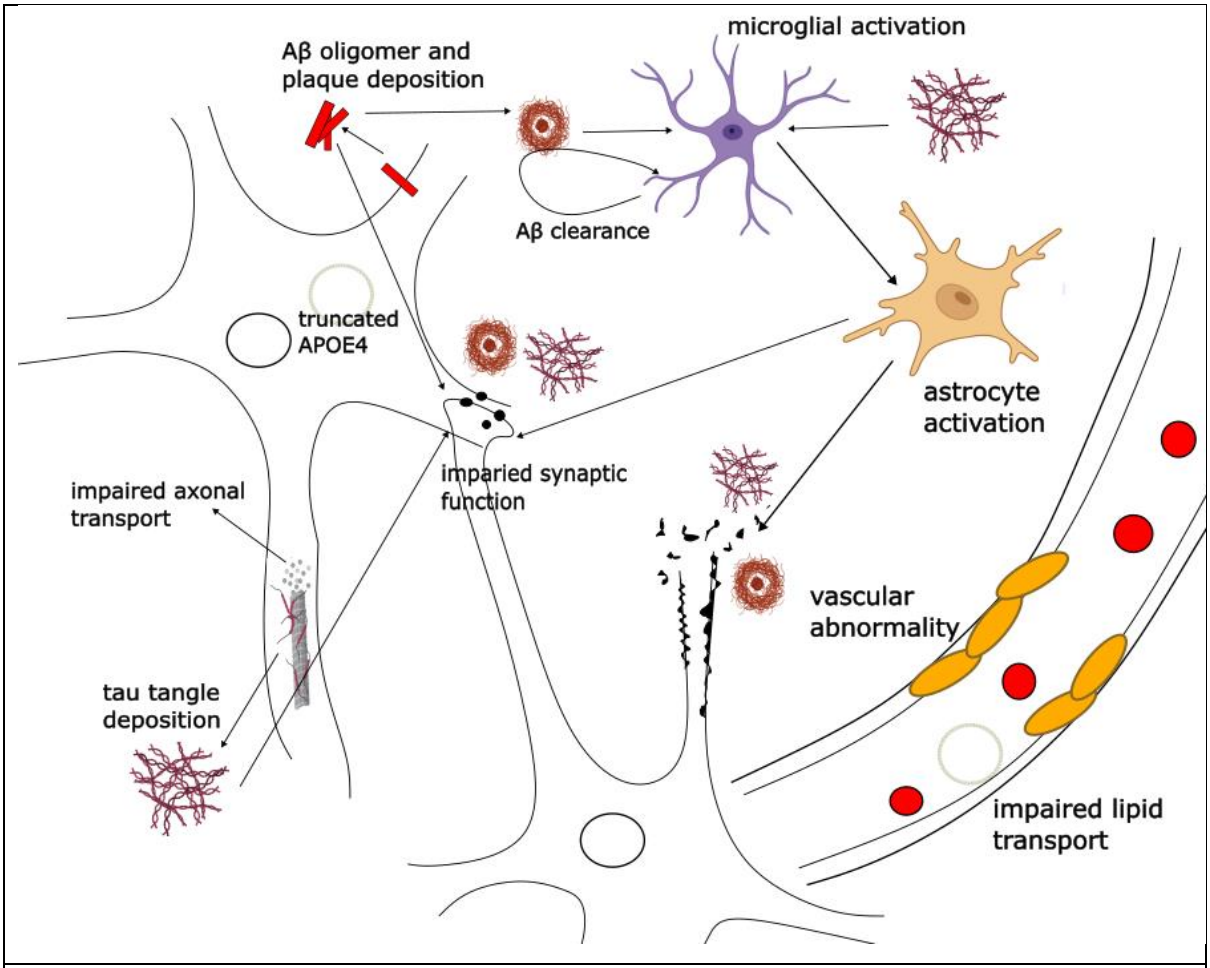

Figure 2: Key pathological events in AD.

Aβ oligomers and insoluble plaque deposition cause neuronal toxicity, and can initiate tau phosphorylation, leading to synaptic dysfunction and toxicity. Vascular dysfunction is associated with AD and may reduce cerebral blood flow and decrease clearance of Aβ. Microglial activation due to tau and Aβ accumulation is likely to be initially neuroprotective but may induce reactive astrocytes and release pro-inflammatory cytokines and therefore become toxic to neurons later in the disease. APOE4, a major risk factor for AD, is associated with vascular dysfunction, mitochondrial damage and abnormal tau and Aβ accumulation. Figure adapted from [49] using information from [40]. Made using BioRender.com and Inkscape.

1.3 Genetic and epigenetic involvement in Alzheimer's disease pathogenesis

AD is a multifactorial disease, with genetic and environmental risk factors contributing to its initiation and progression. The human genome and its regulation are complex, and genetic variation among individuals can occur in the form of single nucleotide polymorphisms (SNPs), deletions, substitutions, inversions and copy number variants [50]. Many of the variants that contribute to complex traits and diseases like AD occur in non-coding regions, meaning they influence gene regulation rather than protein composition [51]. However, some have an impact on protein function due to a resulting change in amino acid sequence, but this is more common in Mendelian diseases. The human genome is subject to complex epigenetic regulation. These changes primarily consist of DNA methylation and histone acetylation. DNA methylation involves covalent addition of a methyl group at CpG sites by DNA methyltransferases (DNMTs) which typically leads to a decrease in gene expression [52]. Histone acetylation is the transfer of acetyl groups onto lysine residues on histones 3 and 4 by histone acetyltransferases, making the chromatin more accessible causing increased gene expression [53]. Genetic and epigenetic changes are important events in AD pathogenesis, and can arise from spontaneous mutations in DNA, differential patterns of methylation and acetylation caused by environmental factors and aging, or direct effects of Aβ and tau on genomic and epigenomic profiles in the brain [54]. Tau has been shown to promote loss of heterochromatin (the condensed form of DNA) via mitochondrial-induced oxidative stress in *Drosophila* and mouse models of tauopathy [55], which leads to increased aberrant gene expression. This chromatin relaxation was directly linked to neurodegeneration, as restoration of chromatin reduced apoptosis. Heterochromatin was also reduced in the brains of AD patients in this study. Genetic and epigenetic factors influencing AD pathogenesis can also occur independently of amyloid or tau toxicity. SNPs and other variations in the genetic code that do not occur in AD as a direct result of tau or amyloid pathology and epigenetic changes generally due to environmental factors can modify AD pathology [56].

Genome and epigenome-wide association studies are approaches that identify novel loci in the genome with genetic and epigenetic differences in healthy individuals and

individuals with a disease (Figure 3). GWAS involves the use of microarray technology or next-generation sequencing methods to identify SNPs that occur at a higher frequency in individuals with a disease compared to healthy individuals [57]. They can also be used to identify copy-number or sequence variations. Usually, in AD GWAS, tissue samples or genetic and phenotypic data from biobanks is collected from individuals with the disease or trait being investigated, and healthy control individuals. Historically, GWAS has used microarray technology for genotyping, which detects up to 1,000,000 commonly occurring SNPs, determined by linkage disequilibrium in certain ancestral populations to cover the majority of common SNPs in the human genome [58]. However, due to the decreasing cost of whole-genome sequencing, this is becoming more commonly used than microarray technology as it allows for detection of rarer variants [57]. Odds ratios are calculated from the frequency of the SNP in each group, and association tests are used to gain p values for the odds ratios, which are adjusted to control for factors known to influence the trait which include age and sex in AD GWAS. Closest genes to significant SNPs are then identified. Replication tests on different populations and further bioinformatic or molecular techniques can be used to validate and determine the effect of the identified SNPs. GWAS are most effective at finding common genetic variants with a small effect size for disease risk, rather than rare genetic variants with a large effect size provided by linkage studies [58]. These have identified many novel loci which may be involved in AD, most notably the APOE $\varepsilon 4$ allele which is consistently highlighted in GWAS [59, 60] and is the most significant genetic risk factor for LOAD [48].

Epigenome-wide association studies have also become increasingly common as new technology to quantify epigenetic processes evolves. The form of epigenetic regulation most commonly studied is methylation, as it is the most accessible [61]. Post-mortem brain tissue is used for DNA extraction (with intact epigenetic modifications) and a similar microarray technique to GWAS is used in EWAS, which involves quantifying methylation of CpG sites in case and control groups by detecting hybridisation of methylated DNA to the beads on the microarray [62]. Association between differentially methylated positions (DMPs) and AD (using Braak stage as a measure of pathology) are performed [59, 62]. Due to advances in microarray

technology, over 450,000 CpG sites can be tested for differential methylation in disease [61]. Large sample sizes and stringent adjustments to statistical tests are needed for GWAS and EWAS [57], and further meta-analyses of GWAS and EWAS, when performed with appropriate adjustments, increase sample size and allows more loci to be interrogated [59, 63]. Recently, difficulties in the interpretation of GWAS and EWAS have been discussed, as analysis of the contribution of each significant loci in a GWAS to a complex trait has revealed that each SNP has a minor contribution to its heritability, and that complex traits may be omnigenic rather than polygenic such that every gene in a relevant tissue contributes to the trait [51]. This means that GWAS and EWAS are more useful when further information about the connectivity of biochemical networks is available. However, GWAS and EWAS are useful for the detection of common genetic variants that increase the risk of AD development, and despite the small effect sizes of each variant, still aid in identifying networks of genes and their interactions involved in diseases like AD.

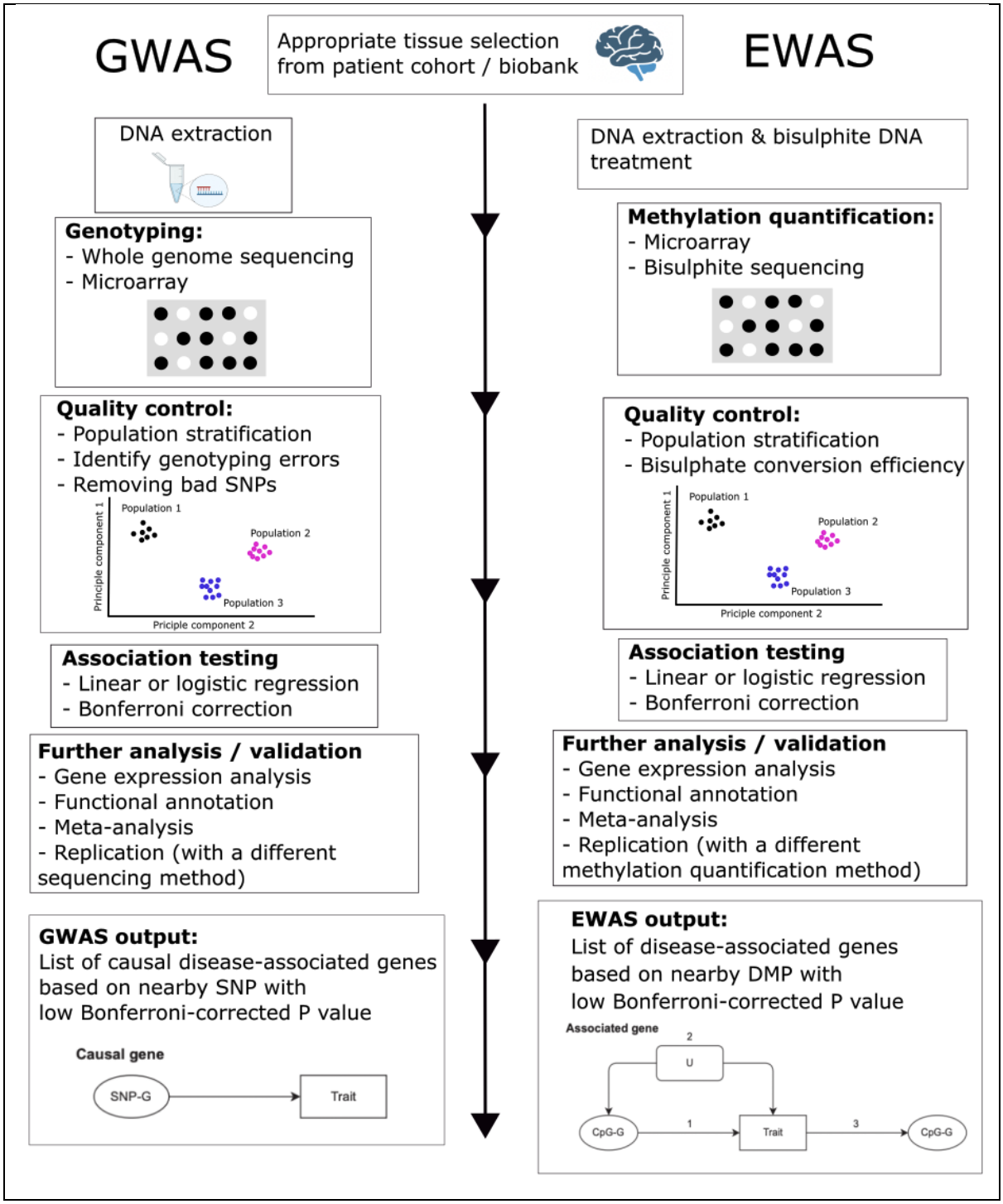
GWAS
Appropriate tissue selection from patient cohort / biobank
EWAS
DNA extraction
DNA extraction & bisulphite DNA treatment
Genotyping:
- Whole genome sequencing
- Microarray
Methylation quantification:
- Microarray
- Bisulphite sequencing
Quality control:
- Population stratification
- Identify genotyping errors
- Removing bad SNPs
Population 1
Population 2
Population 3
Principle component 1
Priciple component 2
Quality control:
- Population stratification
- Bisulphate conversion efficiency
Association testing
- Linear or logistic regression
- Bonferroni correction
Association testing
- Linear or logistic regression
- Bonferroni correction
Further analysis / validation
- Gene expression analysis
- Functional annotation
- Meta-analysis
- Replication (with a different sequencing method)
Further analysis / validation
- Gene expression analysis
- Functional annotation
- Meta-analysis
- Replication (with a different methylation quantification method)
GWAS output:
List of causal disease-associated genes based on nearby SNP with low Bonferroni-corrected P value
Causal gene
SNP-G
Trait
EWAS output:
List of disease-associated genes based on nearby DMP with low Bonferroni-corrected P value
Associated gene
2
U
CpG-G
1
Trait
3
CpG-G

Figure 3: Flow diagram demonstrating methods used in AD GWAS and EWAS and gene-sets identified by each.

Similar methods are used for the design and analysis of GWAS and EWAS. Bisulphite treatment of DNA is required in EWAS to convert unmethylated cytosine to uracil to allow comparison of methylated regions. Diagram of causal and disease-associated genes in GWAS and EWAS outputs from [64], and demonstrates that unlike GWAS, EWAS hits may not be directly causal due to the many factors that affect methylation. Figure made in Inkscape and BioRender using information from [57, 65].

1.4 *Drosophila melanogaster* as a model to study Alzheimer's disease

Once SNPs or DMPs that have significant association with a disease are detected in a GWAS or EWAS, characterising their role in AD and translation to use as a therapeutic target can be difficult. Whilst ancestry and other factors are adjusted for in GWAS and EWAS statistical analysis, some genes identified from significant loci may still be false positives, especially in diverse populations [57, 66] and due to the large number of significant hits, direct translation to rodent models is costly and can take multiple years depending on the methods used. *Drosophila melanogaster* has recently been used as a model to screen candidate genes for involvement in AD pathogenesis [67-69]. Their short generation time, genetic tractability, and presence of *Drosophila* orthologues to approximately 75% of human genes has made them advantageous to molecular and genetic research [70]. Manipulation of the *Drosophila* genome can be easily accomplished using the *GAL4-UAS* binary expression system, which takes advantage of the yeast transcriptional activator *GAL4* under control of a tissue-specific promotor and the upstream activation sequence (*UAS*), which allows for tissue-specific expression of transgenes (Figure 4). When a *GAL4* fly line is crossed with a *UAS*-dependent transgene line, the resulting offspring inherit both the *GAL4* and *UAS* insertions, causing the tissue specific expression of the transgene [71]. The *UAS* insertion can be used to express human genes, overexpress fly genes or knockdown fly genes using RNA interference (*RNAi*). Additionally, inducible promotors such as the temperature sensitive *GAL80* gene (*GAL80ts*) can be used to express or knockdown fly genes in adulthood and old age which is particularly relevant to AD.

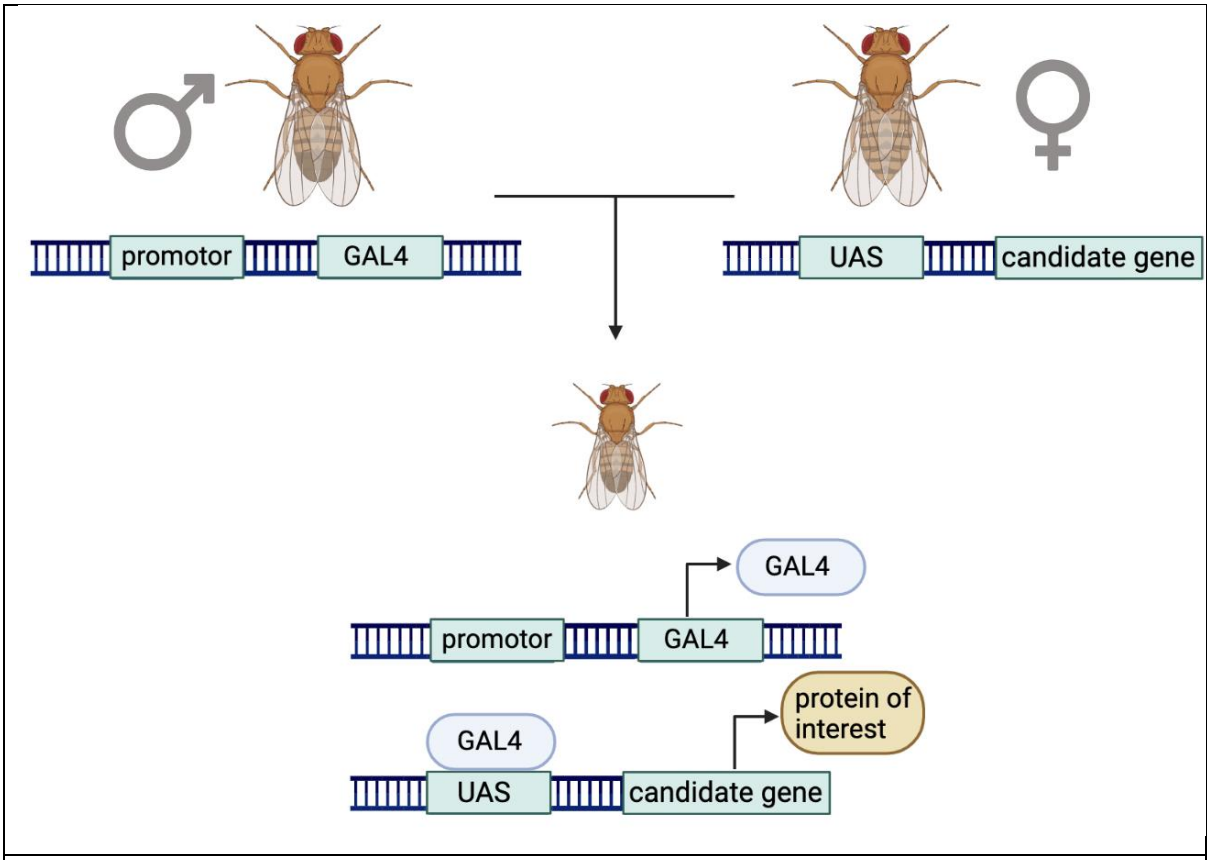

Figure 4: Use of the *GAL4-UAS* system in Drosophila to induce tissue-specific expression of candidate genes.

A *GAL4* line under control of a tissue specific promotor and *UAS* line linked to a candidate gene are crossed to induce tissue specific expression of the candidate gene in the offspring of the cross, which inherit both the *GAL4* and *UAS* insertions. This system can be exploited to induce tissue specific expression of human genes or knockdown of *Drosophila* genes by placing *RNAi* under control of the *UAS*. Figure made using BioRender and adapted from [71].

To model the pathogenesis of AD, human Aβ and tau can be overexpressed in *Drosophila* using the *GAL4-UAS* system. Multiple assays exist to assess neurodegeneration and behavioural phenotypes, including light and electron microscopy on the eye to detect photoreceptor degeneration [72], climbing assays to assess locomotor behaviour [73], lifespan measurements [74], memory assays [75], and circadian and sleep measurements [76]. Overexpression of human *APP* or secreted Aβ in the *Drosophila* eyes causes photoreceptor degeneration and, in the neurons, premature death, and progressive memory and locomotor defects [77, 78]. Overexpression of tau-0N4R in *Drosophila* in neurons also causes premature death,

climbing, and memory deficits [68, 79], and overexpression of both genes simultaneously in *Drosophila* exacerbates their pathology [80, 81]. Additionally, orthologues of *APP* and *MAPT* exist in *Drosophila*. These are *dAPPL* (β amyloid protein precursor-like) and tau, respectively [82, 83], which have also been used to model AD pathology. *dAPPL* in flies can be cleaved by an α-secretase, *Kuz* (fly orthologue of human *ADAM10*), to form an sAPPLα fragment, and the drosophila β-secretase orthologue, *dBACE*, can cleave *dAPPL* to form a toxic Aβ-like fragment [84] (Figure 5), and this study also suggested that intracellular Aβ is important in AD pathogenesis as behavioural deficits preceded extracellular Aβ deposition despite low sequence homology between *Drosophila* and human Aβ domain in APP/*dAPPL* [85]. *dAPPL* in flies appears to be involved in memory formation [86] and neuroprotection [87], whereas the Aβ-like fragment produced by Kuz cleavage is toxic. Additionally, loss of function alleles of Psn, the *Drosophila* orthologue of PSN1 and PSEN2 (Figure 5), causes age-related memory deficits [88].

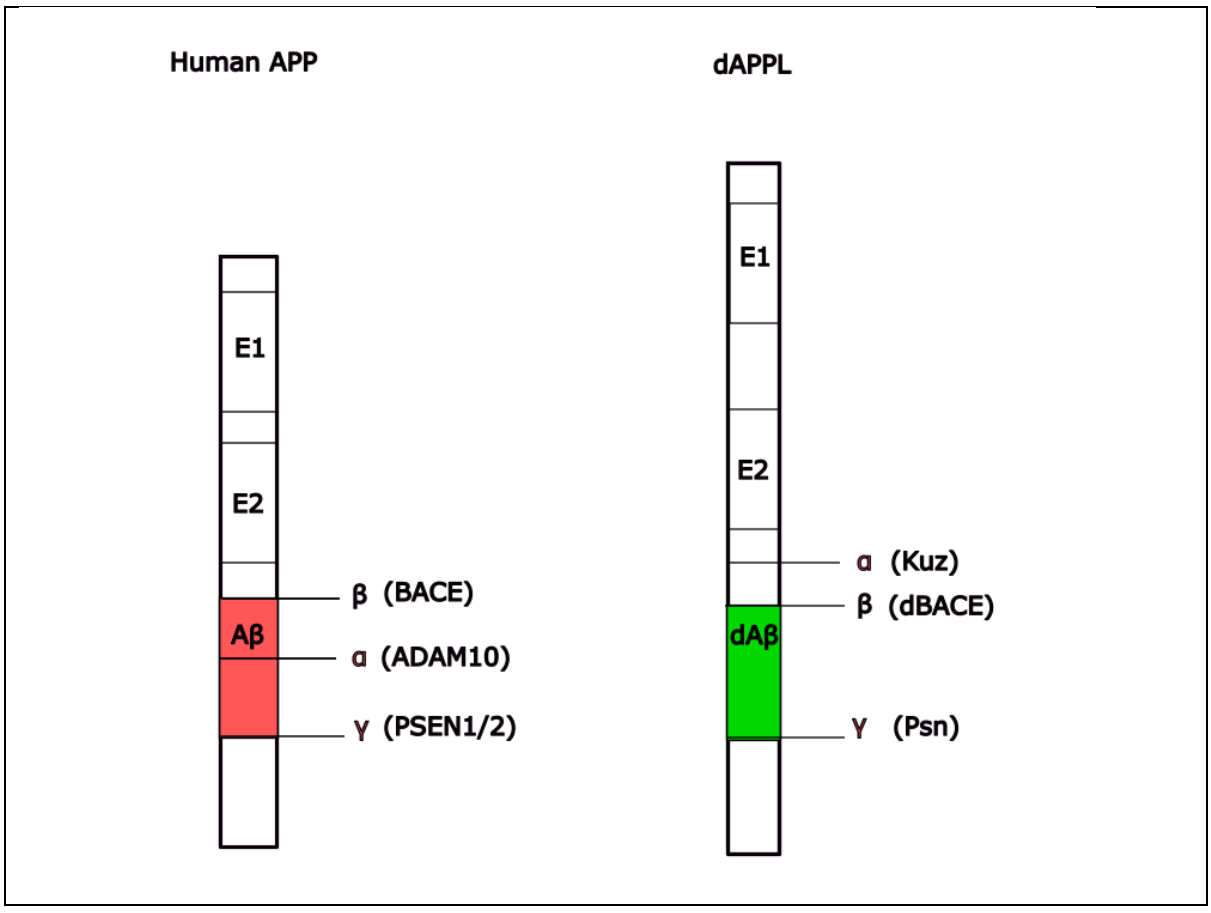

Figure 5: Comparison of the structure and cleavage sites of human *APP* and *dAPPL*.

dAPPL shares a similar overall structure with human *APP,* including two extracellular domains (E1 and E2) and an Aβ-like fragment (dAβ). Secretase cleavage of *dAPPL* differs from human *APP,* as the α-secretase and β-secretase cleavage sites are reversed. However, cleavage by β-secretases in both organisms produces an Aβ fragment. Made in Inkscape with information from [36, 89, 90].

Due to the presence of a relatively conserved AD-associated pathological pathway, their genetic tractability and simple husbandry, *Drosophila* have been used to characterise multiple mechanisms related to AD pathology, including lipid metabolism, mitochondrial dysfunction, and oxidative stress [70, 91]. Oxidative stress is a key pathological feature of AD [92]. A screening study found multiple genes in oxidative stress pathways including superoxide dismutase (SOD) and ferritin had altered expression in flies expressing human Aβ, and these flies were more sensitive to oxidative stress [93]. Downregulation of a *Drosophila* SOD orthologue increased the number of apoptotic cells in tau mutant flies, which may have been due to aberrant cell cycle activation [94]. Furthermore, mitochondrial dysfunction may contribute to reactive oxygen species production during elongation, as in *Drosophila*, overexpression of the RhoGTPase involved in mitochondrial axonal transport, fission and fusion, *Miro*, rescued Aβ and tau-induced AD-associated phenotypes [95]. Tau-induced heterochromatin loss in flies was also linked to inhibition of mitochondrial fission protein *Drp1* associating with mitochondria, leading to ROS production [55]. Localisation of *Drp1* was also observed in places of forced contact between mitochondria and endoplasmic reticulum (ER) in an Aβ42 fly model of AD, where these artificial ER-mitochondria links increased lifespan, likely due to decreased mitochondrial length and stress [96]. Therefore, *Drosophila* do not only provide a system for screening of candidate genes for roles in AD pathogenesis, but functional genomic studies which aid understanding of AD-related pathways and identification of potential drug targets.

1.5 Alzheimer's disease risk genes selected for characterisation have diverse functions

Novel AD risk genes and their fly orthologues screened in this project are summarised in Table 1. They were selected from two recent GWAS and EWAS meta-analyses [59, 60], but some have been previously identified in genetic studies for AD and other diseases. *ADAM10* encodes a disintegrin and metalloproteinase, the dominant α-secretase that cleaves *APP* in the non-amyloidogenic pathway [97], and is well understood in this context. It is therefore likely to modify the risk of AD via an effect on Aβ levels. Kuz, the *Drosophila* orthologue of *ADAM10*, has a similar function in Appl cleavage [86]. Both *ADAM10* and *Kuz* also have conserved functions in neurogenesis and gliogenesis via Notch signalling, and early dysfunction in these processes can increase vulnerability to neurodegeneration [98]. Another gene in the ADAM family, a disintegrin and metalloproteinase with thrombospondin motifs 1 (*ADAMTS1*), has also been identified as a risk factor for AD in a GWAS meta-analysis [60]. *ADAMTS1* is overexpressed in the cerebral cortex of Downs syndrome, Parkinson's and Alzheimer's disease patients [99]. It is a metalloprotease primarily residing in the extracellular matrix [100]. It has been implicated in autosomal recessive hearing impairment [101], and hearing loss is associated with dementia [102]. *ADAMTS1* is also involved cell migration and adhesion, cancer, and inflammatory processes including mediating the inflammatory response to tumours [103]. *AdamTS-A*, its fly orthologue, has also been implicated in cell migration and adhesion via cleavage of extracellular matrix (ECM) proteins [104]. Therefore, *ADAMTS1* may modify the risk of AD through multiple pathways, including neuronal development, hearing loss and inflammation.

Interestingly, multiple AD risk genes identified in GWAS and EWAS have also been implicated in cancer and immune cell function. *FMNL1* encodes Formin-like protein 1 (FRL1), the *Drosophila* orthologue of which (*Frl*) has been implicated in actin polymerisation in a *Drosophila* morphological screen [105]. Binding of a small Rho GTPase to the GTPase binding domain prevents inhibition of the FH2 functional domain, leading to FRL1 modulation of acting polymerisation and Rho GTPase signalling via feedback mechanisms [106]. Actin polymerisation and FRL1 signalling has also been implicated in immune cell function [107] and multiple types of cancer

when overexpressed [108]. The *Drosophila* orthologue *Frl* has a conserved role in actin polymerisation [109]. Therefore, *FMNL1* may moderate AD risk via cytoskeletal dynamics, which is one of the pathways involved in tau-mediated neurodegeneration [110]. Metastasis Associated 1 Family Member 3 (*MTA3*) encodes for a protein that constitutes part of the NuRD complex, which acts as a histone deacetylase and is involved in ATP-dependent nucleosome disruption [111]. This process has also been implicated in multiple cancers [112]. The *Drosophila* orthologue of *MTA3*, *MTA1-like*, is also involved in chromatin remodelling via the macromolecular NuRD complex, as well as correct localisation of the histone variant CENP-A to centromeres for chromosome segregation [113]. Therefore, like tau [55], *MTA3* may modify the risk of AD by regulating gene expression via chromatin remodelling. Lysine demethylase 2 (*KDM2B*) has been shown to demethylate histones H3K36me1/2, H3K4me3 and K3K79me3 to repress gene expression, including NF-κB (involved in innate immunity signalling) and β-catenin (involved in the Wnt cell fate, migration and immunity-related signalling pathway) [114]. *Drosophila Kdm2* also specifically demethylates histone H3K4me3, and is involved in nucleolar structure [115] as well as regulation of genes involved in circadian behaviour [116]. Like *MTA3*, the contribution of *KDM2B* to AD is likely to be via epigenetic regulation of disease-relevant gene expression.

Enoyl-CoA Hydratase Domain Containing 3 (*ECHDC3*) encodes a protein involved in the β-oxidation step in mitochondrial fatty acid metabolism, implicated in cardiovascular disease [117, 118], a major risk factor for AD. An association analysis indicated that a polymorphism near *ECHDC3* did not increase risk of AD in APOE4 carriers [119], but decreased *ECHDC3* expression was detected in the blood of AD patients and correlated with increased neurodegeneration [120]. *CG6984* is the *Drosophila* orthologue of *ECHDC3*, but little is known about its function other than a putative role in lipid metabolism due to homology with *ECHDC3* and its identification as a potential modifier of an Na_V channel seizure mutant phenotype [121]. Therefore, *ECHDC3* is more likely to contribute to AD pathogenesis via modification of lipid metabolism.

SLC44A2 encodes for choline transporter like protein 2 (*CTL2*), which has also been associated with autoimmune hearing loss [122] and Parkinson's disease in a recent GWAS meta-analysis [123]. In mice, *CTL2* is expressed in the lungs, inner ear, kidney, muscle, heart, and brain [124], and relevant to AD pathology, is expressed in the plasma membrane and mitochondria of human brain microvascular endothelial cells [125], participating in membrane potential and pH-dependent choline transport into the brain side of the BBB [126]. This transport of choline is likely to provide the choline needed for acetylcholine synthesis, a neurotransmitter relevant to AD and memory, and phosphatidylcholine synthesis, an important constituent of cell membranes. In *Drosophila*, *Ctl2* has not been characterised specifically in the central nervous system (CNS), but global Ctl2 knockdown caused lethality and knockdown in the wing disc induced abnormal wing growth [127]. However, the modification of AD risk by *CTL2* is likely to occur through altered choline transport causing neuronal and synaptic dysfunction.

Palmitoyl protein thioesterase 2 (*PPT2*) is localised to the lysosome and catalyses the hydrolysis of thioester bonds in enzymes involved in fatty acid metabolism, as part of their protein degradation process [128]. It has been implicated in neurodegenerative lysosomal storage disorders when knocked out in mice [129, 130]. In these mouse models, spasticity, increased mortality, apoptotic bodies in the cortex, thalamus and pyramidal neurons of the hippocampus and abnormal spleen and pancreas appearance were observed, resembling a milder neuronal ceroid lipofuscinoses phenotype (a disease caused by *PPT1* deficiency). In *Drosophila*, *Ppt2* also acts as a lysosomal palmitoyl protein thioesterase [131], and knockdown of *Ppt1*, which shares some substrates with *Ppt2*, causes premature death in *Drosophila* [132]. *PPT2* may modify the risk of AD via impaired lysosomal storage, and lipid metabolism via impaired degradation of lipid metabolism enzymes.

STARD13 encodes Deleted in Liver Cancer 2 (*DLC2*), which is expressed in most tissues in mice and is a Rho GTPase activating protein (RhoGAP), regulating Rho GTPase signalling which is involved in cell morphology, migration and proliferation [133]. Additionally, DLC2 localises to the mitochondria and the StAR related lipid transfer (START) domain may interact with HMG-CoA reductase, which catalyses the rate limiting step of cholesterol synthesis [134]. Altered expression of *STARD13*

has also been observed in many cancers [135, 136], likely due to dysregulated Rho GTPase signalling. Whilst *DLC1*, *DLC2* and *DLC3* have distinct functions [133], *Drosophila* only has one orthologue, crossliveliness-c (*cv-c*), which is also acts as a RhoGAP involved in cytoskeletal regulation [137] and homeostatic sleep regulation [138]. *DLC2* may contribute to AD pathogenesis through dysfunctional Rho GTPase signalling or cholesterol metabolism.

Homeobox A5 (*HOXA5*) encodes a transcription factor important in organ morphogenesis, and in mice, knockout of *HOXA5* causes abnormal axial skeleton, lung, stomach, mammary gland, and ovary development [139]. *HOXA5* is also involved in neuronal development, as a transcriptome study in *HOXA5* knockout mice identified downregulation of multiple genes involved in synaptic function, and the *HOXA5* protein is primarily expressed in glutamatergic and GABAergic synapses [140], and abnormal glutamatergic activity is detected in AD [39]. *HOXA5* dysregulation has also been implicated in many cancers, including glioma lung cancer and breast cancer [141]. *HOX* genes were first identified in *Drosophila* as regulators of segmentation [142], and the *Drosophila* orthologue of *HOXA5* is *Scr*, which is also a transcription factor involved in development of the head along with other genes in the Antennapedia complex [143]. Therefore, *HOXA5* may influence AD pathology through abnormal gene transcription at the synapse.

Kinesin Family Member 21B (*KIF21B*) encodes a kinesin protein which associates with the plus end of microtubules to reduce their growth [144]. It is involved in transport of brain-derived neurotrophic factor (BDNF) [145], and *KIF21B* knockout mice have slower growing microtubules, decreased cell surface levels of AMPA and $GABA_A$ receptors, and defects in learning and memory [146]. GWAS have implicated *KIF21B* as a risk gene for multiple sclerosis and ulcerative colitis [147]. The *Drosophila* orthologue of *KIF21B* is *Klp31E*, a kinesin also linked to memory function. In a large screen for memory-related genes, *RNAi*-mediated knockdown of *Klp31E* caused a memory deficit in the olfactory shock assay [148]. Therefore, *KIF21B* may be linked to AD via microtubule and synaptic dysfunction.

Table 1: Summary of suggested functions of human AD risk genes and their *Drosophila* orthologues chosen for screening in this project.

Human function according to the NCBI Gene database and GeneRIFs (gene references into functions). *Drosophila* orthologue function according to Flybase.com.

Human AD risk gene	**Suggested human function**	***Drosophila* orthologue**	**Suggested *Drosophila* function**	**GWAS or EWAS meta-analysis**
ECHDC3	Fatty acid metabolism via Enoyl-CoA hydratase activity in mitochondria.	*CG6984*	Hydro-lyase activity in mitochondria.	[60]
ADAMTS1	Disintegrin and metalloproteinase activity, associated with inflammatory processes.	*AdamTS-A*	Matrix metalloprotease that may be involved in cell migration.	[60]
ADAM10	A cell surface protein that cleaves Notch, TNF-α and E-cadherin. α-secretase that cleaves APP.	*Kuz*	Metalloendopeptidase involved in nervous system development and Notch cleavage. α-secretase that cleaves Appl.	[59, 60]
SLC44A2	Transmembrane choline transporter.	*Ctl2*	Transmembrane choline transporter.	[59]
PPT2	Lysosomal palmitoyl protein thioesterase.	*Ppt2*	Lysosomal palmitoyl protein thioesterase.	[59]
HOXA5	Transcription factor that upregulates p53 and other genes.	*Scr*	Transcription factor involved in head and thoracic segment identity.	[59]

KIF21B	ATP-dependent microtubule motor protein.	*Klp31E*	Likely to be ATP-dependent microtubule motor protein.	[59]
STARD13	May be involved in cytoskeletal reorganisation and cell motility and proliferation and has GTPase activating protein domain and lipid transfer domain.	*cv-c*	RhoGTPase activating protein, involved in actin organisation, synaptic homeostasis, and sleep homeostasis.	[59]
MTA3	Part of the NuRD complex and may be involved in histone deacetylase binding and transcription regulation.	*MTA1-like*	Part of the NuRD complex and may be involved in chromatin condensation.	[59]
KDM2B	An F-box protein involved in phosphorylation-dependent ubiquitination.	*Kdm2*	Histone demethylase at histone H3.	[59]
FMNL1	Formin-related protein involved in cell polarity and morphogenesis.	*Frl*	Binds GTPase and actin and involved in cell motility and neuronal development.	[59]

1.6 Aims

Whilst GWAS and EWAS have detected hundreds of common genetic variants that confer a small increase in the risk of developing AD, many of these may be false positives or peripherally involved in the disease and therefore have little therapeutic potential. The challenge remains in identifying those that are directly involved and that can be taken forward for further characterisation and tested as candidates for

therapies. In this project, I aim to use the highly genetically tractable *Drosophila melanogaster* to identify novel risk genes for AD identified by GWAS and EWAS that are likely to be involved in the pathogenesis of AD. I will use bioinformatic analysis to identify *Drosophila* orthologues of candidate genes and *RNAi* lines for each orthologue, based on the observed downregulation of human genes in GWAS and EWAS. I will use multiple behavioural and molecular assays to detect AD-associated phenotypes arising due to knockdown of candidate genes by *RNAi*, using established fly models of AD (human Aβ and tau 0N4R overexpressing flies) as positive controls. Firstly, light microscopy will be used to observed whether knockdown of candidate genes in the eye using the *GMR-GAL4* driver causes photoreceptor degeneration. Secondly, I will use the negative geotaxis assay to detect progressive changes in locomotor behaviour resulting from candidate gene knockdown and a longevity assay to detect changes in lifespan due to candidate gene knockdown. I will also use the aversive olfactory shock assay to detect whether candidate gene knockdown causes short-term memory deficits, and the *Drosophila* Activity Monitor (DAM) to assess the sleep and circadian phenotypes. RT-qPCR will be used to validate knockdown of genes causing severe phenotypes. Based on this data, I will identify genes with significant AD-associated phenotypes that merit further characterisation.

2 Methods

2.1 Bioinformatic analysis

Human genes closest to significant loci in GWAS and EWAS were identified, and *Drosophila* orthologues searched on DRSC Integrative Orthologue Prediction Tool (DIOPT), available at https://www.fly*RNAi*.org/cgi-bin/DRSC_orthologs.pl and selected for screening if protein similarity >40% and DIOPT score >6. Genes with higher protein similarities and DIOPT scores were prioritised. The Aerts_Fly_AdultBrain_Filtered_57k scRNAseq dataset on SCope (available at https://scope.aertslab.org/#/Davie_et_al_Cell_2018/*/welcome) was used for gene expression analysis to determine relative fly orthologue expression per cluster in the *Drosophila* brain. Each fly orthologue was searched and the whole brain lassoed.

The resulting data set (Seurat Resolution 2.0 clustering, age annotated) was downloaded into a spreadsheet calculating gene expression (CPM) for the candidate gene by cluster. An expression heatmap was created for each gene from the calculated CPM per cluster averaged over all ages in GraphPad Prism 9.

2.2 Fly stocks and husbandry

Unless stated otherwise in results, all flies were maintained at 25°C in a 12hr light-dark (LD) cycle with standard cornmeal food (0.7% agar, 1.0% soya flour, 8.0% polenta/maize, 1.8% yeast, 8.0% malt extract, 4.0% molasses, 0.8% propionic acid and 2.3% nipagin). *GAL4* and *UAS* lines used in this project are summarised in Tables 2 and 3.

Table 2: *GAL4* fly lines used in this project, their cytology, expression patterns, and sources.

BDSC, Bloomington *Drosophila* Stock Centre, VDRC, Vienna *Drosophila* Resource Centre.

Fly line and cytology	Description	Source
Elav-GAL4/cyo (II)	*GAL4* expressed in all neurons during development and adulthood	BDSC (8765)
Repo-GAL4/TM6b (III)	*GAL4* expressed in all glial cells during development and adulthood	BDSC (7415)
Tim-GAL4/cyo (II)	*GAL4* expressed in all clock cells during development and adulthood	Prof. Ralf Stanewsky, University of Münster [149]
OK107-GAL4 (IV)	*GAL4* expressed in mushroom bodies. Used for original 3 repeats of old genes L&M	BDSC (854)
Tub-GAL80ts (II); elav-GAL4 (III)	Ubiquitous GAL80ts expression, pan-neuronal *GAL4* expression at temperatures ≥29°C (GAL80ts blocks *GAL4* transcriptional activation at temperatures below 29°C)	BDSC (8760)

JO15-GAL4 (III)	*GAL4* expressed in the Johnstons organ during development and adulthood	BDSC (6753)
GMR-GAL4/cyo(II)	*GAL4* expressed in the eye during development and adulthood	BDSC (9146)
PDF-GAL4 (II)	*GAL4* expressed in ventrolateral neurons (LNv)	Prof. Ralf Stanewsky, University of Münster [149]
TH-GAL4 (II)	*GAL4* expressed in dopamine neurons	BDSC (854)
+/cyo (II); Clk4.1M-GAL4/TM3 (III)	*GAL4* expressed in dorsal pacemaker (DN1) neurons during development and adulthood	BDSC (36316)

Table 3: *UAS* and control fly lines used in this project.

BDSC, Bloomington *Drosophila* Stock Centre, VDRC, Vienna *Drosophila* Resource Centre.

Fly Line	**Description**	**Source**
Csw-	Wild type control, white eyes	Prof. Scott Waddell, University of Oxford
UAS-tAB42/cyo (II)	Human Aβ42 with a tandem linker overexpressor to cause increased aggregation	Dr. Damian Crowther, University of Cambridge [150]
UAS-Tau-0N4R (II)	Human 0N4R isoform of tau overexpressor	Dr. Linda Partridge, University College London [151]
UAS-Frl-RNAi (III)	*RNAi* for *Frl*	BDSC (32447)
UAS-MTA1-like-RNAi (III)	*RNAi* for *MTA1-like*	BDSC (33745)
UAS-Kdm2-RNAi (III)	*RNAi* for *Kdm2*	BDSC (31360)
UAS-Klp31E-RNAi (II)	*RNAi* for *Klp31E*	BDSC (40943)
UAS-cv-c-RNAi (II)	*RNAi* for *cv-c*	BDSC (64030)
UAS-Scr-RNAi (III)	*RNAi* for *Scr*	BDSC (28676)
UAS-Kuz-RNAi (II)	*RNAi* for *Kuz*	BDSC (66958)

UAS-CG6984-RNAi (III)	*RNAi* for *CG6984*	BDSC (31753)
UAS-Ppt2-RNAi (III)	*RNAi* for *Ppt2*	BDSC (28362)
UAS-Ctl2-RNAi (II)	Primary *RNAi* for *Ctl2* (used in all assays involving *Ctl2* knockdown)	BDSC (44113)
UAS-Ctl2-RNAi (III)	Secondary *Ctl2 RNAi* line (used in hearing assay)	VDRC (22869)
UAS-AdamTS-A-RNAi (III)	*RNAi RNAi* for *AdamTS-A*	VDRC (33347)

2.3 RT-qPCR

Reverse-transcriptase quantitative polymerase chain reaction (RT-qPCR) was used to confirm the efficacy of *RNAi*-mediated knockdown for selected candidate genes. Firstly, RNA extraction from whole *Drosophila* heads was performed. 30-50 male and female flies were anaesthetised on CO_2 pads 2-3 days post-eclosion, and sterilised tweezers used to remove their heads. Whole *Drosophila* heads were placed in 400 μl Trizol reagent (Ambion) in a 1.5 ml Eppendorf microcentrifuge tube on ice. A motorised autoclaved plastic pestle (Argos Technologies) was used to homogenise the heads, then 400 μl Trizol added. The tube was shaken briefly to mix, then incubated at room temperature (25 °C) for 5 minutes. 180 μl of chloroform was added to the mixture, then shaken vigorously for 15 s before incubation at room temperature for 3 minutes. The mixtures were centrifuged at 4 °C for 20 minutes, and the aqueous phase transferred to a new RNAse free 1.5 ml Eppendorf tube. 600 μl isopropanol was added, and the mixture gently shaken, then incubated at room temperature for 10 minutes to precipitate the RNA. The mixtures were then centrifuged for 5 minutes at 12000 rpm at 4 °C to produce an RNA pellet. The supernatant was discarded, then ethanol added to the pellet and vortexed, then centrifuged again to clean the pellet. The supernatant was discarded, and the pellet left to air dry, then resuspended in 55 μl nuclease-free water at 55 °C before freezing for storage.

Following RNA extraction, RNA was quantified using a NanoDrop 2000 (ThermoFisher Scientific). 1 μl nuclease-free water was added to the NanoDrop and

used as a blank. RNA samples were loaded onto the NanoDrop and the purity (OD 260/280 ratio) was recorded. The concentration of RNA was recorded to calculate the volume needed to synthesise 1.5 μg of cDNA in the reverse transcriptase step. The RevertAid First Strand cDNA Synthesis Kit (ThermoFisher) was used in the reverse transcriptase step. RNA samples dissolved in nuclease free water were added to 1 μl oligo(dT) primer in a 1.5 ml Eppendorf tube and made up to 12 μl. 4 μl of 5X reaction buffer, 1μl of RiboLock RNAse inhibitor, 2 μl of 10 μM dNTP mix and 1 μl RevertAid reverse transcriptase were added to the reaction mixture, tapped gently and centrifuged for 5 seconds to mix. The reaction mixture was then incubated at 42 °C for 1 hour, then at 70 °C for 5 minutes to terminate the reaction. cDNA was stored at -20 °C until qPCR step.

Primers for *Drosophila* orthologues of risk genes were designed using the PrimerQuest tool (Integrated DNA Technologies) based on coding sequences of *Drosophila* candidate gene orthologues obtained from the NCBI Nucleotide database (Table 4). Primers were diluted in nuclease-free water to 100 μM. α-tubulin was used as the endogenous control and *Elav/+* was used as the reference sample. For each genotype, 3 technical repeats were run, and in each reaction the following reagents were used: 2 μl of cDNA template, 2 μl of primer (forward and reverse), 6μl of distilled H_2O and 10 μl of PowerUp™ SYBR™ Green Master Mix (Thermo Fisher). Reaction mixtures (including three technical repeats for each cDNA sample) were added to a MicroAmp™ Fast Optical 96-Well Reaction Plate (Thermo Fisher), covered with an optical adhesive cover (Applied Biosystems), then centrifuged at 1000 rpm in a Heraeus Labofuge 400 centrifuge (Thermo Fisher) for 2 minutes to remove air bubbles. A QuantStudio 3 Real-Time PCR machine (Thermo Fisher) was used with steps and corresponding cycles and temperatures in Table 5. Comparative ΔCT used to calculate relative gene expression normalised to *Elav/+* control, which was presented as relative mRNA (%). Three biological repeats (meaning 3 separate RNA extractions, RT steps and qPCR plates run) were conducted where possible. A one-way ANOVA with Dunnett's post-hoc was used to test for significant differences between relative mRNA expression of *Elav/+* control and experimental genotypes.

Table 4: Forward and reverse primers used for RT-qPCR experiments.

Primers designed using the PrimerQuest tool (Integrated DNA Technologies) based on the coding mRNA sequence for the *Drosophila* gene obtained from the NCBI Nucleotide database, available at https://www.ncbi.nlm.nih.gov/nuccore.

Gene	Forward primer	Reverse primer
α-tubulin	5'- CCTCGAAATCGTAGCTCTACAC-3'	5'-CAGCCTGACCAACATGGATA-3'
Ctl2	5'- GGCTTGCTGGTGGGTATTTA-3'	5'- CATTCTTGACCGTGGAGTGTAG-3'
Scr	5'- TACGCCTAACCTGTATCCAAAC-3'	5'- CTGCGTGTAGTCCACCATATC-3'
CG6984	5'-CCTACATATCGGGAATGGTCAC-3'	5'-GAGATGACGGCACGACTTT-3'
Frl	5'-ATTGCCGATGCTCTGGATAG-3'	5'- GATAGCTCGCAGGCACATAA-3'
MTA1-like	5'- GATGGCAGCTTGGTGTATGA-3'	5'- TGGCTTGCGTGGGAATTAT-3'
Kuz	5'- GCCAGCAGCTTCCAGAATA-3'	5'- AAGTTCGTCCTCGGCATTAC-3'

Table 5: Cycling mode used for qPCR in QuantStudio 3 Real-Time **PCR machine.**

Step	Temperature	Duration	Cycles
UDG activation	50°C	2 minutes	Hold
Dual-Lock DNA polymerase	95°C	2 minutes	Hold
Denature	95°C	15 seconds	40
Anneal/extend	60°C	1 minute	

2.4 Eye degeneration assay

The *GMR-GAL4* driver was used to drive expression of candidate gene *RNAi* in the developing *Drosophila* eye. 2–3-day old male and female flies were collected for each genotype and anaesthetised using ethanol solution to prevent their movement during imaging. Due to sex differences between eye surface area, five female and five male flies for each genotype were anaesthetised by submerging them in ethanol and placed under a Zeiss dissecting microscope at 8x magnification and consistent orientation (facing right) to take an image of the eye. Morphology of the eye was observed, noting any changes in the arrangement and shape of the regular

ommatidia structures or evidence of necrotic patches. The lasso tool in Zeiss Zen programme was used to encircle the eye to calculate surface area (mm^2). Average surface area was calculated from the 10 flies tested for each genotype and a one-way ANOVA with Dunnett's post hoc test for multiple comparisons was used to test the for significant differences between the mean surface area of *GMR*/+ control flies and experimental groups. Assumptions for parametric tests were checked and a non-parametric test performed if assumptions were not met.

2.5 Climbing assay

To determine the effect of candidate gene knockdown on locomotor ability, a climbing assay was used. 50 male flies of each genotype were collected at 1-2 days post-eclosion and housed in 5 vials of 10 flies. Every 7 days, their climbing performance was measured. Flies were transferred into a food free vial with a line at 10cm up the vial, which was tapped twice on a mat to cause the flies to fall to the bottom and induce the startle (negative geotaxis) reflex, which causes flies to climb upwards. The climbing performance was measured as the number of flies that reached the 10cm threshold line in 10 seconds (s), calculated as percentage success. Average percentage success for each genotype was analysed in a two-way ANOVA with Dunnett's post hoc analysis was used to test for significant differences between climbing performance between experimental genotypes and *elav/+* and *repo/+* controls across age. Assumptions for the parametric two-way ANOVA were checked and when not met, a non-parametric equivalent (mixed effects analysis) was used.

2.6 Longevity assay

To determine the effect of candidate gene knockdown on the lifespan of flies, a longevity assay was used. 50 mated female flies of each genotype were collected at 1-2 days post-eclosion and housed in 5 vials containing 10 flies each. Every 3-4 days, flies were flipped into fresh food vials and the number of dead flies was counted. Female flies were chosen because egg laying prevents flies getting stuck in the food which can cause inaccurate survival counts. Kaplan-Meier survival curves were constructed, and a log-rank test was used to test for significant differences in survival curves between experimental genotypes and *elav/+* and *repo/+* controls.

2.7 Memory assay

To determine the effect of candidate gene knockdown on short-term memory, an aversive olfactory shock assay (AOSA) was used, which is based on flies avoidance of an odour trained to be associated with an electric shock [75]. The *OK107-GAL4* driver was used to express candidate gene *RNAi* in mushroom body neurons. At least 50 male and female flies of each genotype were collected 1-2 days post eclosion and housed in two vials with approximately equal numbers of flies and placed in a behavioural assessment room (25°C, 70% humidity) to acclimatise for 1-2 days. 4-methylcyclohexanol (MCH) (Sigma Aldrich) and 3-octanol (OCT) (Sigma Aldrich) were diluted in 10ml of mineral oil in concentrations of 3:250 and 3:125 respectively, at which flies had an approximately equal preference for both odours. Training and testing phases were always performed in the afternoon to reduce time-of-day effects. During the training phase, flies were transferred into the top chamber of a T-maze (Figure 6) and allowed to acclimatise while exposed to air for 90 seconds. Flies were then exposed to either MCH or OCT simultaneously with a 70V electric shot for 1.5s every 5s for 60s (CS+). Flies were exposed to air for 45 s, then the non-shock associated odour for 60s (CS-). Flies were then transferred to a tube with standard food to rest for 1-hour. During the testing phase, flies were transferred to the central chamber of the T-maze and allowed to acclimatise for 90 s, then exposed to both MCH and OCT on either side of the T-maze for 120 s. The number of flies in the MCH and OCT chambers was counted. For each genotype, two vials were trained and tested with MCH and OCT each used in one trial as the shock associated odour (CS+) to control for odour bias. A performance index (PI) calculated from the number of flies in each chamber for the MCH and OCT repeats was calculated using the formula below.

$$PI = (N_{CS-} - N_{CS+})/(N_{CS-} + N_{CS+})$$

N_{CS-} = number of flies in non-shock associated chamber
N_{CS+} = number of flies in shock associated chamber

An average from the PIs for OCT and MCH repeats was calculated for each genotype to make one experimental repeat. Average PIs were inputted into GraphPad Prism 9 and a one-way ANOVA with Dunnett's post hoc analysis was used to test for significant differences in average PI between *OK107/+* control and experimental genotypes. Assumptions for a parametric test were checked.

Shock avoidance was assessed by transferring flies into the central chamber of the T-maze and allowed to acclimatise while exposed to air for 90s, then exposed to a non-shock tube and a shock tube for 120s, then the number of flies in each tube counted to calculate percentage avoidance.

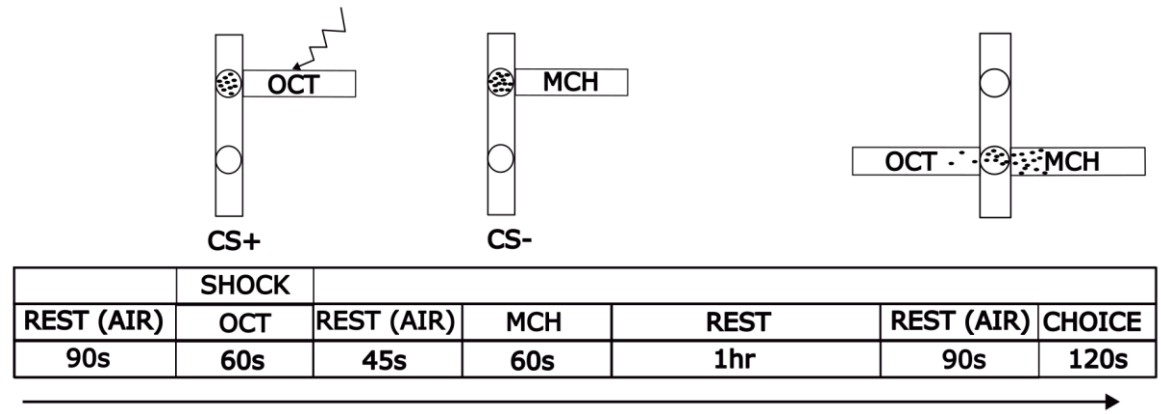

Figure 6: T maze set up for olfactory shock aversive assay for memory assessment.

Flies were transferred into the top chamber of a T maze and allowed to acclimatise while exposed to air for 90 s. Flies were exposed to an odour (OCT) with a 90 V electric shock (CS+), then allowed to rest while exposed to air for 45 s before being exposed to an odour (MCH) without electric shock (CS-). After 1 hr rest while housed in a standard tube with access to food, flies were transferred into the bottom chamber, allowed to rest while exposed to air for 90 s then exposed to both odours via a chamber on each side for 120 s. The number of flies in each chamber was then counted to calculate performance index. For each experimental repeat for a gene, the odour exposed with the electric shock was reversed in a second trial to control for odour bias. Figure made using information from [75].

2.8 Sleep and circadian rhythms assay

To determine the effects of candidate gene knockdown on sleep and circadian rhythms, *Drosophila* activity monitors (DAM) were used, which count the number of

infrared beam breaks caused by the movement of individual flies housed in tubes, as a measure of activity (Figure 7). The *Tim-GAL4* driver was used to express candidate gene *RNAi* in all clock cells. This driver was cantonised (backcrossed to csw- for 3 generations) to control for genetic background, which can have a strong effect on activity and sleep behaviours. Male flies were collected at 3-5 days post-eclosion and placed in individual tubes filled with approximately 1cm of food at one end. Each DAM monitor (Trikinetics) housed 32 flies and was placed in an incubator at 25°C for 5 days in a 12hr light-dark (LD) cycle, and then switched to 5 days in constant darkness (DD). Activity data from raw monitor files was extracted using the DAMFileScan113X program (Trikinetics). The Sleep and Circadian Analysis MATLAB Program (SCAMP) scripts in MATLAB were used to analyse the extracted activity data to calculate average total activity counts, total sleep, period length and rhythmicity statistic for each genotype. Activity data from LD was used to analyse sleep and activity data from DD was used to calculate circadian period length and rhythmicity statistic. Total sleep and total activity counts were analysed in a two-way ANOVA with Dunnett's post hoc to test for significant differences between genotypes and *Tim/+* and *UAS/+* controls and time of day (day/night). Period length and rhythmicity statistic were analysed using a one-way ANOVA with Tukey's post hoc. Assumptions for parametric tests were checked and a non-parametric equivalent used if not met.

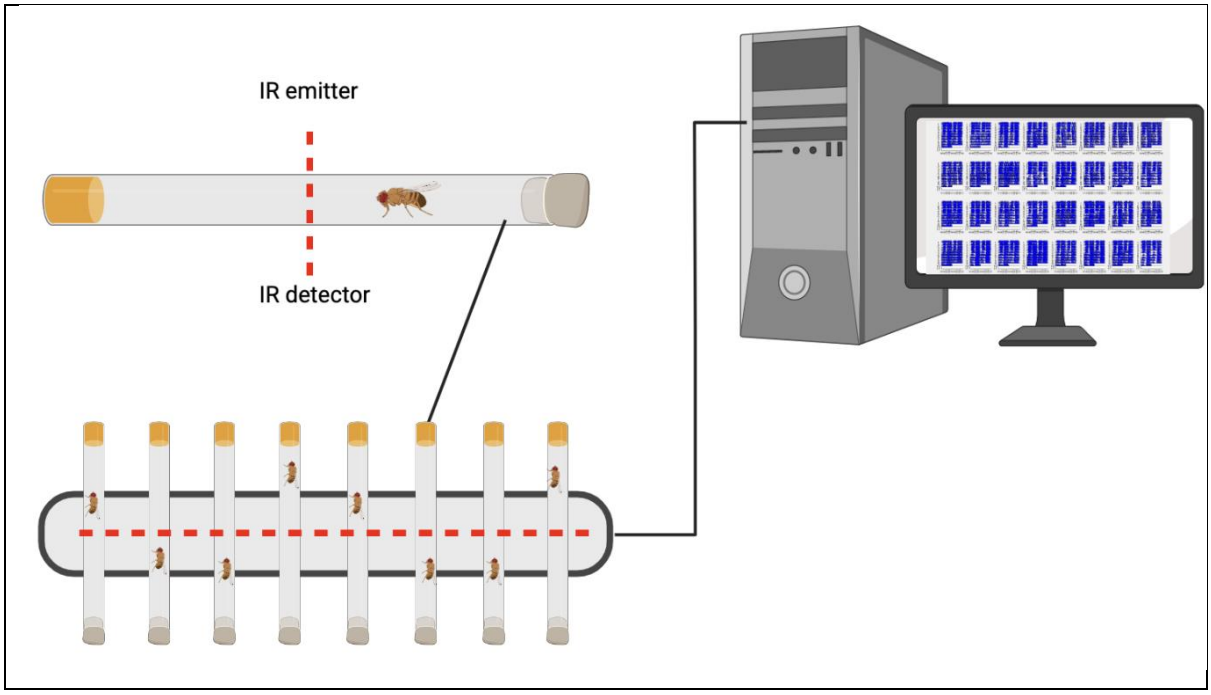

Figure 7: *Drosophila* activity monitor (DAM) system set-up.

32 flies are housed in individual tubes in a DAM. The number of times the infrared beam is broken by a fly crossing it is used as a measure of activity, and >5 minutes of inactivity is counted as sleep. DAM monitors are kept at 25°C for 5 days in a 12hr LD cycle and 5 days in constant darkness for sleep and circadian analysis respectively. Raw activity data is extracted using the DAMFileScan programme (TriKinetics) and analysed in MATLAB using SCAMP scripts. Figure made in BioRender.com.

2.9 Courtship Assay

Protocol adapted from [152]. *Drosophila* courtship relies on the male 'wing song' created by wing beating. Virgin males and virgin females were collected from producing vials of each genotype. Males were housed individually, and females housed in vials of 5-6 females, each on standard food and 12hr light-dark cycle. After allowing flies to age to 4-5 days old, a male and female fly were transferred into the chamber of a clean mating wheel (Figure 8) using a fly aspirator (built using a clean pipette tip, mesh, and tubing) to avoid the use of CO_2 anaesthesia which can interfere with courtship behaviour. Flies were observed for 15 minutes (900 s) and their latency in seconds (s) to courtship behaviours and the number of pairs performing each courtship behaviour was recorded as frequency. The latency from wing song to successful copulation was also measured as a proxy for hearing sensitivity. If no successful copulation occurred during the 15 minutes, the pair was assigned a copulation latency and wing song-copulation latency of 900 s. After experimentation, the mating wheel was soaked in Alconox Powdered Precision Cleaner (Alconox Inc.) soap for 24hrs then washed in distilled water to remove traces of pheromones before the next use. All courtship experiments took place at 25°C, 70% humidity and always performed in the afternoon to reduce circadian effects. Assumptions were not met for parametric statistical testing due to small sample sizes.

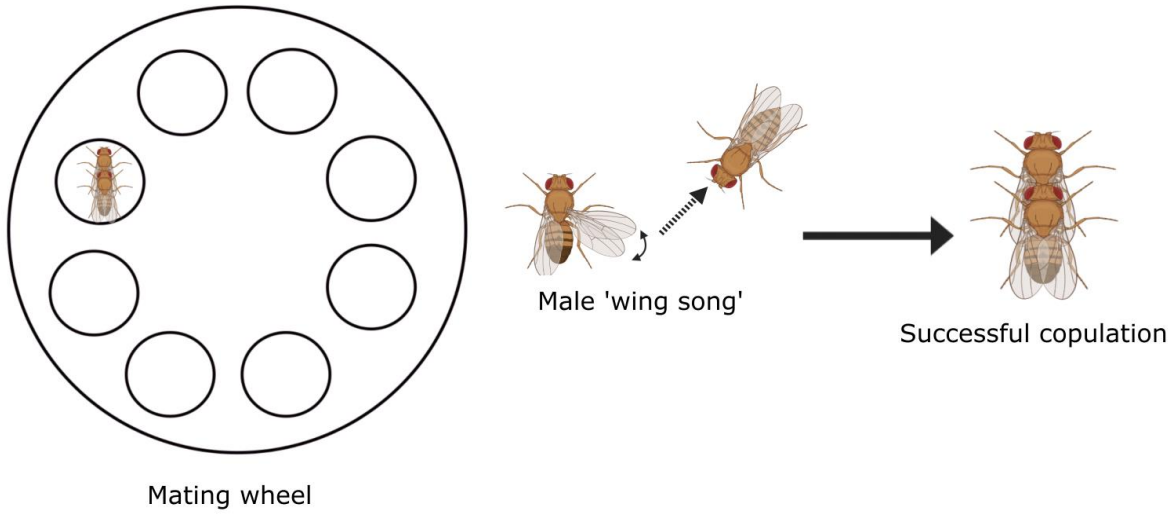

Figure 8: Mating wheel used for courtship assay and behaviours observed.

A male and female of each genotype was transferred into the mating wheel and observed for 15 minutes (900 s). Latency to successful courtship and latency to wing song was measured to calculate wing song-copulation latency, used as a measure of hearing ability. Figure made using BioRender.com.

3. Results

3.1 Bioinformatic analysis and verification of fly lines

Human genes identified as closest to significant loci from Kunkle et al's 2019 GWAS meta-analysis study [60] and Smith et al's 2021 EWAS meta-analysis [59] for LOAD were selected based on high significance and functions of interest to AD pathology. Selected genes were searched using the online DRSC Integrative Orthologue Prediction Tool (DIOPT) [153] to find their closest *Drosophila* orthologues (Tables 6 and 7). *Drosophila* orthologues were selected for screening in flies if protein similarity was >40%, protein identity >30% and DIOPT score >6. In Kunkle et al's GWAS meta-analysis, hits were searched in AlzBase, a database with gene, network, and expression information integrated from human and animal model genetic and studies of AD [154] to find whether upregulation or downregulation was associated with Braak stage [60]. *ECHDC3* was more frequently downregulated in transcriptome studies of AD, whereas *ADAMTS1* was more frequently upregulated in transcriptome studies of AD (Table 1). Smith et al assigned DMPs from their EWAS meta-analysis

a calculated methylation effect size for their association with Braak stage, which was positive if hypermethylation was associated with higher Braak stage and negative if hypomethylation was associated with higher Braak stage, indicated in Table 3. Hypermethylation was associated with higher Braak stage for all EWAS hits selected for screening in this project (Table 2).

Table 6: AD risk genes selected and relevant annotations from Kunkle et al's 2019 GWAS meta-analysis and their *Drosophila* orthologues screened in this project.

Single nucleotide polymorphism (SNP) rsID, up- or downregulation association with Braak stage based on AlzBase searches and DIOPT score (a measure of the number of tools that support the human-*Drosophila* orthologue relationship) are listed for each gene. Protein similarity and protein identity from DIOPT are also included.

Human AD risk gene	**SNP**	**AlzBase search regulation results**	***Drosophila* orthologue**	**DIOPT score**	**Protein similarity (%)**	**Protein identity (%)**
ECHDC3	rs7920721	Down-regulation	*CG6984*	15	61	42
ADAMTS1	rs2830500	Up-regulation	*AdamTS-A*	7	47	32

Table 7: AD risk genes selected and relevant annotations from Smith et al's 2021 EWAS meta-analysis and their *Drosophila* orthologues screened in this project.

Differentially methylated position (DMP) and direction of effect for methylation associated with higher Braak stage are included. DIOPT score, protein similarity and protein identity from DIOPT are also included.

Human AD risk gene	**DMP**	**Methylation associated with Braak stage**	***Drosophila* orthologue**	**DIOPT score**	**Protein similarity (%)**	**Protein identity (%)**
ADAM10	chr15: 59042684	Hyper-methylation	*Kuz*	14	48	35
SLC44A2	chr19: 10736059	Hyper-methylation	*Ctl2*	13	49	32

PPT2	chr6: 32120826	Hyper-methylation	*Ppt2*	13	57	40
HOXA5	chr7: 27184461	Hyper-methylation	*Scr*	7	56	43
KIF21B	chr1: 200983238	Hyper-methylation	*Klp31E*	10	56	40
STARD13	chr13: 33780307	Hyper-methylation	*cv-c*	8	49	34
MTA3	chr2: 42795262	Hyper-methylation	*MTA1-like*	13	56	43
KDM2B	chr12: 121890907	Hyper-methylation	*Kdm2*	11	43	31
FMNL1	chr17: 43318900	Hyper-methylation	*Frl*	13	58	41

All but one (*ADAMTS1*) of the candidate genes selected showed downregulation or hypermethylation associated with increased Braak stage (Tables 6 and 7). Whilst hypermethylation can have positive or negative effects on gene expression depending on where it occurs [52], methylation of CpG islands is generally considered to reduce gene expression [155], indicating that the human AD risk genes with hypermethylation associated with increased Braak stage likely have reduced expression in the brains of AD patients (Table 7). Therefore, decreasing gene expression was considered the best approach to detect AD-associated phenotypes associated with candidate genes in the following assays used in this project.

Search Tool for the Retrieval of Interacting Genes/Proteins (STRING) is an online bioinformatics database used to search both predicted and confirmed protein-protein interactions [156]. For this project, a STRING search for both human (Figure 9a) and *Drosophila* orthologues of AD risk genes (Figure 9b) was used to create protein-protein interaction networks. In humans, interaction between *ADAM10* and *ADAMTS1*, *APP, BACE1* and *MAPT* was inferred through text mining, indicating that there are multiple papers that co-mention gene names in their abstract. Coexpression and experimental data also supports the interaction of *ADAM10* with

APP and *BACE1* (Figure 1a). *ADAM10* is an α-secretase involved in non-amyloidogenic processing of *APP,* whereas *BACE1* is involved in the amyloidogenic processing of *APP* via its role as a β-secretase [157], and can form a α-/β-secretase binary complex with *ADAM10* [158]. Only text mining indicated an *ADAM10-MAPT* interaction, but no direct interaction between *MAPT* or tau protein and *ADAM10* was found when searching these abstracts. The interaction between the *Drosophila* orthologue of *APP, dAPPL* (annotated as Appl below) and *Kuz* (orthologue of human *ADAM10*) was conserved, but no other interactions between *Drosophila* candidate gene orthologues were detected at medium confidence (Figure 9b).

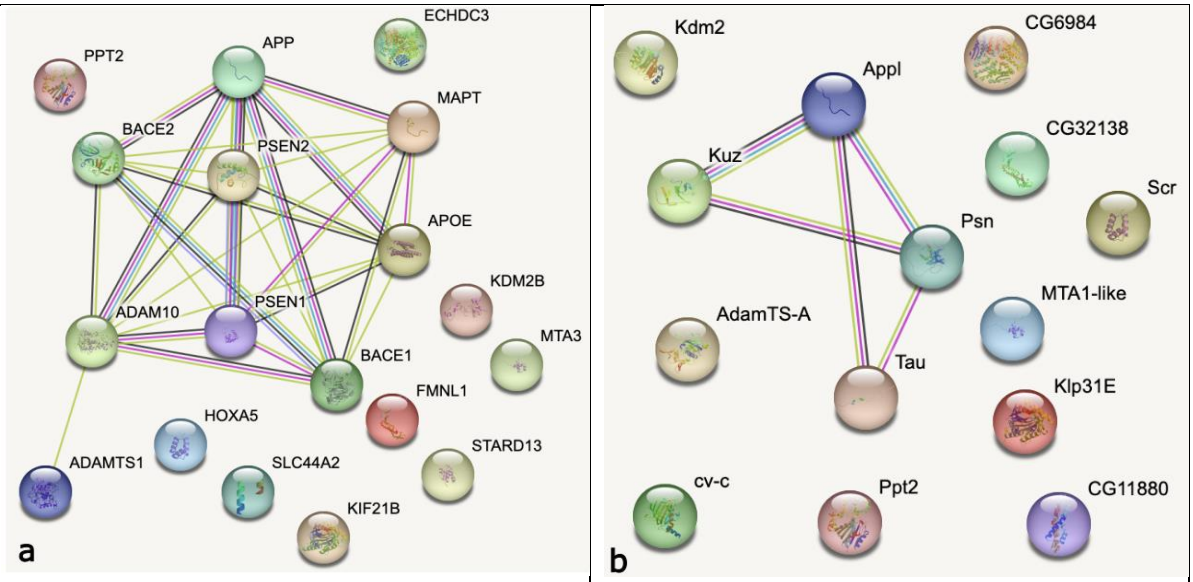

Figure 9: Protein-protein interaction network for risk genes and hallmark AD proteins in humans and *Drosophila*.

(a) Human GWAS and EWAS hits and hallmark AD proteins (*APP,* amyloid precursor protein, *MAPT,* microtubule-associated protein, BACE1, β secretase 1, BACE2, β secretase 2, *PSEN1*, Presenilin-1, PSEN2, Presenilin-2) were searched in STRING to create a protein-protein interaction network. (b) *Drosophila* orthologues of GWAS and EWAS hits and hallmark AD proteins (Appl, *Drosophila* orthologue of *APP, Psn*, orthologue of human *PSEN1* and *PSEN2*, and tau) were searched in STRING to create a protein-protein interaction network. *CG32138* is *Frl*, *CG11880* is *Ctl2*. Both networks are medium confidence (0.400). Green lines indicate interactions based on text mining, pink lines indicate experimentally determined interactions, blue lines indicate curated databases, and black lines indicate interactions based on co-expression data.

Table 8: Expression of selected human risk genes in human tissues.

Five human tissues with highest expression of risk gene and brain expression level (RPKM), using the HPA RNA-seq normal tissues dataset [159] expression graph for each gene from NCBI Gene database (https://www.ncbi.nlm.nih.gov/gene/).

Human gene	**Tissues with highest expression (RPKM)**	**Brain expression (RPKM)**
ECHDC3	Fat (46.0), kidney (40.5), liver (26.3), heart (9.5), thyroid (9.4)	0.5
ADAMTS1	Ovary (125.4), placenta (76.7), gall bladder (71.3), prostate (49.9), urinary bladder (48.1)	5.5
ADAM10	Urinary bladder (31.1), thyroid (26.9), placenta (24.5), spleen (22.4), prostate (21.5)	16.7
SLC44A2	Placenta (81.4), spleen (68.7), testis (62.6), lung (62.0), stomach (50.9)	34.2
PPT2	Ovary (15.4), placenta (11.8), skin (10.6), endometrium (10.2), bone marrow (9.5)	7.1
HOXA5	Adrenal (47.8), lung (14.3), kidney (9.6), endometrium (8.1), fat (7.7)	0
KIF21B	Bone marrow (11.9), brain (10.4), testis (6.9), lymph node (6.6), spleen (6.3)	10.4
STARD13	Placenta (8.5), thyroid (7.1), fat (7.0), endometrium (6.3), gall bladder (5.1)	2.8
MTA3	Brain (3.7), ovary (3.5), adrenal (3.1), testis (3.0), endometrium (2.2)	3.7
KDM2B	Lymph node (6.1), appendix (5.5), spleen (5.4), skin (4.7), testis (4.5)	3.7
FMNL1	Bone marrow (44.1), appendix (23.0), spleen (22.6), lymph node (19.5), lung (9.4)	3.7

SCope is an online single cell RNAseq database which allows analysis of gene expression in the *Drosophila* brain across different cell clusters and ages [160]. *Drosophila* orthologues of the annotated genes were searched in SCope.com to build an expression heatmap (Figure 10). *Frl* and *Kuz* (fly orthologues of *FMNL1* and *ADAM10*) showed the highest overall expression in the fly brain. *Ctl2*, *cv-c*, *Kdm2* and *Ppt2* show higher expression in glial cell clusters compared to most other clusters (Figure 10). *Kdm2*, *Frl*, *Klp31E*, *Kuz* and *Ppt2* show comparatively high expression in peptidergic neurons, which are abundant in the CNS of *Drosophila* and are involved in regulation of locomotor behaviour, courtship, metabolism, feeding and sleep [161], among other behaviours.

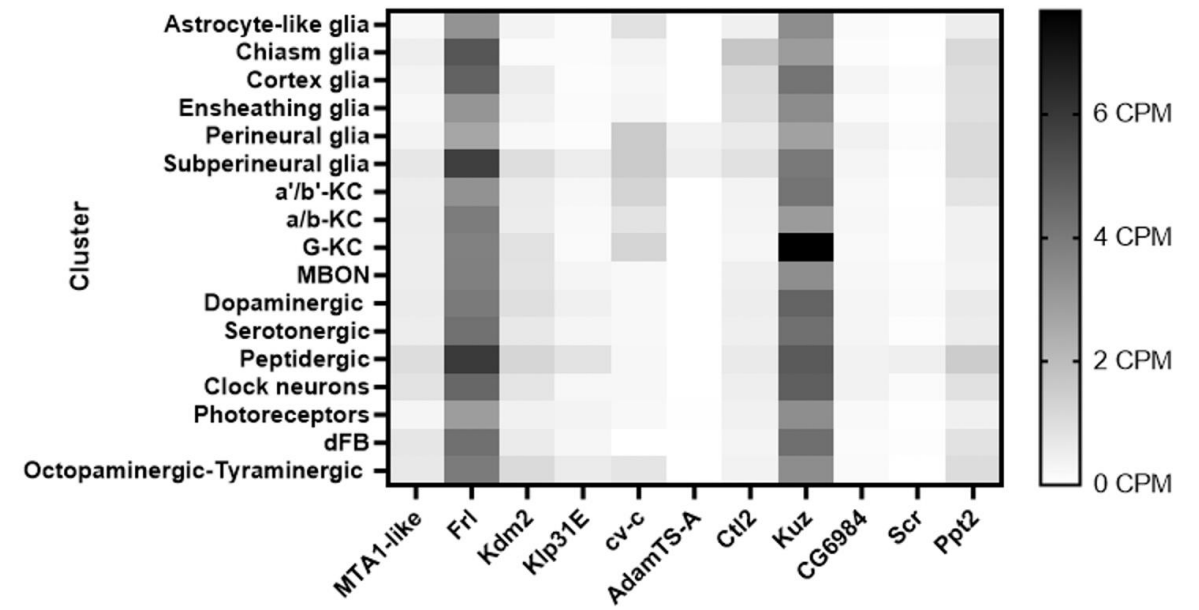

Figure 10: Drosophila orthologues of AD risk genes show differential expression across cell types in the Drosophila brain.

Heatmap of gene expression (CPM) by cluster, using single cell RNAseq data from the Aerts_Fly_AdultBrain_Filtered_57k database on SCope.com. Units for expression are counts per million (CPM).

Following behavioural screening, some genes which exhibited AD-associated phenotypes or unusual effects upon *RNAi* expression were chosen for RT-qPCR experiments to confirm their knockdown and validate their phenotype. RT-qPCR data is included here as it informs behavioural assay data in the following results chapters. The Elav-*GAL4* driver was used to express *RNAi* for each candidate gene

in all neurons, and mRNA was extracted from whole *Drosophila* heads for RT-qPCR (Figure 11a). Due to partial lethality caused by pan-neuronal Ctl2 *RNAi* expression, only one biological replicate was produced using *Elav>Ctl2-RNAi*. Therefore, the temperature-sensitive *GAL80ts, Elav-GAL4* driver was used to express *Ctl2 RNAi* only in adulthood using temperature manipulation (Figure 11b) to increase the number of surviving flies. Pan-neuronal expression of *Scr-RNAi* lead to no change in relative mRNA (Figure 11a) but pan-neuronal expression of *CG6984 RNAi* and *MTA1-like RNAi* lead to an increase in CG6984 and *MTA1-like* mRNA to 218.7% and 140%, respectively (Figure 11a). Pan-neuronal expression of *Frl* and *Ctl2 RNAi* caused a decrease in relative mRNA to 44.3% and 56%, respectively. However, when analysed in a one-way ANOVA, these changes in relative mRNA were not significant.

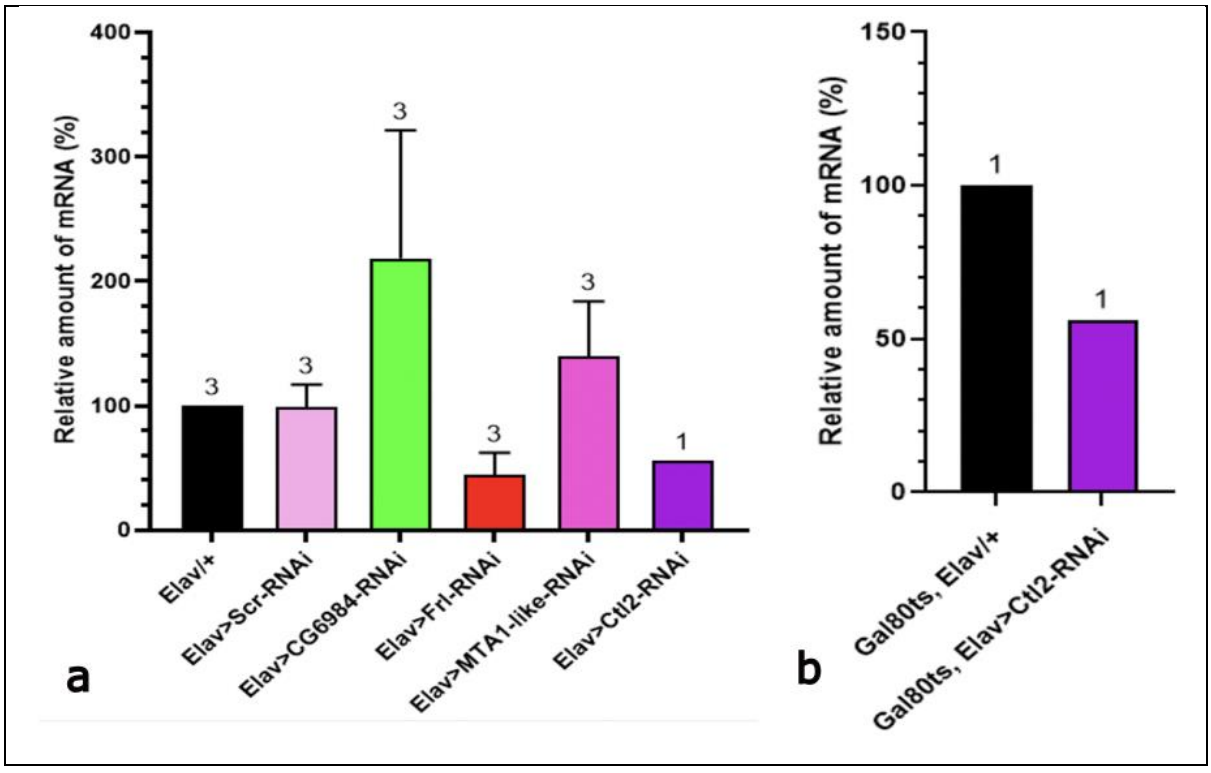

Figure 11: Pan-neuronal expression of *Frl RNAi* and *Ctl2 RNAi* caused a reduction in *Frl* and *Ctl2* mRNA.

The *Elav-GAL4* driver was used to express candidate gene *RNAi* in neurons during development and the *GAL80ts-Elav* driver was used to express candidate gene *RNAi* in neurons just during adulthood. RT-qPCR was used to measure mRNA (%) relative to *Elav/+* control. The number above bars indicates the number of biological replicates (one biological replicate is one RNA extraction from 20-30 *Drosophila* heads). (a) Relative amount of mRNA compared to *Elav/+* control (100%). (b) Relative amount of mRNA compared to *Gal80ts, Elav/+* control (100%). Relative amount of mRNA in (a) analysed in a one-way ANOVA with Dunnett's post hoc for multiple comparisons. No statistical analysis performed on (b) due to N=1. Error bars are mean ± SEM. Numbers above bars indicate the number of experimental repeats per genotype.

3.2 Knockdown of candidate genes in the eye did not cause a change in gross morphology or surface area

The adult *Drosophila* eye contains approximately 750-800 ommatidia [162], individual hexagonally shaped units. These units include three types of pigment cell which prevent light reaching adjacent ommatidia [163], non-neuronal cone cells which contribute to lens formation via secretion [164] and eight central photoreceptor neurons [165]. The arrangement of ommatidia needs to be precise to provide high visual acuity [162]. Because of this highly regular arrangement, the *Drosophila* compound eye can be used for both forward and reverse screens for genes affecting neurodevelopment and neurodegeneration [166]. Previously, light microscopy measures of surface area and gross morphology of the adult *Drosophila* eye have been used to quantify changes in the number and arrangement of ommatidia caused by misexpression of Aβ and tau peptides and co-expression or knockdown of AD risk genes identified by GWAS [68]. In this project, a similar approach was used as an initial screen of selected risk genes for neurotoxic effects when knocked down. Fly orthologues of AD risk genes were knocked down in the eye from development onwards using the *GMR-GAL4* driver and corresponding *RNAi* lines under *UAS* control. Light microscopy was used to image the eye and measure surface area, to look for a 'rough eye' phenotype (characteristic of neurotoxicity) and decrease in

surface area associated with a change in the number and arrangement of photoreceptors. *GMR/+* was used as a wild-type control, and overexpression of human tau isoform 0N4R and human tAβ42 were used as positive controls.

Overexpression of human tau-0N4R and tAβ42 caused disorganised eye morphology (Figure 12a) and a decrease in eye surface area ($p<0.0001$, one-way ANOVA, Dunnett's post-hoc) compared to the *GMR/+* wild type control. This result is consistent with previous studies involving overexpression of human tau and Aβ isoforms in the *Drosophila* eye [68, 72, 110]. However, no noticeable change in gross morphology of the eye or decrease in eye surface area was observed when risk genes were knocked down compared to the *GMR/+* control (Figure 12a and b).

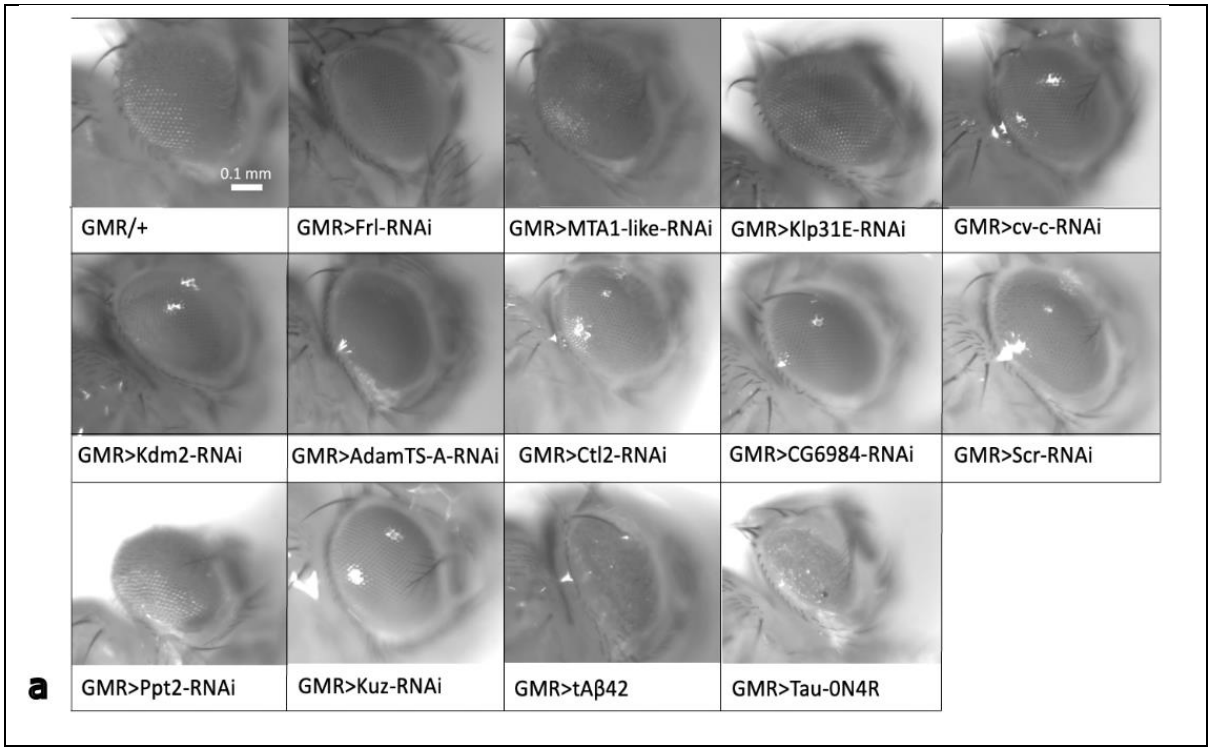

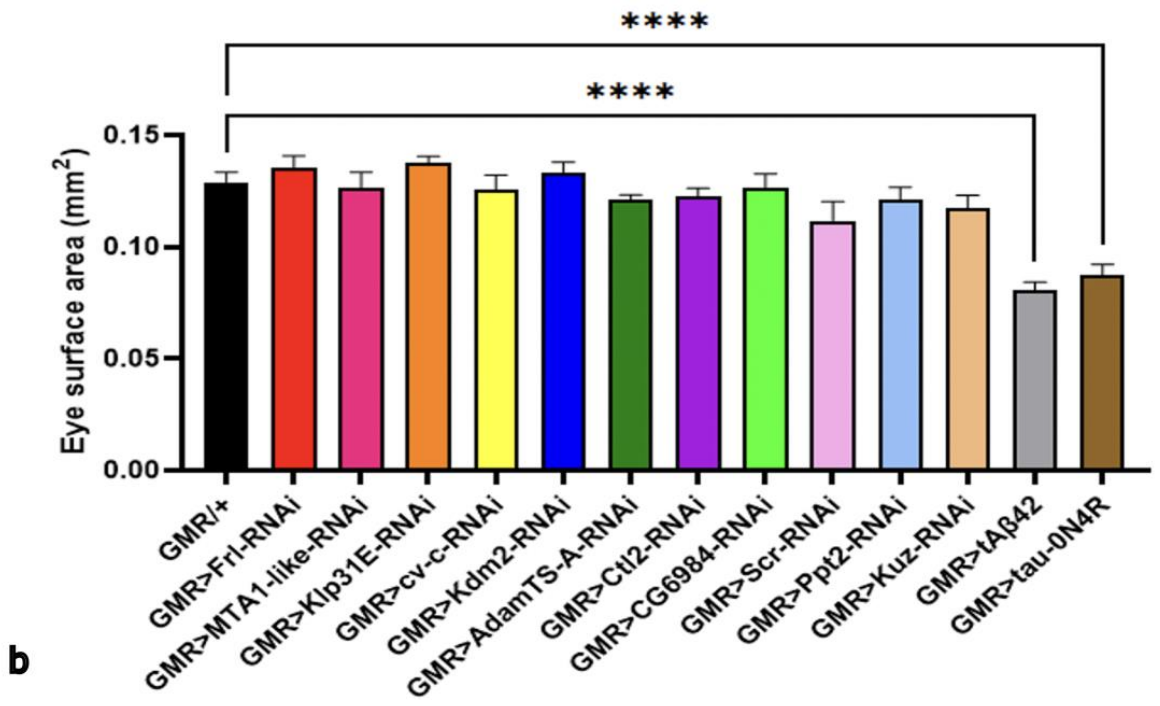

Figure 12: Overexpression of human tAB42 and tau-0N4R in the developing *Drosophila* eye caused a decrease in eye surface area and change in gross morphology.

The *GMR-GAL4* driver was used to knockdown candidate genes in the *Drosophila* eye by expressing candidate gene *RNAi*. (a) Representative images of the eyes taken at 8x magnification. (b) Average eye surface area for each genotype, measured by lassoing the eye on the Zeiss Zen programme. N=10 (5 males, 5 females) for each genotype. Averaged eye surface area analysed in a one-way ANOVA with Dunnett's post-hoc. All error bars are mean ± SEM. ****P<0.0001.

No change in gross eye morphology or surface area were observed upon expression of candidate gene *RNAi* in the eye. The purpose of this screen was to detect genes which may have a significant role in neurotoxicity or neurodegeneration, as it is unusual for knockdown of a single gene to cause a 'rough eye' phenotype unless it is centrally involved in neurotoxicity, such as Aβ. Therefore, as I did not detect a rough eye phenotype with any of the candidate genes, I decided to screen all genes further using behavioural assays included in the following chapters to characterise other possible effects of knockdown.

3.3 Knockdown of candidate genes in neurons and glia affected locomotor ability

Expression of human tau isoforms and amyloid β peptides in *Drosophila* causes a progressive defect in locomotor behaviour that can be quantified in a climbing assay [73]. This measures the negative geotaxis, or 'startle' reflex, where flies climb upwards when tapped to the bottom of a vial. This response is primarily mediated by dopaminergic and mushroom body neurons [167], but glial cell signalling can also mediate motor behaviour [168]. In this project, the climbing assay was used to assess neurotoxic effects of each candidate gene knocked down in neurons and glia involved in this behaviour. The *Elav-GAL4* driver was used to knockdown genes in all neurons during development and adulthood, or the *Repo-GAL4* driver was used to knockdown genes in all glial cells during development and adulthood. Male offspring were collected and climbing performance measured as percentage success and was assessed every 7 days from their day of eclosion (day 0) to 21 days of age to record the effect of aging on climbing performance and the effect of gene knockdown on climbing performance. Due to the large number of genes screened and labour-intensive experiments, genes were split into two groups that were screened together in each assay for simplified presentation and analysis. These are presented separately due to the use of separate *GAL4*/+ controls.

Interestingly, *Kuz* and *Ctl2* consistently caused developmental lethality when knocked down in neurons using the *Elav-GAL4* driver, meaning between 0-5 flies eclosed from each cross that would normally produce 50-100 offspring of the correct genotype. Additionally, *Ctl2* caused developmental lethality when knocked down in glia using the *Repo-GAL4* driver. These genes are therefore not included in climbing assays with these drivers. In all experiments, overexpression of human tAβ42 in neurons or glia caused a reduction in climbing ability of varying severity and a steeper age-dependent decline in climbing ability (Figures 13-17), as previously observed [73] and was used as a positive control. Unexpectedly, expression of *RNAi* for *Scr* and *CG6984*, fly orthologues of HOXA5 and ECHDC3 respectively, in all neurons resulted in increased climbing performance compared to the *Elav/+* control genotype at 21 days ($P<0.01$). Pan-neuronal expression of *Ppt2-RNAi* caused no change in climbing ability at all ages (Figure 13).

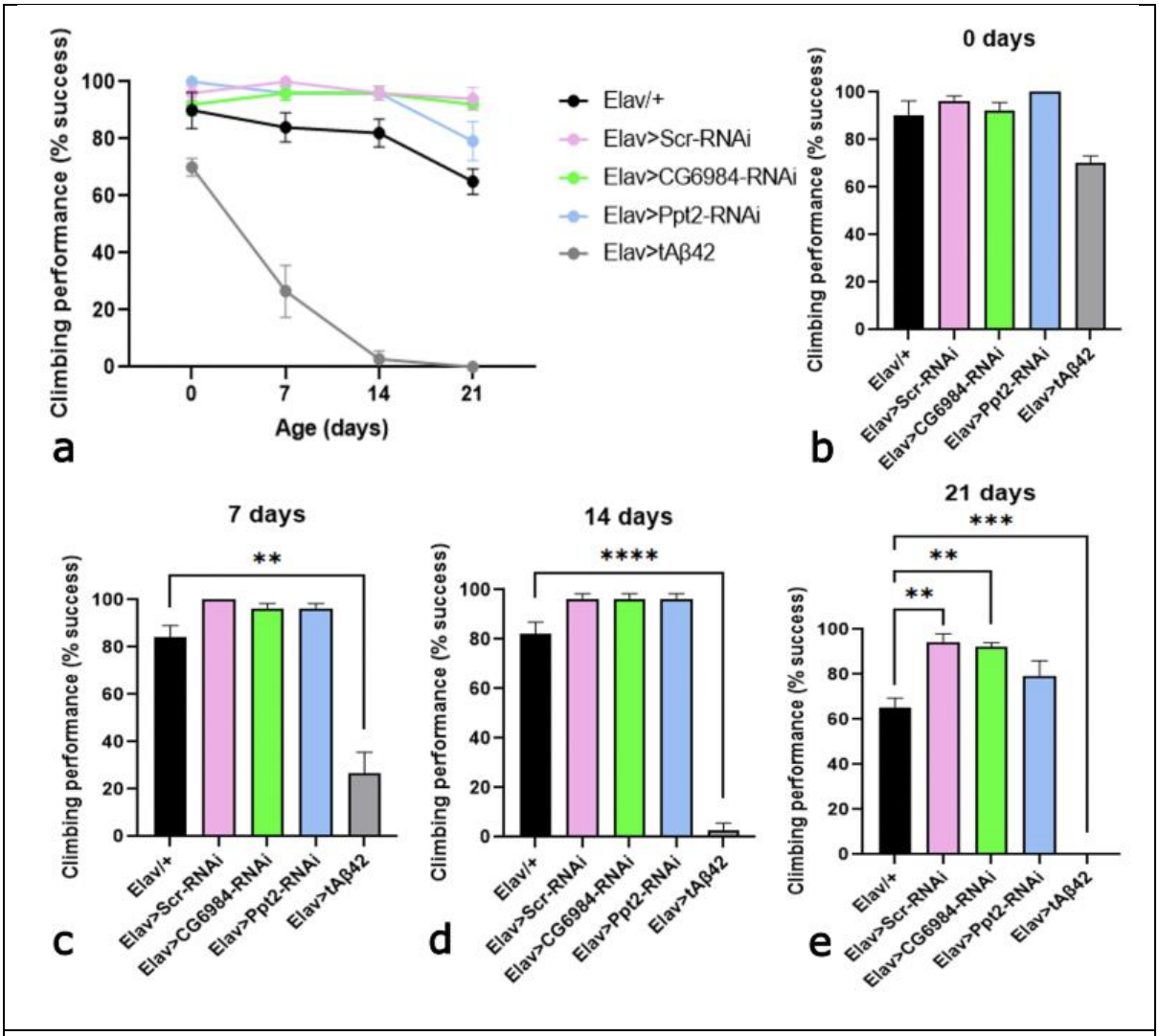

Figure 13: Pan-neuronal knockdown of *Scr* and *CG6984* rescued age-dependent decline in climbing performance.

RNAi for candidate genes was expressed in all neurons using the *Elav-GAL4* driver. The negative geotaxis response was measured as average percentage success during aging. (a) Climbing performance over time for each genotype. Climbing performance at 0 (b), 7 (c), 14 (d) and 21 days (e) post-eclosion. Mixed effects analysis, Dunnett's post hoc. All error bars are mean ± SEM. N≥50 flies for all genotypes except tAβ42 at day 21 due to premature death. *P<0.05, **P<0.01, ***P<0.001, ****P<0.0001.

Pan-neuronal expression of *RNAi* against *cv-c (STARD13)*, *Klp31E (KIF21B)*, *Kdm2 (KDM2B)* or *AdamTS-A (ADAMTS1)* caused no change in climbing ability compared to *Elav/+* control at all ages (Figure 14). However, pan-neuronal expression of *Frl* and *MTA1-like RNAi* caused a reduction in climbing ability at all ages (Figure 15). As

a separate control to *Elav/+*, *Frl-RNAi* and *MTA1-like-RNAi* lines were crossed to *csw-* to create *UAS* controls (*Frl/+* and *MTA1-like/+*). These are used to demonstrate no effect of the *UAS* insertion without the *GAL4* present. The *MTA1-like/+* control had similar climbing ability compared to the *Elav/+* control, but the *Frl/+* control showed significantly reduced climbing ability to the *Elav/+* control at 0, 14 and 21 days (Figure 15).

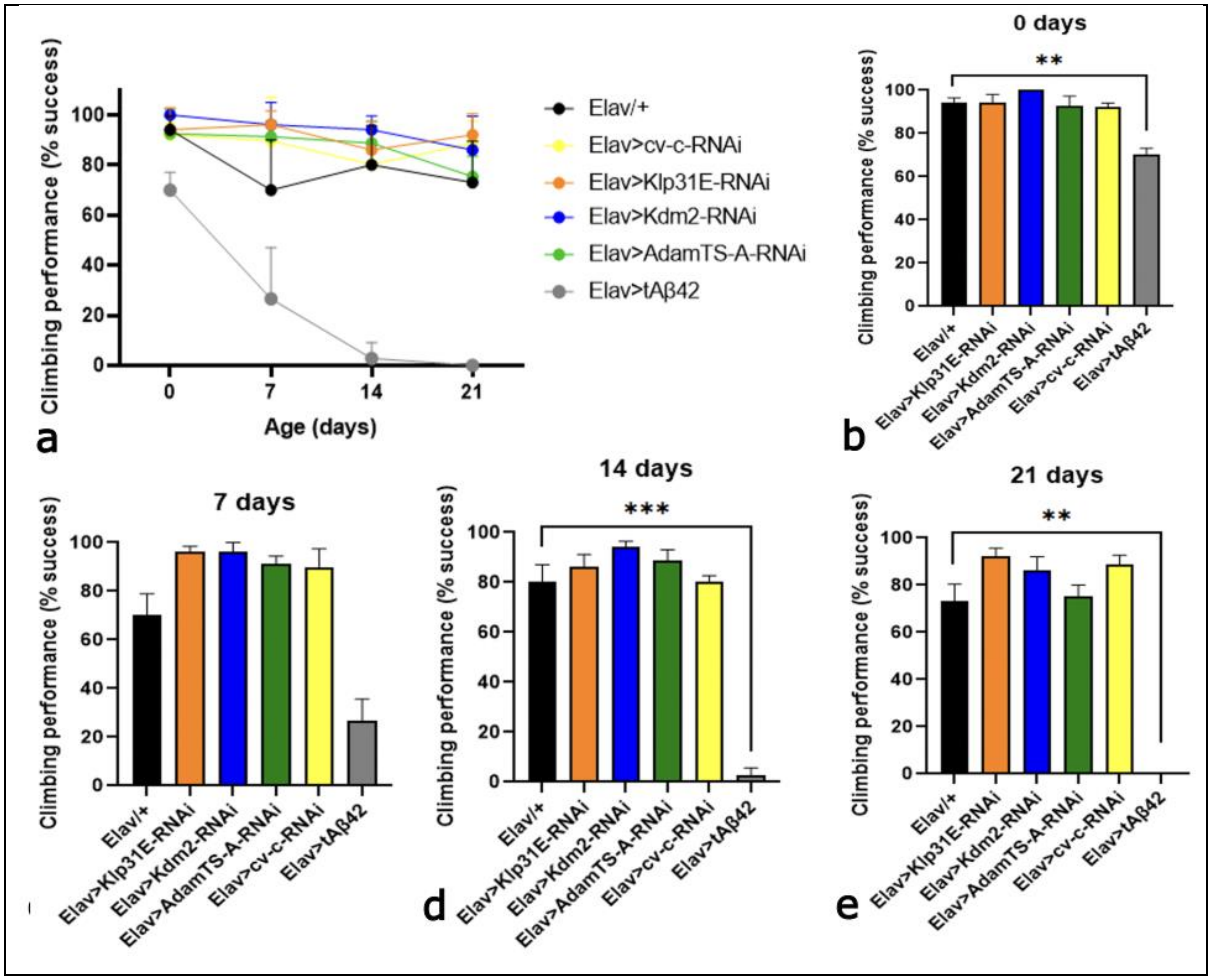

Figure 14: Pan-neuronal knockdown of *Klp31E, Kdm2, AdamTS-A*, and *cv-c* did not cause a change in climbing performance of flies compared to *Elav-GAL4/+* control.

Neuronal overexpression of human tAβ42 caused a steep decline in climbing performance. The negative geotaxis response was measured as average percentage success during aging. (a) Climbing performance over Time for each genotype. Data analysed in a mixed effects analysis, Dunnett's post-hoc with Figure 7 presented separately for interpretation with *UAS* controls. Climbing performance at 0 (b), 7 (c), 14 (d) and 21 days (e) post-eclosion. All error bars are mean ± SEM. N≥50 flies for all genotypes except tAβ42 at day 21 due to premature death. **P<0.01, ***P<0.001.

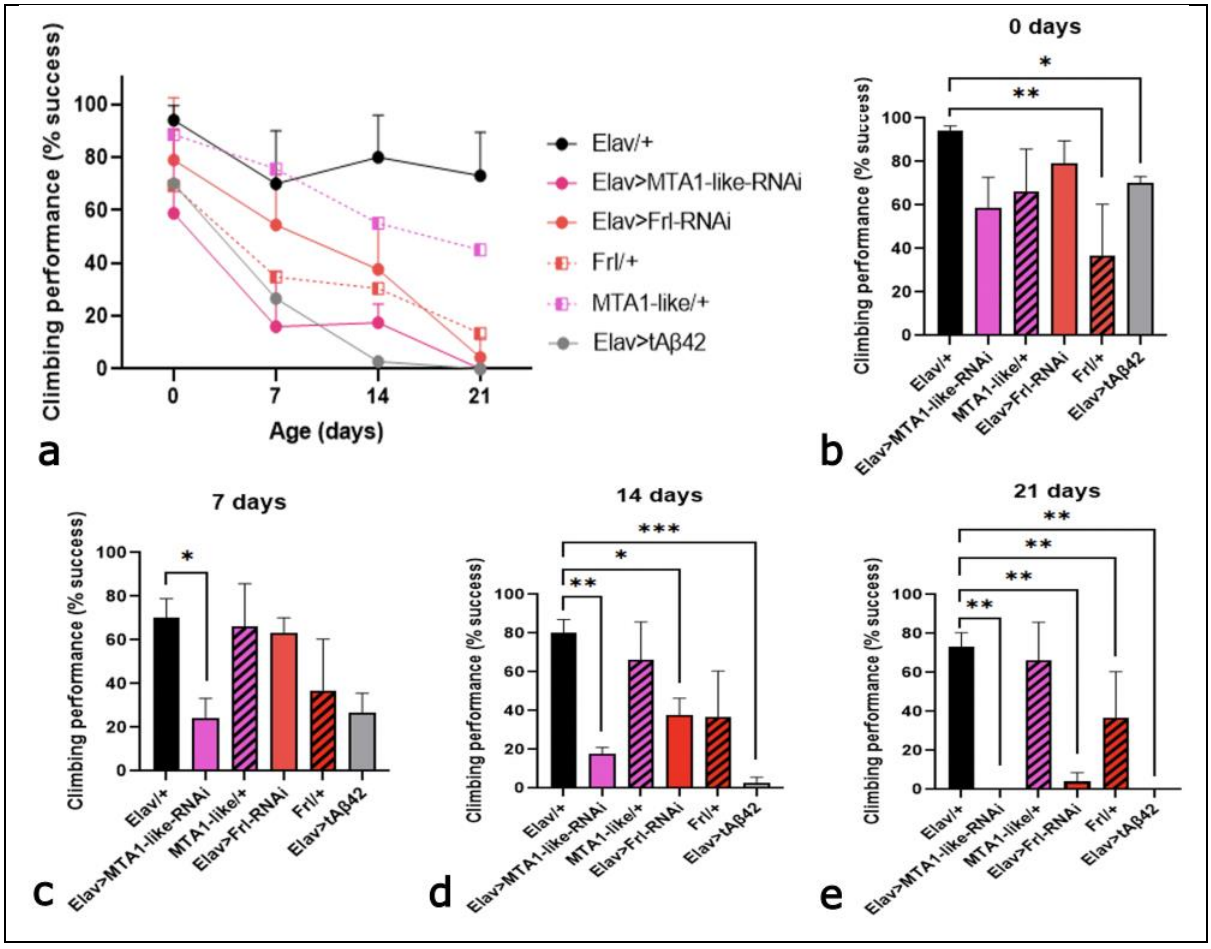

Figure 15: Pan-neuronal knockdown of *Frl* and *MTA1-like* induced an age-dependent climbing defect.

Negative geotaxis response was measured as average percentage success during aging. (a) Climbing performance for each genotype decreases over Time. Climbing performance at 0 (b), 7 (c), 14 (d) and 21 days (e) post-eclosion. Mixed effects analysis, Dunnett's post-hoc with Figure 7 (presented separately for interpretation with *UAS* controls). All error bars are mean ± SEM. N≥50 flies for all genotypes except tAβ42 at day 21 due to premature death. *P<0.05, **P<0.01, ***P<0.001.

In humans, glial cells exist in higher abundance than neurons and perform supportive functions within the nervous system [169], and are heavily involved in AD pathology [40]. *Drosophila* glial cells exhibit similar subtypes and functions to human glia [170]. Multiple candidate genes are expressed in glial cells in *Drosophila* according to SCope analysis (Figure 10), so to test whether reduction in candidate gene function causes glial dysfunction that could lead to a change in locomotor behaviour, the *Repo-GAL4* driver was used to express candidate gene *RNAi* in all glial cells. Climbing ability over 4 weeks was measured using the negative geotaxis assay. Glial overexpression of human tau-0N4R caused lethality and is therefore not included in the flowing results. Glial overexpression of tAβ42 caused a reduction in climbing ability at 14 and 21 days of age (Figure 16), but this was non-significant when tested in a mixed effects analysis. Glial expression of *Kuz-RNAi* caused a reduction in climbing ability at 7, 14 and 21 days, but this was only significant at 7 days (Mixed effects analysis, Dunnett's post hoc, P<0.01).

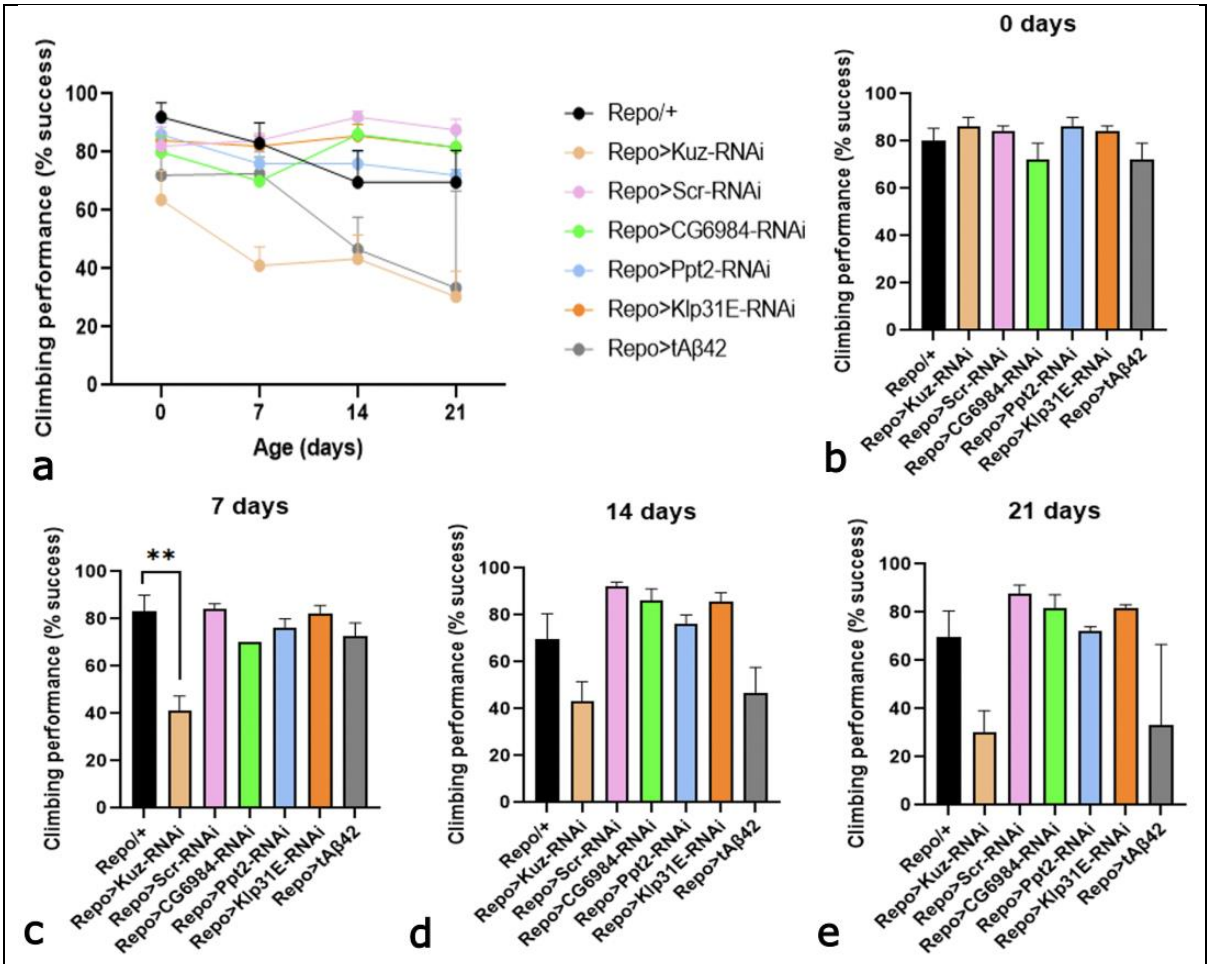

Figure 16: Glial knockdown of *Kuz* reduced climbing performance at 7 days post-eclosion.

Glial overexpression of human tAβ42 caused a non-significant decrease in climbing performance. Candidate gene *RNAi* was expressed in all glial cells using the Repo-*GAL4* driver. The negative geotaxis response was measured as average percentage success during aging. (a) Climbing performance over Time for each genotype. Mixed effects analysis, Dunnett's post hoc. Climbing performance at 0 (b), 7 (c), 14 (d) and 21 days (e) post-eclosion. All error bars are mean ± SEM. N≥50 flies for all genotypes except tAβ42 at day 21 due to premature death. *P<0.05, **P<0.01.

Glial expression of *Frl RNAi* decreased climbing ability compared to *Elav/+* control at 0, 7, 14 and 21 days (Figure 17). Glial knockdown of *MTA1-like* decreased climbing ability compared to Elav/+ control at 7, 14 and 28 days (Figure 17). The reduction in climbing ability of *Repo>tAβ42* positive control flies was significant at ages 7 to 28 days compared to *Elav/+* control. Glial expression of *RNAi* for *Kdm2* caused no significant change in climbing ability compared to *Elav/+* at all ages (Figure 17a).

Glial expression of *cv-c RNAi* caused a small reduction in climbing ability at all ages, but this was non-significant when compared to the *Elav/+* control in a two-way ANOVA (Figure 17).

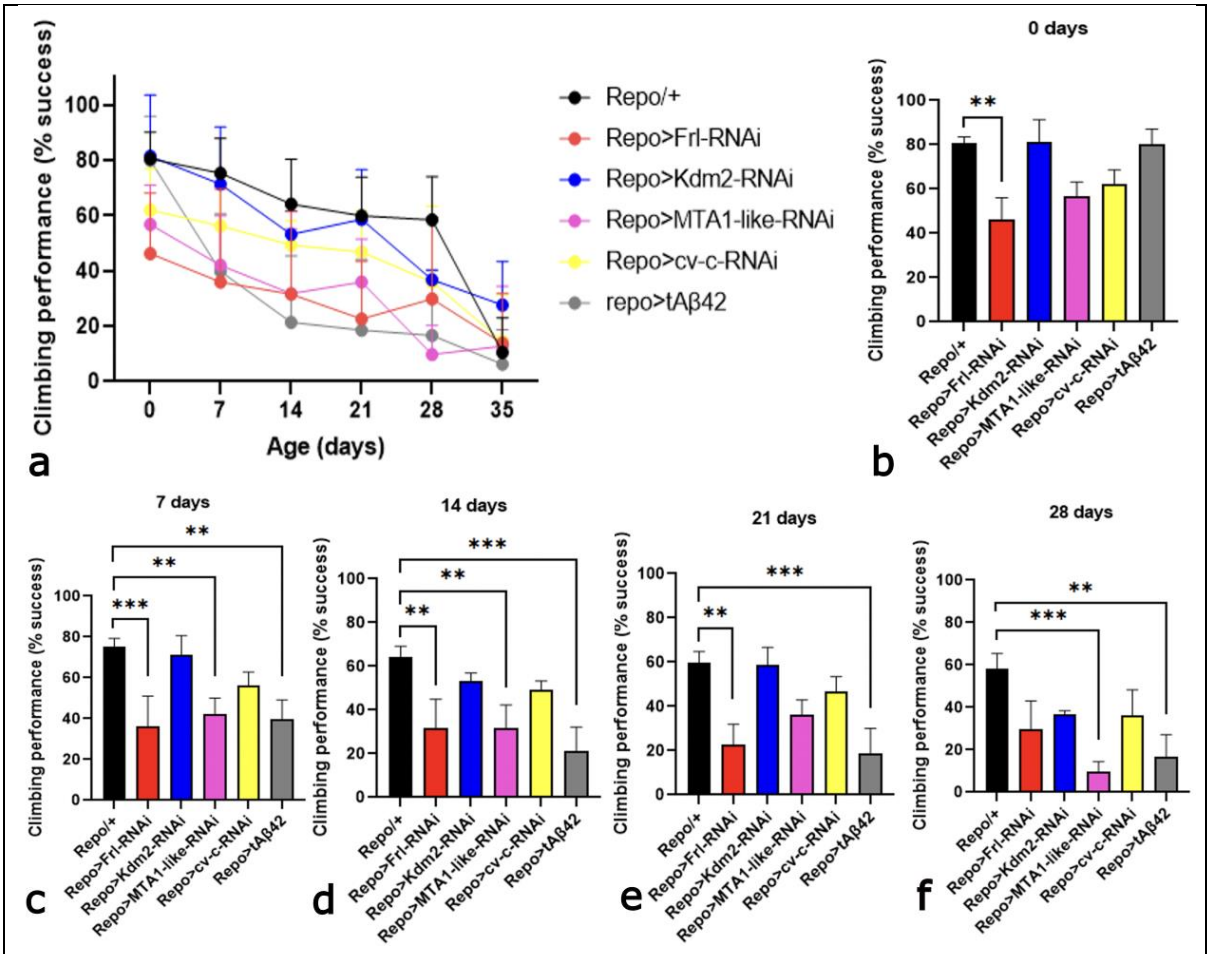

Figure 17: Glial knockdown of *Frl* and *MTA1-like* decreased climbing ability.

The *Repo-GAL4* driver was used to knockdown candidate genes in glial cells. The negative geotaxis response was measured as average percentage success during aging. Flies reared and tested at 22°C, 12hr LD cycle. (a) All flies exhibited age-dependent decline in climbing performance. Climbing performance at 0 (b), 7 (c), 14 (d) and 21 days (e) post-eclosion. Two-way ANOVA, Dunnett's post hoc. All error bars are mean ± SEM. N≥50 flies for all genotypes except *Repo>tAβ42* at day 35 due to premature death. *P<0.05, **P<0.01, ***P<0.001.

3.4 Knockdown of candidate genes in neurons and glia affected lifespan

The prognosis of AD generally includes survival of 3 to 12 years from diagnosis [8]. This is easily modelled in Drosophila by measuring their lifespan. Typically, the

lifespan of healthy flies is approximately 80 days [171], however, overexpression of tau and amyloid β isoforms cause a reduction in lifespan of flies [68, 172]. To measure lifespan, mated female flies are collected into vials of 10 flies, flipped into fresh food every 3-4 days and the number of dead flies counted [74]. Survival curves (Figures 18-22) were plotted and analysed using a log-rank test.

Pan-neuronal overexpression of tAβ42 consistently caused a decrease in median survival compared to the *Elav/+* control median survival (Figures 18-21). Expression of *Ppt2 RNAi* caused a median survival of 50 days, which was significantly shorter than the Elav/+ control median survival of 63 days. Pan-neuronal expression of *RNAi* for *Scr* and *CG6984* did not cause a change in lifespan (Figure 18). Expression of *Kdm2* and *MTA1-like RNAi* in neurons caused no change in median survival or survival curves (Figure 19). However, expression of *RNAi* for *Klp31E*, *AdamTS-A*, *cv-c* and *Frl* increased median survival compared to the *Elav/+* control (Figure 19b).

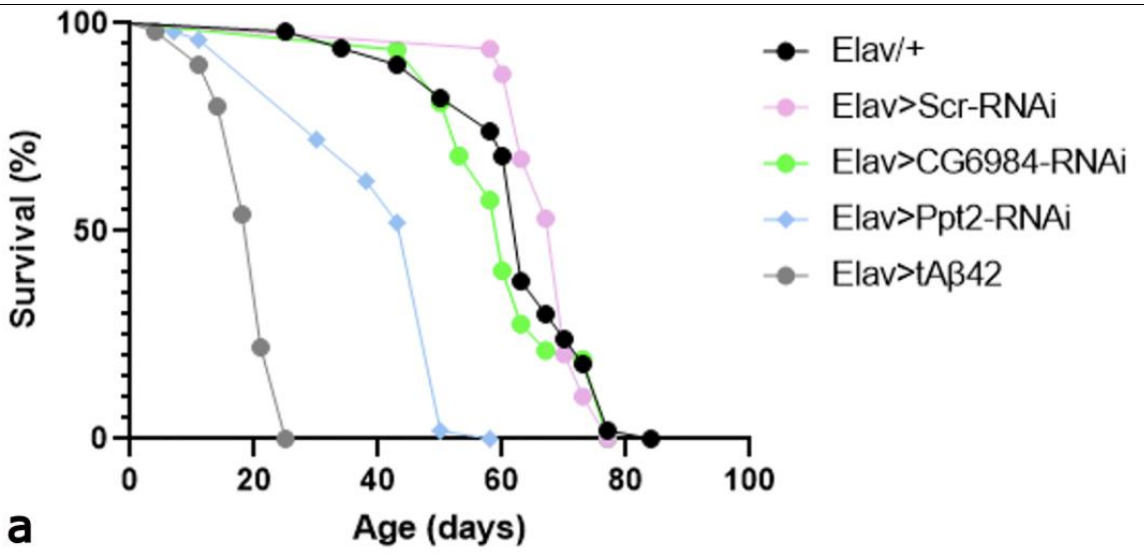

a

b

Genotype	Median survival (days)	Significance level
Elav/+	63	
Elav>Ppt2-RNAi	50	****
Elav>Scr-RNAi	70	ns
Elav>CG6984-RNAi	60	ns
Elav>tAβ42	21	****

Figure 18: Pan-neuronal expression of *Ppt2 RNAi* significantly reduced lifespan.

Pan-neuronal overexpression of tAβ42 significantly reduced lifespan. Mated female flies were flipped into fresh food vials every 3-4 days and the number of dead flies counted. (a) Survival curves for all genotypes. (b) Median survival and significance level compared to Elav/+ WT control. Data analysed in a log rank survival analysis in Prism. ****P<0.0001

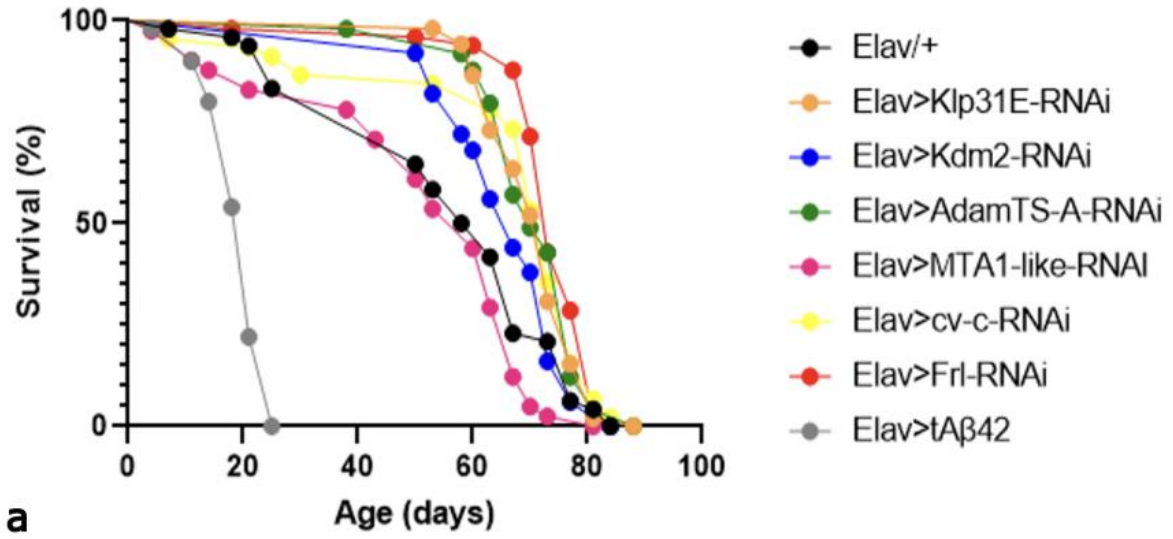

a

b

Genotype	Median survival (days)	Significance level
Elav/+	60.5	
Elav>Klp31E-RNAi	73	**
Elav>Kdm2-RNAi	67	ns
Elav>AdamTS-A-RNAi	70	***
Elav>MTA1-like-RNAi	60	ns
Elav>cv-c-RNAi	73	**
Elav>Frl-RNAi	73	****
Elav>tAβ42	21	****

Figure 19: Pan-neuronal expression of *RNAi* for *Klp31E, AdamTS-A, cv*-c and *Frl* affected the lifespan of flies.

Mated female flies were flipped into fresh food vials every 3-4 days and the number of dead flies counted. (a) Survival curves for all genotypes. (b) Median survival and significance level compared to *Elav/+* control. Data analysed in a log rank survival analysis in Prism. **P<0.01, ****P<0.0001

Glial cells, and particularly microglia, have been reported to perform both neuroprotective and neurotoxic functions in AD [40]. Although their functions are not yet well defined, glial cells in *Drosophila* have some similar subtypes and functions to human glial cells, including astrocyte-like glia and ensheathing glia [170]. Cortex glia

envelope cell bodies of neurons in the cortex [173] and ensheathing glia can also enwrap neuropils and phagocytose neuronal debris after axonal injury [174]. Loss of Draper, the glial engulfment receptor in ensheathing glia, exacerbated the Aβ42^{arc}-induced decrease in lifespan in *Drosophila* [175], indicating that these cells are involved in Aβ42 clearance. As glial cells have a major function in AD, the *Repo-GAL4* driver was used to test whether knockdown of candidate genes in glial cells can cause premature death. *RNAi* for candidate genes was expressed in glia using the Repo-*GAL4* driver, and the lifespan of these flies assessed in a longevity assay (Figures 20 and 21). Glial overexpression of tAβ42 caused a significant reduction in lifespan compared to the Repo/+ wild-type control in both longevity assays (log rank test, $P<0.0001$). Glial expression of *CG6984* and *Klp31E RNAi* caused no change in median survival or survival curves (Figure 20). Glial expression of *Ppt2 RNAi* caused a small reduction in median survival ($P<0.05$). Glial expression of *Kuz RNAi* resulted in a median survival of 67 days, which was the same as the *Repo/+* control, but there was a small difference between the survival curves of these genotypes ($P<0.05$). Glial expression of *Scr RNAi* caused an increase in median survival compared to the *Repo/+* control ($P<0.0001$). Glial expression of *cv-c*, *Frl* and *MTA1-like RNAi* caused no change in median survival or survival curves (Figure 21). However, glial expression of *Kdm2 RNAi* caused a small decrease in median survival (log rank test, $P<0.05$).

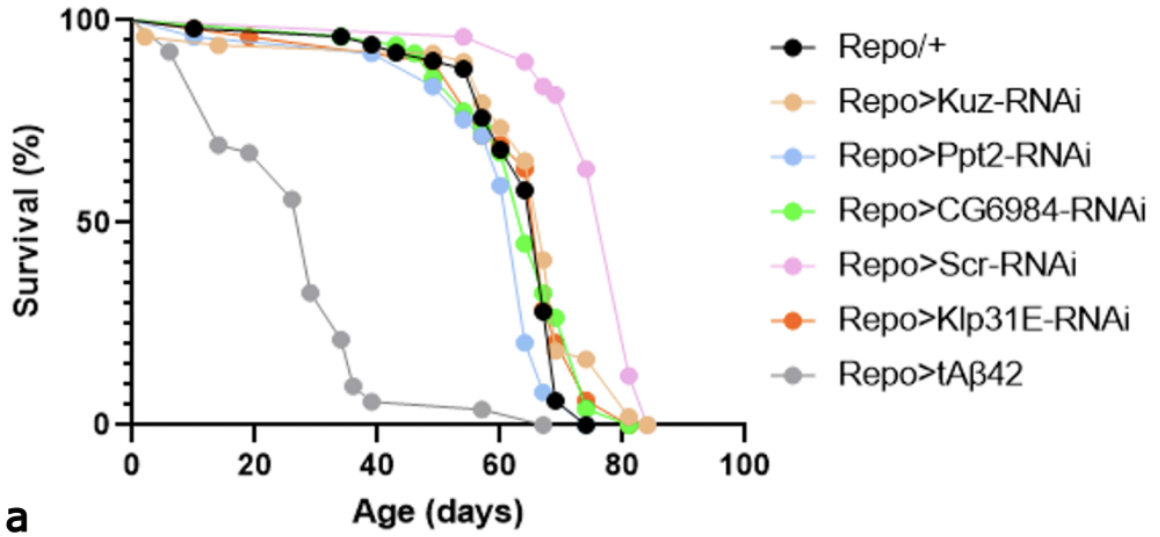

a

b

Genotype	Median survival (days)	Significance level
Repo/+	67	
Repo>Kuz-RNAi	67	ns
Repo>Ppt2-RNAi	64	*
Repo>CG6984-RNAi	64	ns
Repo>Scr-RNAi	81	****
Repo>Klp31E-RNAi	67	ns
Repo>tAβ42	29	****

Figure 20: Glial expression of *RNAi* for *Kuz*, *Ppt2*, and *Scr* affected lifespan.

Mated female flies were flipped into fresh food vials every 3-4 days and the number of dead flies counted. (a) Survival curves for all genotypes. (b) Median survival and significance level compared to Repo/+ WT control. Data analysed in a log rank survival analysis in Prism. *P<0.05, ****P<0.0001

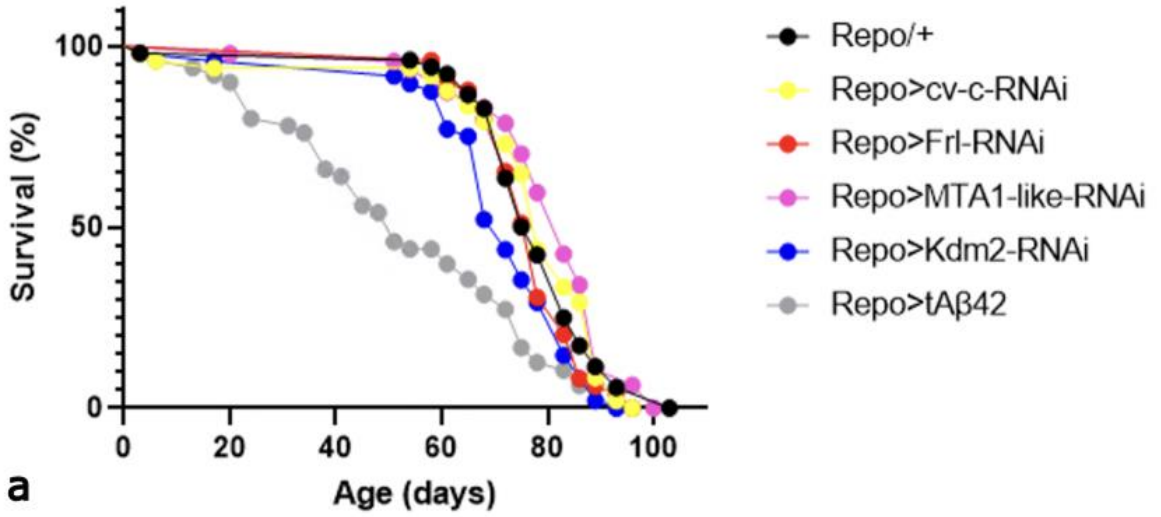

a

b

Genotype	Median survival (days)	Significance level
Repo/+	76.5	
Repo>cv-c-RNAi	78	ns
Repo>Frl-RNAi	78	ns
Repo>MTA1-like-RNAi	83	ns
Repo>Kdm2-RNAi	72	*
Repo>tAβ42	51	****

Figure 21: Glial expression of *Kdm2 RNAi* caused a small reduction in lifespan.

Mated female flies were flipped into fresh food vials every 3-4 days and the number of dead flies counted. (a) Survival curves for all genotypes. (b) Median survival and significance level compared to *Repo/+* control. Data analysed in a log rank survival analysis in Prism. *P<0.05, ****P<0.0001

The gene *Ctl2* (fly orthologue of *SLC44A2*) caused lethality when knocked down in neurons and glia, so a longevity assay run using the *Elav-GAL4* driver was not possible. Therefore, the *GAL80ts-Elav-GAL4* driver was used to drive pan-neuronal expression of *Ctl2 RNAi* only in adulthood without causing developmental lethality, by changing the temperature from 18°C to 29°C following eclosion to prevent *GAL80ts* block of Elav-*GAL4* transcriptional activation. Flies were kept at 29°C and flipped into fresh food vials every 2-3 days and the number of dead flies counted. These results are presented in Figure 22. Pan-neuronal knockdown of *Ctl2* restricted to adulthood caused a reduction in median lifespan to 3 days, significantly shorter than both the *Gal80ts-Elav-GAL4/+* and *Ctl2-RNAi/+* controls (log-rank test, P<0.0001). However, the *Ctl2-RNAi/+* control median survival was significantly shorter than the *Gal80ts-Elav/+* control.

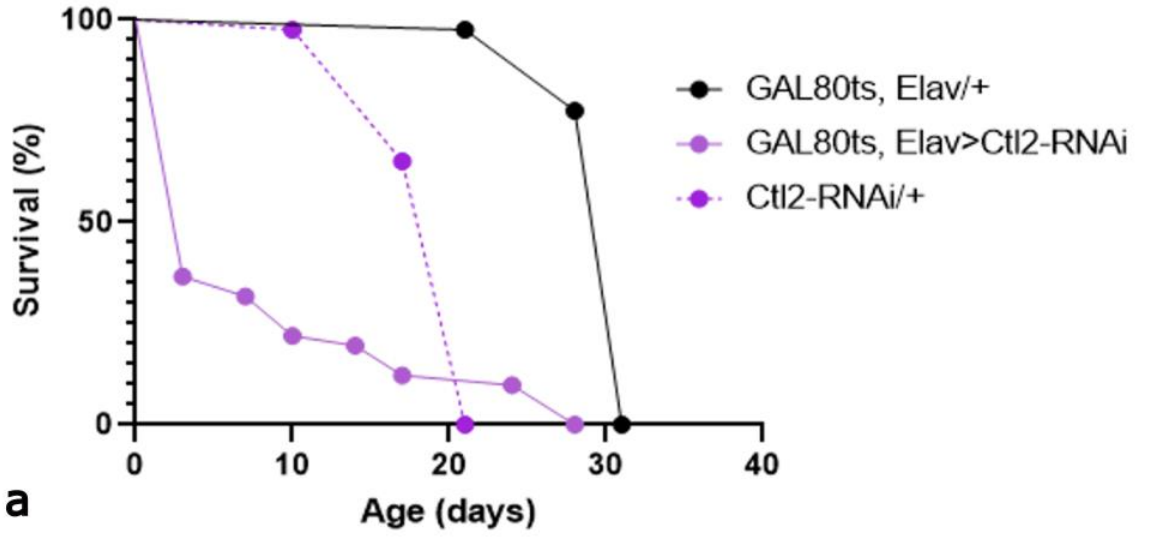

b

Genotype	Median survival (days)	Significance level
GAL80ts-Elav/+	31	
Ctl2-RNAi/+	21	****
GAL80ts-Elav>Ctl2-RNAi	3	****

Figure 22: Pan-neuronal knockdown of *Ctl2* in adult flies significantly reduced lifespan.

Mated female flies were flipped into fresh food vials every 2-3 days and the number of dead flies counted. (a) Survival curves for all genotypes. (b) Median survival and significance level compared to *Gal80ts-Elav/+* WT control. N = 40 flies per genotype. Data analysed in a log rank survival analysis in Prism. ****P<0.0001

3.5 Knockdown of Ctl2 in mushroom body neurons reduced 1-hr memory

Memory loss, including semantic and episodic memory, is usually one of the first symptoms to occur in AD patients [176]. Multiple assays exist in *Drosophila* to assess memory, but the most commonly used is the olfactory shock aversive conditioning assay [75, 177], which is a form of classical conditioning that involves exposing flies to an odour paired with a shock (CS+) and an odour with no shock (CS-), to allow learned association between the paired odour and the aversive shock (Figure 6). The time between training (odour presentation) and testing (choice chamber) can be changed depending on the type of memory being tested. Immediate testing is used to assess learning, or memory acquisition [178], an

interval of 3 minutes is often used to test short term memory, whereas an interval of 1 to a few hours is typically used for assessment of mid-term memory [179]. Long-term memory is usually tested using spaced learning protocols as it is a form of consolidated memory [180]. Aging has been shown to specifically impair 1-hour memory in *Drosophila* [181, 182]. Additionally, 1-hour memory performance is significantly reduced by overexpression of tau-0N4R and Aβ42 in *Drosophila* [68], so 1-hour memory was used in this project to detect AD-associated memory defects due to candidate gene knockdown.

The mushroom body is responsible for olfactory learning via odour representation [183]. Simultaneous arrival of aversive dopaminergic neuron input (from the unconditioned shock stimulus) and projection neuron activation of mushroom body Kenyon cells (from the conditioned odour stimulus) strengthens Kenyon cell synapses onto mushroom body output neurons (MBONs), which lead to avoidance of the odour [179, 183]. The *OK107-GAL4* driver was used to express candidate gene *RNAi* in the mushroom body. 3-5 day-old flies were tested in a 1-hour olfactory shock aversive conditioning assay as described above [75] and performance index calculated as a measure of avoidance of the conditioned stimulus (shock odour). Overexpression of Tau-0N4R in the mushroom body caused a 0.2 decrease in performance index, but this was non-significant when tested in a one-way ANOVA with Dunnett's post-hoc. However, mushroom body knockdown of Ctl2 caused a 0.35 reduction in performance index ($P<0.05$). The performance index of *OK107>Scr-RNAi* and *OK107>Kuz-RNAi* flies was also decreased, but this was non-significant when tested in a one-way ANOVA (Figure 23).

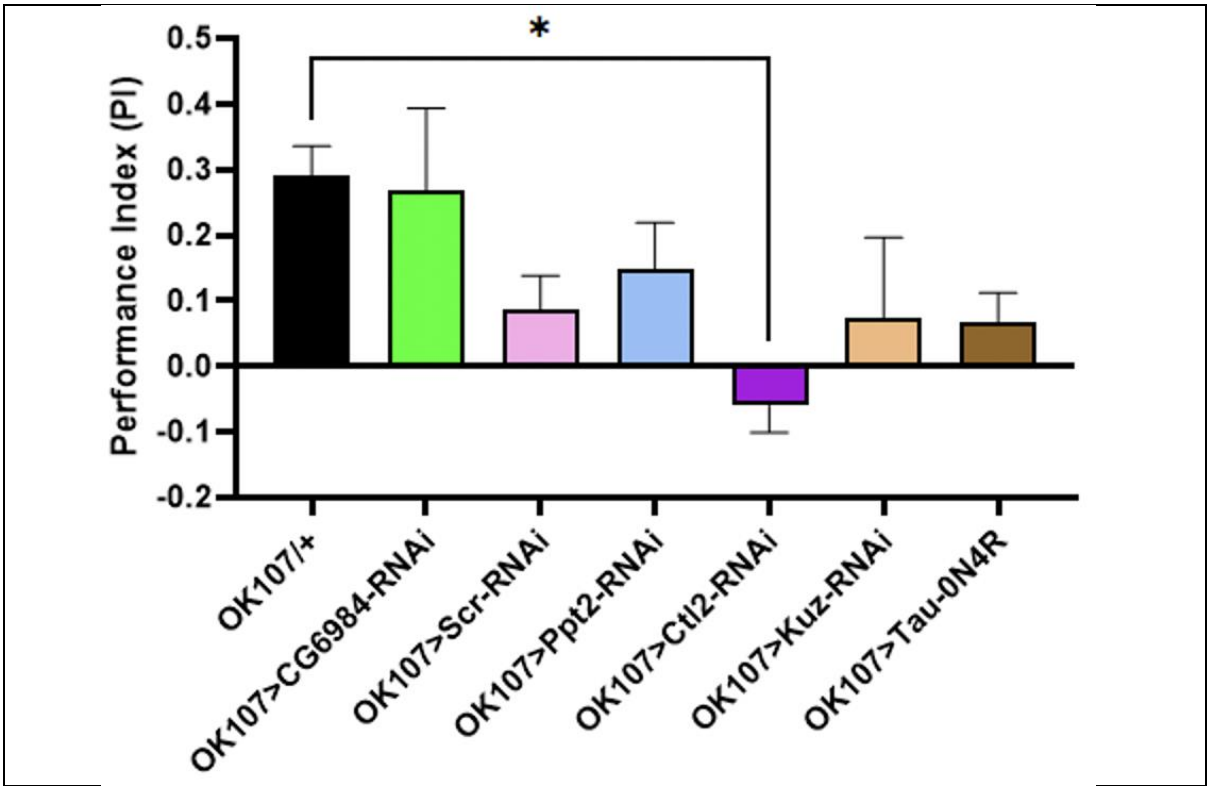

Figure 23: Knockdown of *Ctl2* in the mushroom body in Drosophila reduced 1-hour memory performance in the olfactory shock assay.

Flies were exposed to one odour (MCH or OCT) paired with a 1.5 second 60V shock every 5 seconds for a minute, and one odour with no shock. 1 hour after training, flies were put in a choice chamber and the performance index calculated as (number of flies avoiding shock odour/number of flies not avoiding shock odour)/total flies. (a) Performance index of candidate genes in the olfactory shock assay. N = 3 experiments, 20-60 flies per experiment. One-way ANOVA, Dunnett's post-hoc. All error bars are mean ± SEM. *P<0.05

3.6 Knockdown of candidate genes in clock cells affected sleep and circadian activity

Sleep and circadian rhythm disruption affects approximately 25% of AD patients and correlates with cognitive decline, including attention deficits and aggressiveness [4, 184]. AD patients have more pronounced sleep loss and sleep fragmentation than aging individuals and disrupted activity cycles with increased activity at night [185]. A bidirectional relationship between sleep and circadian rhythm disruption and AD exists, as sleep disruption is likely a result of neurodegeneration but may also

contribute to accelerated cognitive decline [186]. As sleep and circadian rhythm disturbance is reciprocally involved in AD pathology, I investigated whether knockdown of AD candidate gene orthologues in clock cells caused changes in the sleep and circadian rhythms of flies. Sleep and circadian rhythms are disrupted in aging flies [187], and overexpression of human amyloid β and tau proteins in clock cells has previously been shown to cause sleep and circadian rhythm disruption [79, 188]. I used the *Tim-GAL4* driver to express candidate gene *RNAi* in all clock cells, which includes 150 neurons in the fly brain [189]. This driver was cantonised, meaning it was backcrossed to csw- flies for 3 generations to control for genetic background effects, as this fly line had been used in the lab for many years and therefore may have acquired mutations in sleep-related genes. I used the *Drosophila* activity monitor (DAM) system [76], to measure activity and sleep of 3-5-day-old flies in a standard 12-hr LD cycle, and circadian behaviour (including period length and rhythmicity) in a DD cycle.

Flies overexpressing tAβ42 and Tau-0N4R had were hyperactive at night (Figures 24 and 25). *Tim>tAβ42* flies also slept less at night (P<0.0001). Expression of *RNAi* for *Scr*, *CG6984*, *Ppt2* and *Kuz* caused no change in amount of activity, sleep or circadian behaviour compared to *Tim*/+ or *RNAi*/+ controls (Figure 24). However, expression of *Kdm2 RNAi* caused an increase in night-time activity (P<0.0001) and decrease in night-time total sleep (P<0.0001, Figure 25). *Tim*>cv-c-*RNAi* flies also had a small decrease in night-Time total sleep (P<0.05) and increase in night-time activity (P<0.05, Figure 25). Although *Tim*>cv-c-*RNAi* flies had no change in rhythmicity statistic, cv-c-*RNAi*/+ flies had a decrease in rhythmicity statistic (P<0.05). *Tim*>Frl-*RNAi* flies were hyperactive (P<0.0001) and slept less (P<0.01) only during the day (Figure 25a and b). *Tim*>Frl-*RNAi* flies also had a rhythmicity statistic of 1.23 (Figure 25d), which was significantly lower than *Tim*/+ and Frl/+ control flies and classed as arrhythmic. Expression of *RNAi* for *MTA1-like* and *Klp31E* did not cause changes in sleep and circadian rhythms (Figure 25).

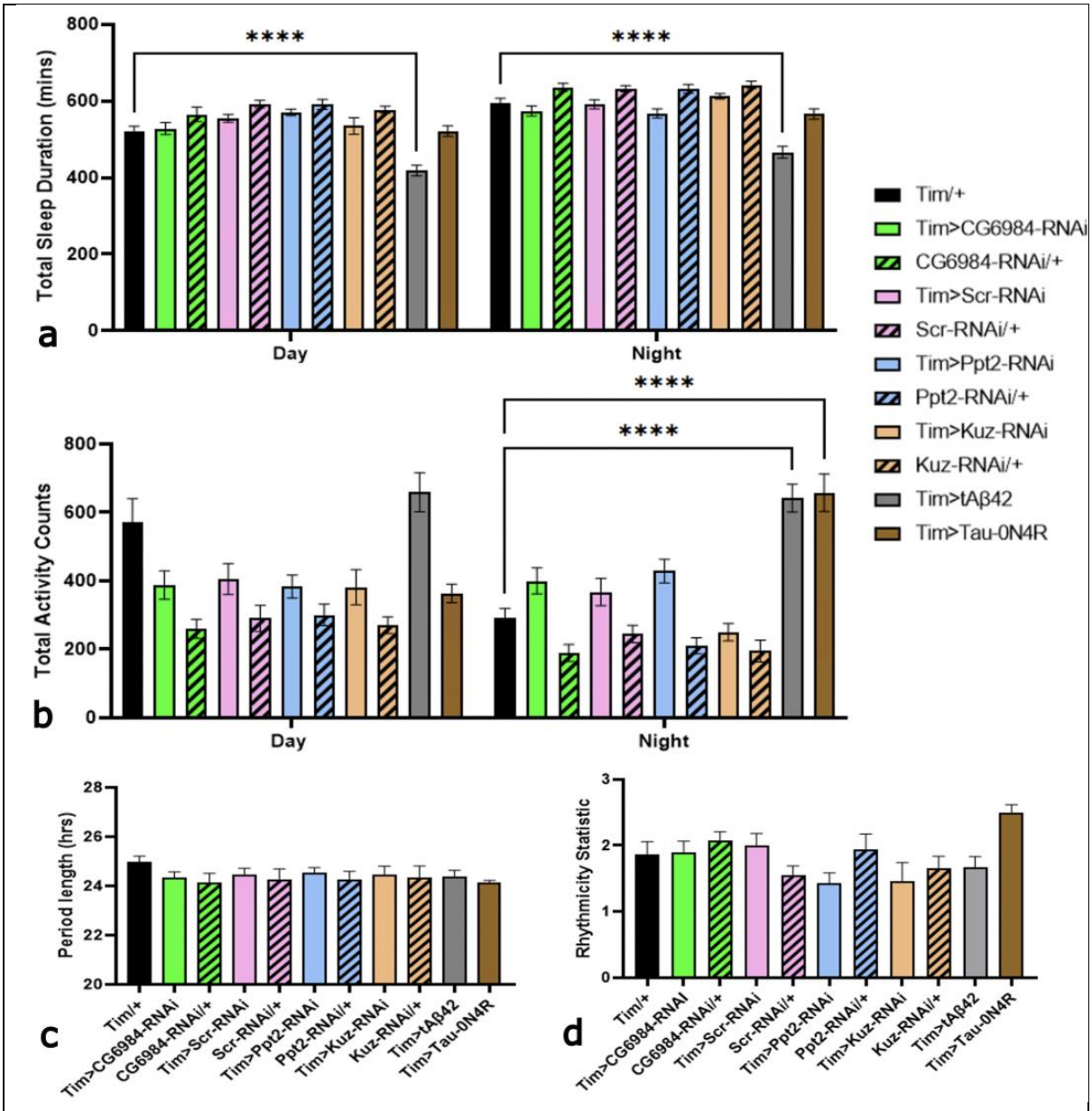

Figure 24: Overexpression of human Tau-0N4R and tAB42 increased total activity at night and decreased total sleep at night.

Expression of candidate gene *RNAi* did not cause a change in total activity, total sleep, period length and rhythmicity of flies. *Tim-GAL4* was used to express candidate gene *RNAi* in clock cells. (a) Total sleep duration in the day (first 12-hr bin) and night (second 12-hr bin). (b) Total activity counts (beam crosses) during the day and night. (c) Circadian period length in hours. (d) Rhythmicity statistic, flies with <1.5 are considered arrhythmic. Total activity counts and total sleep duration were analysed in a two-way ANOVA, with Dunnett's post hoc for multiple comparisons. Period length and rhythmicity statistic were analysed in a one-way ANOVA with Dunnett's post hoc for multiple comparisons. All error bars are mean ± SEM. ****P<0.0001.

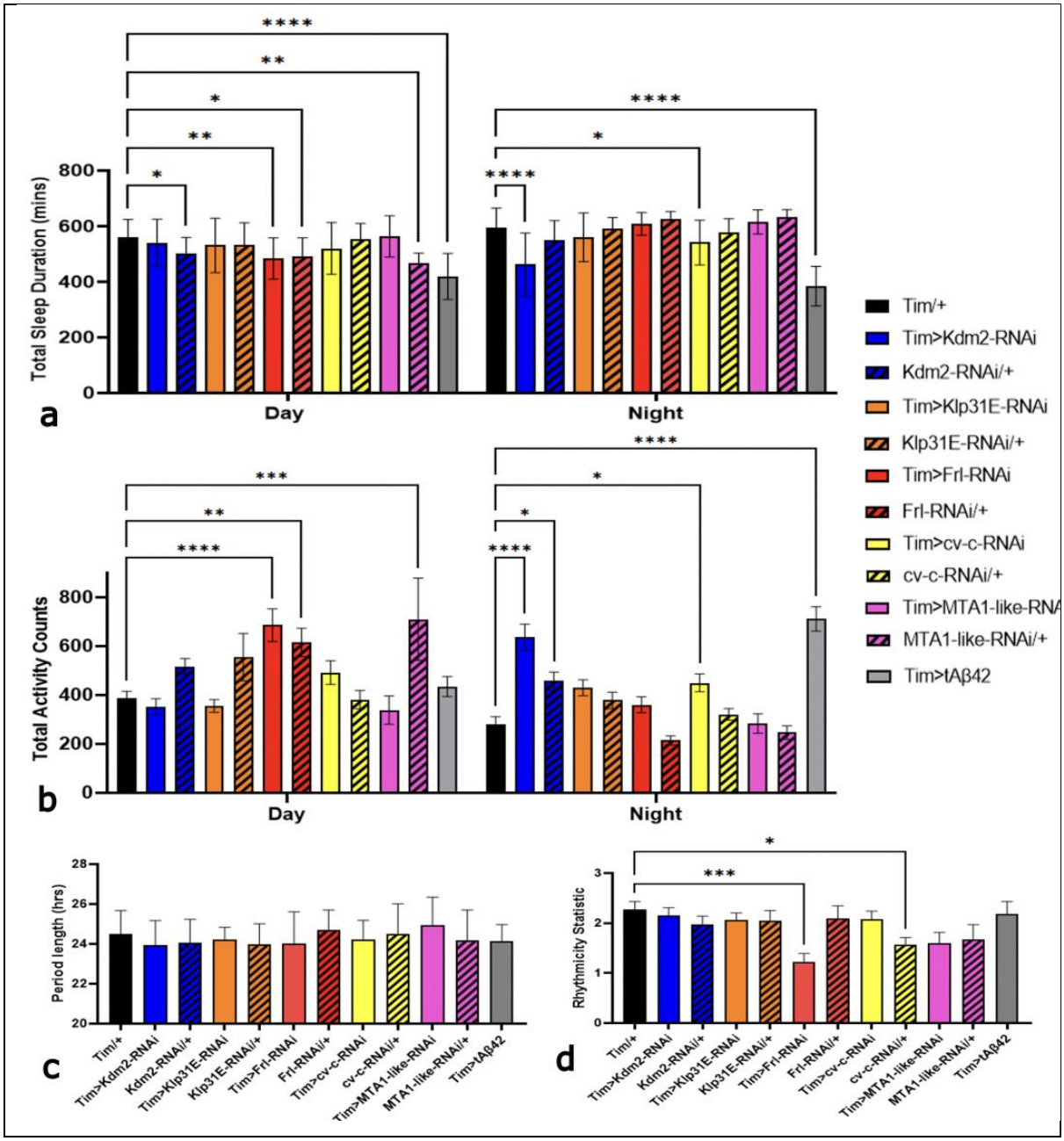
a
Total Sleep Duration (mins)
Day
Night
b
Total Activity Counts
Day
Night
Tim/+
Tim>Kdm2-RNAi
Kdm2-RNAi/+
Tim>Klp31E-RNAi
Klp31E-RNAi/+
Tim>Frl-RNAi
Frl-RNAi/+
Tim>cv-c-RNAi
cv-c-RNAi/+
Tim>MTA1-like-RNA
MTA1-like-RNAi/+
Tim>tAβ42
c
Period length (hrs)
d
Rhythmicity Statistic

Figure 25: Expression of candidate gene *RNAi* affected activity, sleep and circadian rhythmicity and period length.

Tim-GAL4 was used to express candidate gene *RNAi* in clock cells. (a) Total sleep duration in the day (first 12-hr bin) and night (second 12-hr bin). (b) Total activity counts (beam crosses) during the day and night. (c) Circadian period length in hours. (d) Rhythmicity statistic, flies with <1.5 are considered arrhythmic. Total activity counts and total sleep duration were analysed in a two-way ANOVA, with Dunnett's post hoc for multiple comparisons. Period length and rhythmicity statistic were analysed in a one-way ANOVA with Dunnett's post hoc for multiple comparisons. All error bars are mean ± SEM. *P<0.05, **P<0.01, ***P<0.001, ****P<0.0001.

Interestingly, knockdown of *Ctl2* in clock cells using the *Tim-GAL4* caused developmental lethality. Therefore, no sleep and circadian rhythm data was collected for *Tim>Ctl2* flies. Instead, other sleep-related, and clock cell-specific drivers were used to characterise the effect of *Ctl2* knockdown on sleep and circadian rhythms. These included a DN1 neuron-specific driver, *Clk4.1M-GAL4*, *TH-GAL4*, a dopamine neuron driver, and *PDF-GAL4*, a driver for PDF neurons. DN1 neurons are a subset of clock neurons in the fly brain referred to as sleep-promoting cells [190]. In *Drosophila*, *Ctl2* is highly expressed in DN1 cells at 1 and 9 days of age (Appendix Figure 1), so this driver was used to determine whether these cells are involved in the observed lethality. PDF is a neuropeptide only expressed in large and small LNv clock neurons which function in regulation of rest-activity rhythms in constant darkness [191]. The *PDF-GAL4* driver therefore does not drive overlapping expression with the *Clk4.1M-GAL4* driver and was also therefore chosen to characterise the effect of Ctl2 knockdown on sleep and circadian rhythms. As *Ctl2* is also a Parkinson's disease GWAS hit [123], and dopamine is involved in sleep regulation[192], the *TH-GAL4* dopaminergic driver was used to assess whether knockdown of Ctl2 in dopamine neurons affected sleep. Knockdown of Ctl2 in PDF neurons caused no changes to sleep or total activity of flies, but decreased the rhythmicity statistic (P<0.05, Figure 26a). Knockdown of *Ctl2* in dopaminergic neurons using the *TH-GAL4* driver caused a decrease in total activity and increase in total sleep in the night and day (Figure 26a and b), as well as a decrease in rhythmicity statistic (Figure 26c) and increase in sleep episode frequency at night (Figure 26e). *Ctl2* knockdown in DN1 neurons using the *Clk4.1M-GAL4* driver

caused a decrease in night-time activity (P<0.001, Figure 26a) and increase in total sleep duration in the day and night (Figure 26b). *Clk4.1M>Ctl2-RNAi* flies also had a decreased rhythmicity statistic (Figure 26c). Interestingly, very few *Clk4.1M>Ctl2-RNAi* flies eclosed from each cross, indicating partial lethality.

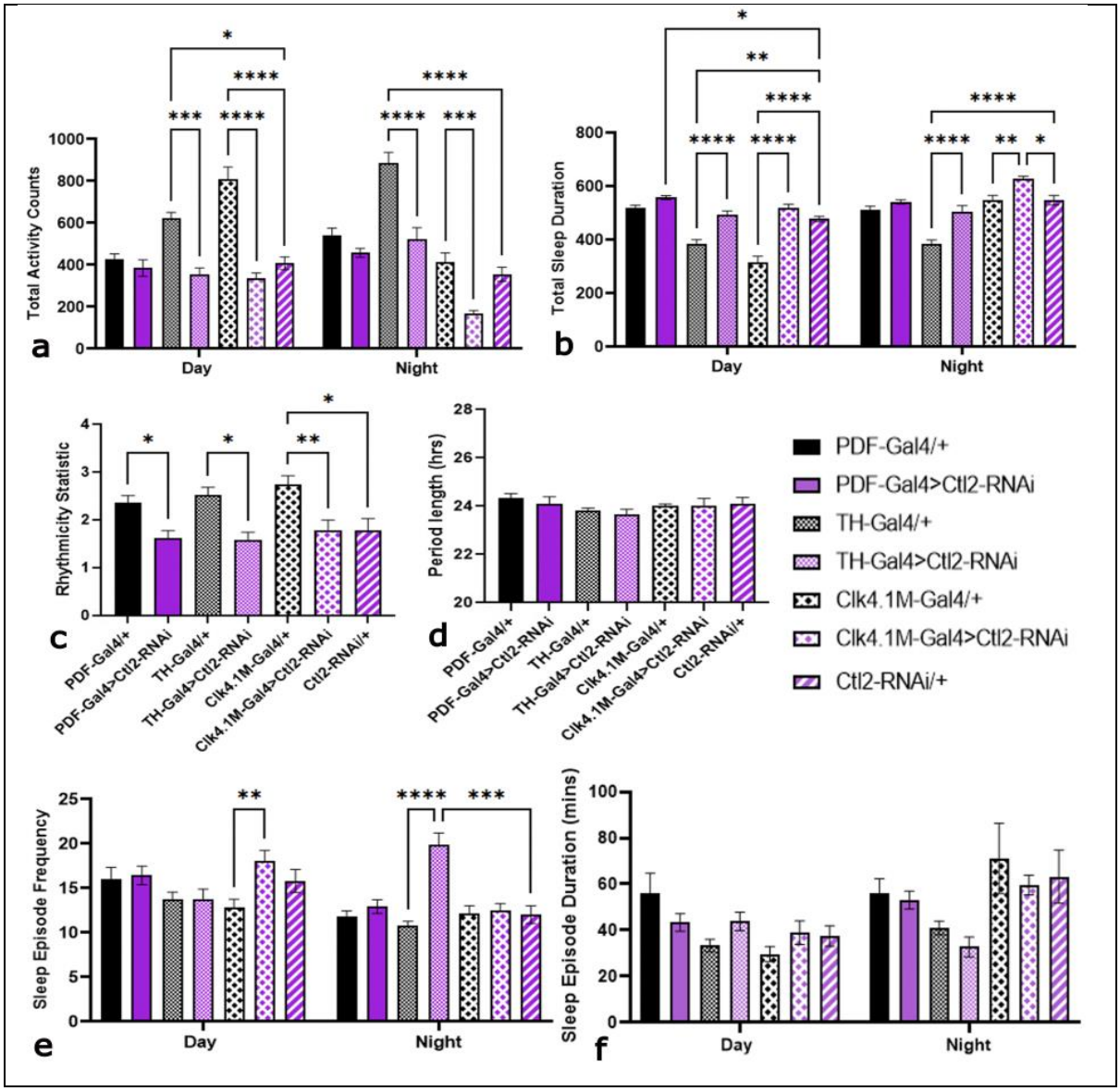

Figure 26: Knockdown of Ctl2 in PDF neurons, dopamine neurons, and DN1 neurons caused changed in sleep and circadian rhythmicity.

The PDF-*GAL4* driver was used to knock down *Ctl2* in PDF neurons, the TH-*GAL4* drivers was used to knockdown *Ctl2* in dopamine neurons and the Clk4.1M-*GAL4* driver was used to knockdown *Ctl2* in DN1 neurons. Ctl2-*RNAi*/+ is *UAS* control. (a) Total activity counts (beam crosses) in the day and night. (b) Total sleep duration in minutes in the day and night. (c) Rhythmicity statistic, <1.5 is considered arrhythmic. (d) Period length in hours. (e) Mean sleep episode frequency in the day and night. (f) Mean sleep episode duration in minutes in the day and night. Total activity counts, total sleep duration, sleep episode frequency and sleep episode duration analysed in a two-way ANOVA with Tukey post hoc test for multiple comparisons. Rhythmicity statistic and period length analyses in a one-way ANOVA with Tukey post hoc. All error bars are mean ± SEM. *P<0.05, **P<0.01, ***P<0.001, ****P<0.0001. Significant differences between *GAL4*/+ controls not included.

3.7 Knockdown of *Ctl2* in the Johnston's organ did not affect courtship behaviour

Ctl2, the *Drosophila* orthologue of human *SLC44A2* (or *CTL2*), caused developmental lethality when knocked down in neurons, glia and clock cells using the *Elav*, *Repo* and *Tim-GAL4* drivers, indicating its importance in the *Drosophila* nervous system. *SLC44A2*, in addition to being an AD risk gene, has also been linked to autoimmune hearing loss as *CTL2* is a target for autoantibodies in the inner ear [122]. Hearing loss is also a risk factor for the development of AD [102]. In *Drosophila*, the Johnston's organ acts as a mechanoreceptor to enable hearing capable of sensing wing beating vibrations [193]. *Drosophila* courtship relies on females hearing these wing vibrations made by males [194]. Factors affecting courtship success, including hearing, can be assessed in a courtship assay [152], where a male and female fly of a specific genotype are placed in a mating wheel and observed to score mating behaviours and copulation success rates. This assay was used to collect preliminary data on the effect of *Ctl2* knockdown in the Johnston's organ on hearing, using courtship success as a proxy measure. The *JO-GAL4* driver was used to express two *RNAi* lines for *Ctl2* (*Ctl2-RNAi*-A, which has been used in all previous chapters, and *Ctl2-RNAi-B*, which was obtained for further *Ctl2*

screening). *JO>TNT-E* was used to express tetanus toxin in the Johnston's organ to silence Johnston's organ neurons [195], as a control to confirm that silencing of the Johnston's organ (and therefore impairing hearing) reduces courtship. Courtship pairs were observed for 15 minutes (900 seconds) and frequency of copulation (number of pairs successfully copulating), copulation latency (time taken to copulate from start of observation), wing song to copulation latency (time between first wing song and copulation) and wing song latency (time to wing song from start of observation) was scored. Pairs were assigned a latency of 900 seconds if no copulation occurred withing the allotted time.

Johnston's organ expression of tetanus toxin caused an ablation of successful courtship (Figure 27a, b and c). *Ctl2-RNAi-B/+* controls also showed a decreased successful copulation frequency (Figure 27a), but all other genotypes copulated within 900 seconds. Expression of *Ctl2 RNAi* did not affect wing-song to copulation latency (Figure 27c), but JO>Ctl2-*RNAi*-B and Ctl2-*RNAi*-B/+ flies had an increased wing-song latency (Figure 27d). Overexpression of tAβ42 in the Johnston's organ had no effect on courtship measures.

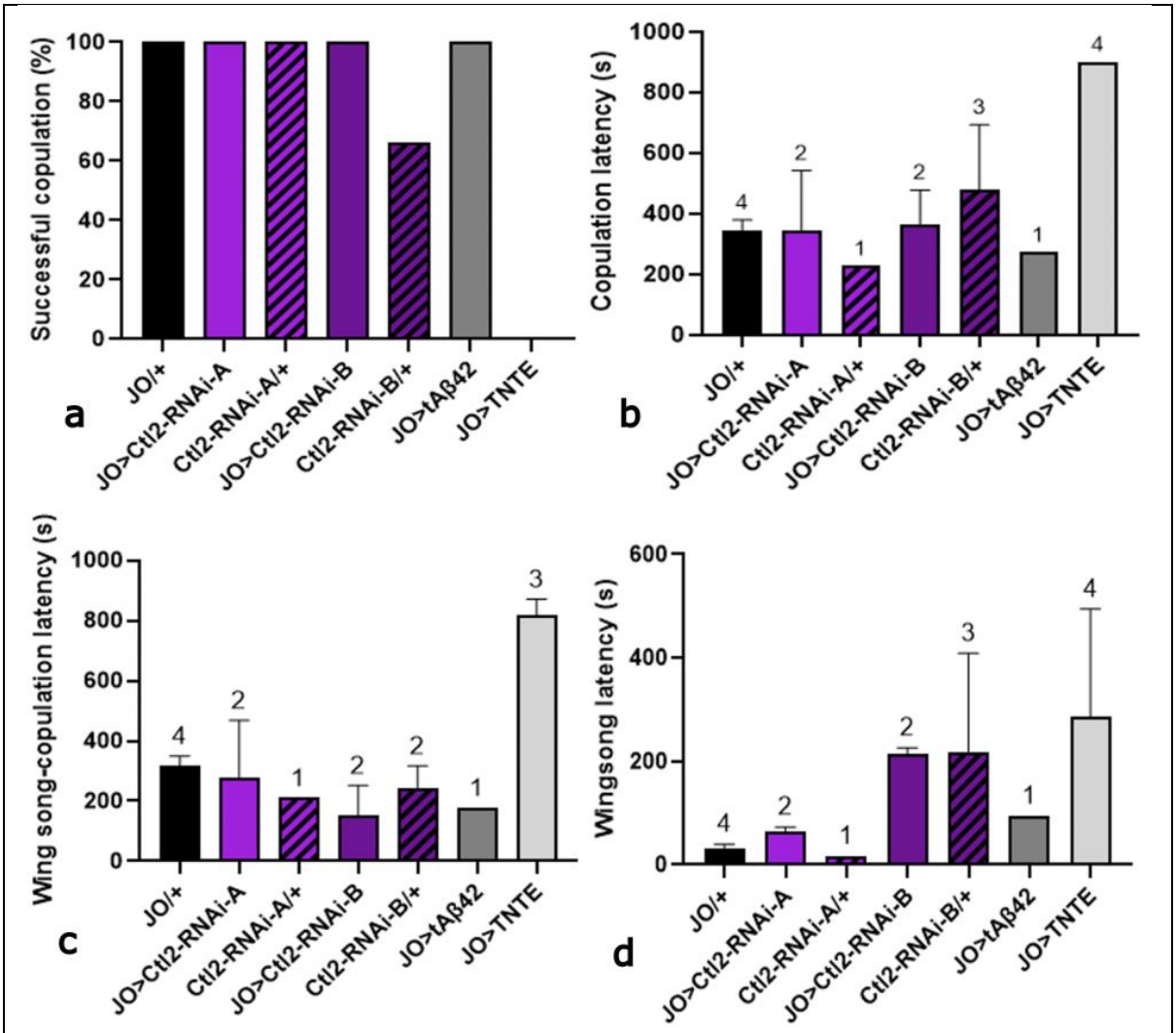

Figure 27: Expression of tetanus toxin in the Johnston's organ affected the rate of successful copulation and wing song-copulation latency.

Preliminary data from the courtship assay used to assess hearing. Pairs were assigned 900 s for the courtship behaviour or copulation latency if the behaviour did not occur within the time observed. (a) Percentage of pairs that successfully copulated. (b) Time from start of observation of copulation. (c) Time between wing song and copulation. (d) Time from start of observation to wing song. Number of pairs used for each genotype is annotated above the bars. All error bars are mean ± SEM. No statistical tests for differences were run as assumptions were not met due to the small sample sizes. Numbers above bars indicate the number of repeats (pairs of flies) for each genotype.

4 Discussion

This project aimed to screen *Drosophila* orthologues of Alzheimer's disease risk genes identified in GWAS and EWAS for AD-associated phenotypes arising due to their knockdown. AD pathology is complex and most drugs targeting Aβ plaque and tau tangle accumulation have been unsuccessful at halting disease progression in clinical trials, with some causing accelerated tau plaque burden and severe adverse effects [196]. As well as earlier and more accurate diagnosis, this indicates the need for exploration of other targets, primarily achieved through identification of risk loci in GWAS and EWAS. Based on an EWAS and a GWAS meta-analysis of LOAD [59, 60], 11 genes were screened in *Drosophila*, with results summarised in Table 9. Six genes induced AD-associated phenotypes in one or more assays when *RNAi* targeting them was expressed. These hits should be prioritised for further characterisation and are summarised in Table 10.

Table 9: Summary of statistically significant results by gene and experimental assay.

Upwards arrows indicate improvement of wild-type phenotype with targeted *RNAi* expression in relevant cell type, downwards arrows indicate impairment of wild-type phenotype, straight horizontal lines indicate no change, and N/A indicates that the assay was not used to test the corresponding gene (ie. due to lethality). Where multiple drivers were used for an assay (climbing and longevity), the cell type is indicated. Where multiple abnormal phenotypes can occur in an assay (sleep and circadian rhythms), the effect of RNAi expression is specified. Developmental lethality is not indicated in the table but occurred with *RNAi* expression against *Kuz* in neurons and *Ctl2* in neurons, glia, and clock cells.

Gene	Eye neuro-degeneration Assay	Climbing assay	Longevity assay	Memory assay	Sleep and circadian rhythms	Courtship assay
Ctl2 / SLC44A2	—	N/A	↓ (Neuronal)	↓	—	—
Kuz / ADAM10	—	↓ (Glial)	—	—	—	N/A
Ppt2 / PPT2	—	—	↓ (Neuronal)	—	—	N/A

Frl / FMNL1	—	↓ (Neuronal and glial)	↑ (Neuronal) ↓ (Glial)	N/A	↓ (Hyper-activity in day) (Reduced Rhythmicity)	N/A
MTA1-like / MTA3	—	↓ (Neuronal and glial)	—	N/A	—	N/A
Kdm2 / KDM2B	—	—	↓ (Glial)	N/A	↓ (Hyper-activity at night)	N/A
CG6984 / ECHDC3	—	↑ (Neuronal)	—	—	—	N/A
AdamTS-A / ADAMTS1	—	—	N/A	N/A	N/A	N/A
Scr / HOXA5	—	↑ (Neuronal)	↑ (Glial)	—	—	N/A
Klp31E / KIF21B	—	—	↑ (Neuronal)	N/A	—	N/A
Cv-c / STARD13	—	—	↑ (Neuronal)	N/A	↓ (Hyperactivity at night)	N/A

4.1 Experimental methods and project limitations

4.1.1 Bioinformatics and RT-qPCR

Due to time constraints, RT-qPCR was not run on all candidate genes showing AD-associated phenotypes, which should be used as a next step to validate the *RNAi*

line and confirm that AD-associated phenotypes were arising due to candidate gene knockdown. Additionally, *Elav>CG6984-RNAi* and Elav>*MTA1-like-RNAi* flies had increased mRNA levels of *CG6984* and *MTA1-like* (Figure 11a), which may be due to an inactive *RNAi* line. It is estimated that inactive *RNAi* lines constitute 15-40% of *RNAi* libraries [197], so it was expected that some lines would not cause mRNA knockdown. However, an increase in mRNA is unusual and may also be a result of an experimental error such as low primer specificity of *CG6984* and *MTA1-like* primers causing non-specific amplification. As significant behavioural phenotypes were observed when *MTA1-like-RNAi* was expressed in the nervous system, *MTA1-like* may have been knocked down despite its increased measured level of relative mRNA. However, use of *RNAi* can lead to off-target effects which may have induced the climbing phenotypes observed with MTA1-like. This would mean that the level of MTA1-like mRNA detected in RT-qPCR would not be reduced as RNAi-mediated knockdown of another gene, not measured using RT-qPCR, could have been responsible for the phenotypes observed. This indicates the importance of using a second RNAi line to confirm the effect of *RNAi* on the gene of interest. Repeats of RT-qPCR on *CG6984*, *MTA1-like* and *Scr* using alternative primers are also needed to confirm whether these *RNAi* lines are active and rule out issues with low primer specificity or off-target effects of *RNAi*.

4.1.2 Eye degeneration assay

In this project, the eye neurodegenerative assay was used as an initial screen for neurodegeneration caused by candidate gene knockdown. In a previous project [198], this initial screen was used to select two candidate genes to take forward for further screening. In this project, no candidate genes caused a change in gross morphology or surface area of the eye when knocked down using the *GMR-GAL4* driver, which could be due to multiple factors. The *RNAi* line may be inactive, candidate genes may not be significantly involved in neuronal function or degeneration, or candidate genes may not be endogenously expressed in the developing eye, meaning no knockdown would have occurred. Alternatively, whilst knockdown of candidate genes did not cause a change in the morphology of the eye or number of photoreceptors when observed using light microscopy, there may be more subtle changes to the ommatidia that could not be observed with light microscopy due to its low resolution and magnification compared to other

microscopy techniques, such as electron microscopy [166]. Electron microscopy has been successfully used to assess rhabdomere morphology in *Drosophila* ommatidia and the effect of overexpression of AD risk gene *BIN1* and its *Drosophila* orthologue on rhabdomere morphology and photoreceptor number [69]. This level of detail is not possible using light microscopy alone, so it is possible that candidate gene knockdown caused smaller changes to photoreceptor number or ommatidia arrangement that was not detected with light microscopy. However, it is rare for knockdown of a single gene alone to cause neurodegeneration, meaning this method could result in failure to detect AD-relevant candidate genes. Double mutant flies that overexpress human tAβ42 or tau, and *RNAi* for each candidate gene, could be used in a more sensitive screen to detect if candidate gene knockdown exacerbates the rough eye phenotype induced by tAβ42 or tau.

4.1.3 Negative geotaxis assay

Pan-neuronal expression of *Frl* and *MTA1-like RNAi* caused a reduction in climbing ability in both young and ageing flies, indicating that a reduction *Frl* and *MTA1-like* may have caused neurotoxicity. The *MTA1-like/+* controls showed similar climbing ability to the *Elav/+* controls, indicating that this this is an effect of *RNAi* expression, although RT-qPCR data only showed knockdown of Frl but no knockdown of *MTA1-like* mRNA levels (Figure 11). However, the *Frl/+* controls showed significantly reduced climbing ability compared to the *Elav/+* controls. This indicates that either the *UAS-Frl-RNAi* insertion is within a gene involved in locomotion and is therefore disrupting it, or the *UAS-Frl-RNAi* insertion is 'leaky', meaning it ubiquitously expresses a small amount of *RNAi* without the *GAL4* driver present, causing the lower level of locomotor behaviour disruption in Figure 7. As RT-qPCR experiments on *Elav>Frl-RNAi* showed decreased mRNA levels of *Frl* (Figure 11), it is more likely that the *UAS-Frl-RNAi* is leaky.

Additionally, aging, and premature death of some flies (particularly with overexpression of tAβ42) meant that a lower number of flies were tested at older ages, likely causing the results to become more variable and lose significance. This may have occurred in Figure 16 and 17, where the significance level of *Repo>tAβ42*

decreased or was non-significant at older ages, indicating the need for a larger starting number of flies used in climbing experiments.

Pan-neuronal and glial knockdown of *Ctl2* caused developmental lethality, meaning no climbing data was collected with this gene. However, additional data should include use of the dopaminergic neuron driver, *TH-GAL4* to test the effect of *Ctl2* knockdown in dopaminergic neurons on climbing ability. Additionally, the *GAL80ts, Elav-GAL4* driver, which includes a temperature-sensitive *GAL80* gene, acts as a negative regulator of *GAL4* at fly ambient body temperature when raised at 18°C [199]. An increase in temperature to 29°C or higher prevents *GAL80* binding to the *GAL4* activator and therefore allows the *GAL4* to drive tissue-specific expression of the desired gene [200]. *GAL80ts-* is therefore useful for driving expression of genes at specific timepoints, including post-developmental if a gene is vital and *RNAi* against it causes developmental lethality. Another climbing assay in *GAL80ts, Elav-GAL4/+* and *GAL80ts, Elav-GAL4>Ctl2* flies with *Ctl2* knockdown restricted to adulthood was attempted, but due to premature death of these flies (most died within 3 days), it was not possible to reliably test their negative geotaxis reflexes. Climbing assays using this driver to cause pan-neuronal *Kuz* knockdown was also attempted, but *GAL80ts, Elav-GAL4>Kuz* flies also did not survive for long enough.

Whilst the negative geotaxis assay is a useful screen for defects in the startle response, it does not pick up more subtle locomotor defects that may occur due to neurodegeneration-related processes [201]. When locomotor behaviour was observed during this assay, neuronal and glial knockdown of *Frl* and *MTA1-like* seemed to cause seizure-like activity which impaired the ability of flies to climb. However, there is no way of recording this given the method of data collection and analysis (percentage success). Other methods of measuring the negative geotactic response employ the use of video cameras as a more sensitive measure of age-dependent decline in motor performance or seizure activity [202, 203].

4.1.4 Longevity assay

As longevity of *Drosophila* is affected by many complex environmental and physiological factors [74, 204], there is some variation between survival curves of the

GAL4/+ control and *GAL4>tAβ42* genotypes (Figures 18-21). A key factor that affects *Drosophila* lifespan is temperature [205]. Typically, flies live to 80 days at 25°C [171], but lifespan increases at lower temperatures and decreases at higher temperatures due to the rate-of-living theory, as a higher metabolic rate causes a shorter lifespan [205]. Flies were kept at approximately 21°C for Figure 21 data collection due to an air conditioning issue, meaning the median survival of these flies was longer than that of the longevity assays run on other groups of candidate genes. This may have also affected the survival curve of the *Repo>tAβ42* flies, which had a decreased median survival, but similar maximum survival compared to the *Repo/+* control (Figure 21) unlike Figures 18-20. Conversely, the longevity assay in Figure 22 included use of the *GAL80ts* driver and was therefore run at 29°C to maintain *GAL4* expression, causing the *GAL80ts, Elav/+* control to have a shorter lifespan than *Elav/+* controls used in assays run at 25°C (Figures 18-20).

Genetic background and inbreeding of fly populations also affects longevity and the change in longevity as a result of temperature [206]. Fly lines used in these longevity assays were not cantonised so there may be differences between their genetic backgrounds that caused the small changes in lifespan observed in Figures 19-21, including mutations in longevity-related genes. Therefore, repeats of these experiments using cantonised *GAL4* and *UAS-RNAi* lines should be conducted for validation.

Due to time constraints, *UAS* controls were not run for most longevity experiments, which would have made this data more robust by confirming that premature death was due to expression of candidate gene *RNAi* and not insertion of the *UAS-RNAi* into a longevity-related gene. However, the *UAS* control (*Ctl2-RNAi/+*) in Figure 14 had a significantly shorter median survival time than the *GAL80ts, Elav/+* control ($P<0.0001$), but a significantly longer lifespan than *GAL80ts, Elav>Ctl2-RNAi* ($P<0.0001$). Although the mRNA level of *Ctl2* in *Ctl2-RNAi/+* flies was not tested, RT-qPCR on *Elav>Ctl2-RNAi* flies showed a decrease in mRNA, indicating that the *RNAi* line is active. Therefore, it is possible that the *UAS-Ctl2-RNAi* line is leaky, causing the *Ctl2-RNAi* to be expressed in the absence of the *GAL4* driver, which may have caused the decrease in lifespan in the *Ctl2-RNAi/+* control flies.

4.1.5 Memory assay

Memory is typically assessed in *Drosophila* using classical conditioning techniques, the most common of which is the aversive olfactory shock assay [75], used in this project. Whilst this is useful for screening candidate genes for involvement in cognitive decline in AD, it can be temperamental and requires stringent controls, and in-depth assessment of cognition and different memory types still requires more complex rodent models [72]. Previous experiments in *Drosophila* using the same Aβ and tau lines as the ones used in this project have also found some small differences between the severity of their phenotypes in each assay, including a more significant learning defect in *OK107>Tau* flies compared to *OK107>tAβ42* flies [207], which was why OK107>Tau flies were used as a positive control in the memory assay.

The performance index of *OK107/+* flies is generally 0.5-0.6 [75], higher than the 0.29 PI of *OK107/+* flies in Figure 15. Due to the complexity of the assay set up, there are multiple factors that could be causing this, including low or unequal airflow for odour delivery, low shock efficiency, and unbalanced odour avoidance (odour bias). Shock avoidance of *OK107/+* flies was 79.5% (Appendix Figure 3), which is within the expected range for the olfactory shock assay [67], so it is more likely that airflow and therefore delivery of the odour was disrupted or there was odour bias in OK107/+ flies (unbalanced odour avoidance).

Following collection of olfactory shock assay data (Figure 23), an equipment break meant that collection of further olfactory shock data was not possible due to a very low performance index of *OK107/+* control flies. As a result, *UAS* controls and sensory controls (including shock avoidance and odour avoidance) were not run to validate the memory deficit of *OK107>Ctl2-RNAi* flies in Figure 23. As previously mentioned, *UAS* controls are important to confirm that the memory deficit is caused by knockdown of the candidate gene and not random *UAS-RNAi* insertion into and disruption of a gene involved in olfactory memory [208]. Additionally, sensory controls including consistently high shock and odour avoidance in all genotypes is necessary to confirm that the memory defect is not a result of a sensory deficit [67]. Further experiments with these controls are needed to validate the memory defect in

OK107>Ctl2-RNAi flies, although the efficacy of the Ctl2-*RNAi* line in Ctl2 mRNA knockdown (Figure 11) increases confidence in this phenotype.

Although 1-hour memory is particularly affected by aging [181], flies tested were 3-5 days old and therefore young. This means age-related effects of candidate gene knockdown were not tested. Additionally, *OK107>Tau-0N4R* showed a decrease in memory that was non-significant, which may be due to the young age as well as the low performance index of *OK107/+* flies, as mushroom body overexpression of tau isoforms has been previously shown to significantly reduce memory [68].

4.1.6 Sleep and circadian rhythm assay

Multiple genes were identified to have AD-associated sleep and circadian phenotypes due to clock cell knockdown, including *Frl, MTA1-like, Kdm2* and *Ctl2*. However, sleep is particularly susceptible to genetic background effects [209, 210]. As only the *Tim-GAL4* driver line was cantonised, but none of the *RNAi* lines used or clock drivers used for *Ctl2* were, genetic background effects in these genotypes cannot be ruled out. This may explain why *UAS*/+ and *GAL4*/+ controls differ from each other in some graphs (Figure 16b and Figure 18). To validate these phenotypes, these DAM assays should be repeated with only cantonised fly lines. Initial data using a non-cantonised *Tim-GAL4* driver to knockdown *Scr, CG6984, Kuz* and *Ppt2* showed multiple AD-associated sleep and circadian phenotypes (Appendix Figure 4) which were not replicated using the cantonised *Tim-GAL4* driver (Figure 16), demonstrating the necessity for controlling the genetic background of flies in sleep assays. Additionally, only 16-32 flies were used for each genotype in these assays, whereas published papers on *Drosophila* circadian rhythms often use approximately 100 flies per genotype [67]. Therefore, more repeats of this assay with cantonised fly lines would increase confidence in the phenotypes observed.

Additionally, use of the *Tim-GAL4* driver to study sleep may be inappropriate. Whilst clock cells expressing *Tim* are involved in the circadian regulation of sleep, multiple non-clock cell neuronal populations in homeostatic regulation of sleep, including dopaminergic [192] and serotonergic inputs [211] inputs to the dorsal fan-shaped body (dFB) and regulation by the mushroom bodies [212]. Therefore, candidate

genes involved in sleep regulation expressed in these neurons would not have shown AD-associated phenotypes in Figures 16 and 17. For example, *cv-c* is a Rho-GTPase-activating protein that mediates the dFB response to sleep deprivation [138]. Although it didn't significantly affect sleep and circadian rhythms when knocked down in clock cells, it likely would have affected sleep if knocked down in dFB neurons. Therefore, the Elav-*GAL4* pan-neuronal driver may be advantageous to sleep analysis in future assays using the DAM system.

The flies that were used were young (3-5 days old), and therefore the interaction effects of aging and candidate gene knockdown on sleep were not studied. This was primarily due to time constraints but sleep and circadian rhythms in aging flies with candidate gene knockdown would be useful to determine whether candidate gene knockdown accelerates the effects of aging on sleep and circadian rhythms.

4.1.7 Hearing assay

As expected, *JO>TNT-E* ablated successful courtship, indicating that silencing of the Johnston's organ prevents females hearing the male wing song, causing them to reject copulation attempts. However, *TNT-E/+* controls were not used to rule out effects of *TNT-E* transgene insertion or 'leakiness' and therefore this ablation may also be partly due to low levels of ubiquitous *TNT-E* expression causing locomotor defects causing abnormal or delayed wing songs, as latency to wing song was increased in *JO>TNT-E* flies (Figure 27d). However, this still suggests that the courtship assay can detect hearing defects.

Interestingly, Johnston's organ overexpression of tAβ42 had no effect on courtship measures. It was expected that these flies would exhibit lower levels of copulation, but effects of tAβ42 overexpression in the Johnston's organ have not been previously published. The unaffected courtship behaviour of *JO>tAβ42* flies (Figure 27) may be due to tAβ42 being less toxic than TNT-E because it causes progressive neuronal loss rather than complete neuronal silencing [213, 214]. It is also likely to be due partly to the sensitivity of the courtship assay for hearing, as many environmental and physiological factors affect courtship behaviour [152, 215], including but not limited to pheromone detection [216], mutations affecting wing song

[217] and visual perception [218]. These can confound the ability to detect hearing defects in the courtship assay. Another assay for *Drosophila* hearing exists, which relies on playing the wing song to a group of males and observing chaining behaviour [219]. This was not possible within the time constraints for this project due to the complexity of the assay and need for new equipment but this is a more sensitive and reliable assay that has been successfully used to screen for mutants affecting hearing [220]. Further characterisation of *Ctl2* mutants in hearing using this assay would be useful. Additionally, larger sample sizes for each genotype are needed to validate this preliminary data as subtle defects may not have been detected.

4.2 Advantages of using *Drosophila* as a model organism to study Alzheimer's disease

Drosophila melanogaster is a useful organism to screen candidate genes for AD-relevant phenotypes, but there are limitations of using *Drosophila* that should be considered when interpreting the results of this project. Firstly, despite the presence of fly orthologues to 75% of human genes, these orthologues tend to have low protein identity and similarity. In this project, the protein identity between human and *Drosophila* orthologues ranged from 31-43% and protein similarity from 43-61% (Tables 6 and 7), meaning that their functions and interactions are likely to differ between humans and flies. Screening of mutated human candidate genes in flies would be more likely to induce an AD-relevant phenotype.

GWAS and EWAS are useful for identifying many genes that may increase the risk of developing AD, but it is likely that not all genes identified are disease relevant, due to the limitations of GWAS and EWAS. Whilst technology is advancing for genetic manipulation of mouse models, generation of knockout or knock-in models for GWAS or EWAS hits is still expensive and time-consuming, and running experiments in rodent models is costly, particularly as many genes identified in GWAS and EWAS may not be involved in the disease, or the direction of effect of SNPs/DMPs (up or downregulation) may be uncertain, meaning that even if the generation of knockout/knock-in mouse models for each gene was more accessible, it may not be meaningful if many are not involved in AD pathogenesis. In contrast,

manipulation of *Drosophila* genes can be achieved within a few weeks using binary expression systems, and *Drosophila* are not subject to strict animal ethics protocols. The relative simplicity of the *Drosophila* CNS, made up of approximately 150,000 neurons which have been mapped in connectome studies, allows the use of genetic drivers to target specific neuronal circuits for characterisation and screening of genes. Therefore, *Drosophila* effectively bridge the gap between GWAS and EWAS and rodent models by identifying and characterising genes that merit further investigation in more complex organisms, reducing the need for higher order animal models and supporting the NC3Rs principles for replacement, reduction, and refinement. *Drosophila* also provide a system for drug screening by introducing drugs to the standard food media. Memantine, an NMDA receptor blocker licensed to treat dementia, increased the performance index of Aβ-expressing flies to wild-type levels [221]. A *DYRK1A* antagonist also rescued tau- and Aβ-induced memory loss in the olfactory shock assay [222], indicating that AD-related pathways are sufficiently conserved to allow basic drug screens, which can be used before trials in more complex organisms.

Many previous experiments have detected neurodegeneration and AD-associated phenotypes due to overexpression of human tau and Aβ peptides in *Drosophila* [68, 77, 79, 214]. In this project, overexpression of human tAβ42 caused photoreceptor neurodegeneration, premature death, an age-dependent locomotor defect and sleep dysfunction. Overexpression of human tau-0N4R caused lethality when targeted to glial cells, a non-significant decrease in 1-hr memory, and sleep dysfunction. This recapitulates the effects of overexpression of both human proteins in previous studies [68, 73]. Despite the relatively low sequence homology between the human and *Drosophila* orthologues, overexpression of *dAPPL*/Aβ-like fragment and *dTau* induces less severe but similar phenotypes to human Aβ and tau [84, 223], indicating that this neurodegenerative pathway is at least partially conserved between *Drosophila* and humans. Ultimately, the genetic tractability, short generation time, and presence of orthologues to approximately 75% of human disease-associated genes make *Drosophila* a useful model to screen candidate genes identified in genetic association studies.

4.3 Knockdown of *Ctl2* induced lethality and a learning defect in *Drosophila*

CTL2 (*SLC44A2*) is a choline transporter [125]. Relative to other candidate genes, *CTL2* had the highest expression in the human brain according to HPA RNA-seq data. In humans, *CTL2* is expressed in the plasma membrane and mitochondria of microvascular endothelial cells and is thought to participate in choline transport into the brain (Figure 28), as circulating choline constitutes the majority of choline required for brain phosphatidylcholine and acetylcholine synthesis and donation of methyl groups for DNA methylation [125, 126]. Perineural and subperineural glial cells comprise the *Drosophila* BBB [224]. In *Drosophila*, *Ctl2* had higher expression in chiasm, perineural and subperineural glia relative to other non-glial clusters, and knockdown of Ctl2 in glial cells caused partial developmental lethality. Therefore, this may be due to reduced available choline during CNS development and indicates conservation between *CTL2/Ctl2* function in *Drosophila* and humans.

The cholinergic hypothesis of Alzheimer's disease proposes that dysfunction in cholinergic neurons in the basal forebrain, the major cholinergic centre of the CNS implicated in sleep, arousal, and cognitive function, principally contributes to cognitive decline in AD patients [225]. Acetylcholinesterase (AChE) inhibitors such as rivastigmine are licensed to treat the symptoms of AD, but they do not reverse or modify disease progression and provide modest symptom relief [35], challenging the cholinergic hypothesis. However, inadequate treatment of symptoms is at least partially due to the continuing loss of cholinergic neurons, causing a reduction in efficacy [226]. A range of epidemiological studies in humans and sleep disturbance studies in rodents support the interaction between choline, sleep disturbance and AD. Reduction in both choline acetyltransferase (ChAT) and AChE has been observed in post-mortem brain tissue of AD patients [227], and inadequate sleep may contribute to cholinergic dysfunction via increased oxidative stress [225]. Acetylcholine acts as a neuromodulator of memory function, as it can produce both long-term potentiation and short-term depression, demonstrating that cholinergic dysfunction in AD may be at least partially responsible for cognitive symptoms such as memory loss [228]. Additionally, a reduction in choline phospholipids, required for cell membrane integrity, has been observed in the prefrontal cortex of Alzheimer's

disease patients [229]. This suggests that there is a general reduction in brain choline availability in AD patients. It is possible that these global changes in cholinergic function in the brains of AD patients could be affected by downregulation of CTL2 (Figure 28), based on its predicted function in choline transport into the brain side of the BBB [125].

Knockdown of *Ctl2* in neurons caused partial developmental lethality in *Drosophila* and knockdown of Ctl2 in neurons restricted to adulthood caused premature death. Knockdown of *Ctl2* targeted to clock cells also caused complete developmental lethality, and *Ctl2* knockdown in DN1 clock neurons caused partial lethality. DN1 neurons were selected for further investigation of *Ctl2* because the SCope analysis performed identified high expression of *Ctl2* in DN1 neurons at 1 and 9 days of age. The viability of *Ctl2* knockdown in mushroom bodies using the *OK107-GAL4* driver indicates that ubiquitous, leaky *Ctl2-RNAi* expression is not likely to be the cause of the lethality. Instead, DN1 neurons, possibly in synergy with another subset of clock neurons, are likely to be responsible for *Ctl2* knockdown-induced lethality. *Ctl2* functions as a low-affinity choline transporter and global *RNAi*-mediated knockdown of *Ctl2* causes lethality [127]. However, whilst choline is involved in both sleep and memory in *Drosophila* [230], it is unusual for a change in choline transport in a subset of clock neurons is to cause lethality alone, as ablation of PDF neurons is viable [191]. Also, arresting circadian rhythms in *Drosophila* causes premature death in neurodegeneration-prone mutants but does not cause developmental lethality [231]. However, DN1 neurons are cholinergic [232] and knockdown of another choline transporter, ChT, in a subset of mushroom body neurons, prevented eclosion, which was posited to be due to reduced neuromuscular junction integrity in these flies [233]. This demonstrates that knockdown of a choline transporter gene in a small neuronal subset can have systemic effects, although the mechanism of Ctl2-induced lethality observed in this project requires further investigation.

Interestingly, knockdown of *Ctl2* in the mushroom bodies, the structures involved in sleep-wake regulation and memory, induced a memory defect in the olfactory shock assay. This memory defect needs further validation using *UAS*/+ and sensory controls, but mushroom body output neuron activation relies on nicotinic acetylcholine receptor activation, and knockdown of vesicular acetylcholine

transporter and choline acetyltransferase in *Drosophila* decreased performance index in an olfactory shock assay [230]. The memory deficit in *OK107>Ctl2-RNAi* flies may therefore be caused by decreased acetylcholine synthesis and decreased nAChR-mediated mushroom body output neuron activation due to a decrease in available choline. In humans, cholinergic innervation of the hippocampus is involved in memory formation [228], so it is possible that *CTL2* is involved in memory loss in neurodegeneration in humans.

CTL2 in humans has also been implicated in Parkinson's disease [123], characterised by progressive degeneration of dopamine neurons of the substantia nigra pars compacta causing locomotor deficits, aspects of which can be modelled in *Drosophila* using the negative geotaxis assay. In this project, assessment of climbing activity of Ctl2 pan-neuronal knockdown flies was not possible because pan-neuronal knockdown caused partial developmental lethality such that only approximately 1/100 flies eclosed, and *Gal80ts-Elav>Ctl2-RNAi* flies died prematurely (male flies only lived 1-2 days on average), which prevented assessment of climbing ability. However, knockdown of *Ctl2* in dopaminergic neurons using the *TH-GAL4* driver was viable, but the climbing ability of these flies was not tested in this project. Therefore, future experiments should assess climbing ability in *TH-GAL4>Ctl2-RNAi* flies to characterise the potential role of *Ctl2* in Parkinson's disease. Additionally, a courtship assay was set up to assess hearing ability in flies with *Ctl2* knockdown in the Johnston's organ (the *Drosophila* auditory centre), as antibodies to *Ctl2* have been detected in autoimmune hearing loss [122]. However, this assay had insufficient repeats and may not have been sufficiently sensitive to detect a change in hearing, so another hearing assay utilising chaining [219] should be used to test whether *Ctl2* knockdown in the Johnston's organ disrupts hearing ability.

In conclusion, *Ctl2* appears to play a major role in *Drosophila* development, survival, and memory. If it has a conserved role in humans, it may contribute to AD pathogenesis and cognitive deficits through disruption of choline transport, oxidation and synthesis of acetylcholine, phosphatidylcholine, and S-Adenosyl methionine (Figure 28). Validation of the memory deficits in *Drosophila* and further

characterisation of *Ctl2* function in *Drosophila* and rodent models are required to understand its role in AD.

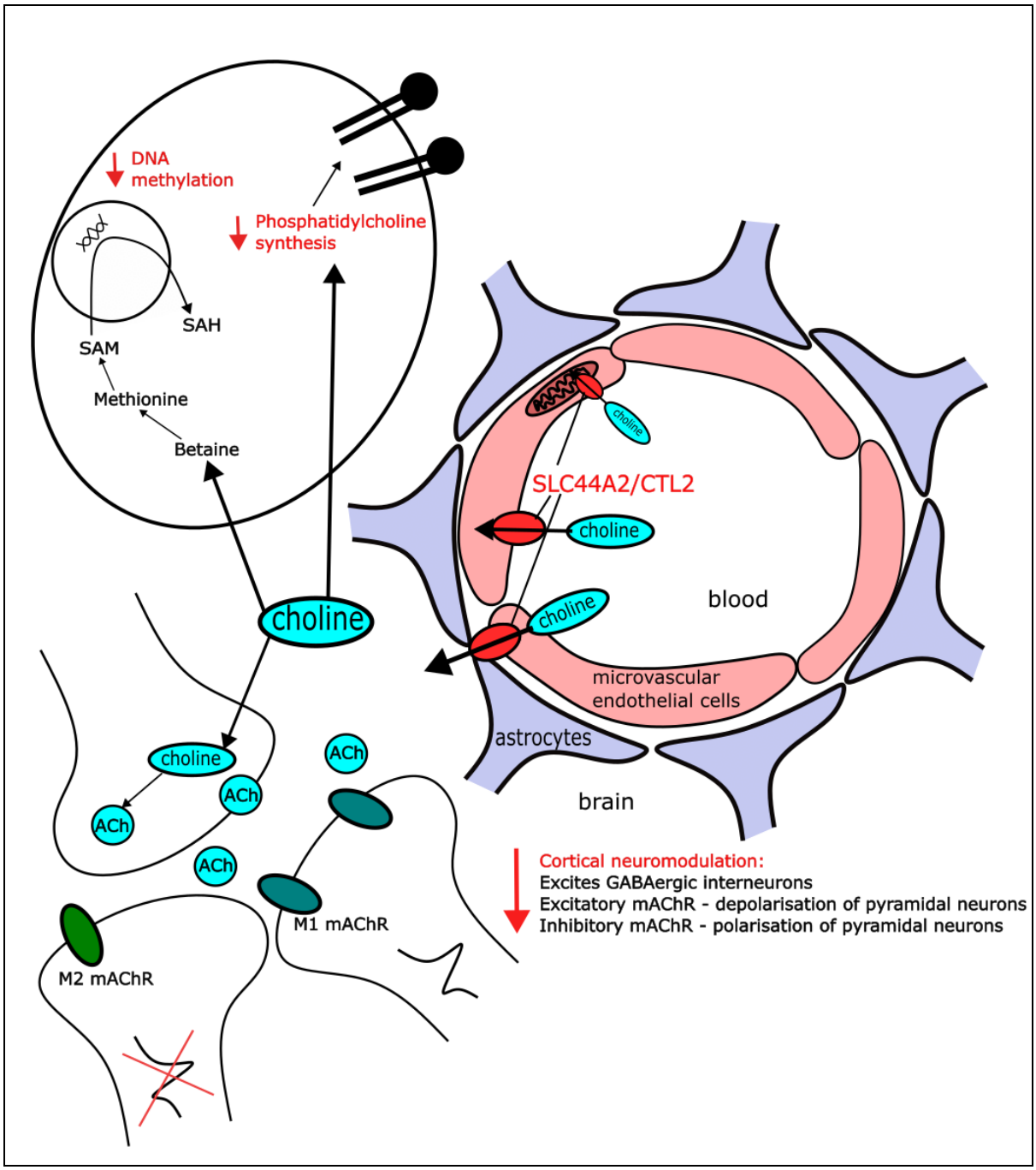

Figure 28: Possible AD-relevant effects of *SLC44A2/CTL2* knockdown in humans.

CTL2 is expressed in microvascular endothelial cells and is considered responsible for choline transport into the brain side of the BBB, required for synthesis of acetylcholine in synaptic boutons, phosphatidylcholine synthesis to maintain plasma membrane integrity and synthesis of S-adenosyl methionine (SAM) for DNA methylation in neurons and glia. Knockdown of *CTL2* may reduce acetylcholine synthesis causing cortical dysregulation, decrease DNA methylation resulting in aberrant gene expression, and decreased phosphatidylcholine and sphingomyelin synthesis causing loss of plasma membrane integrity. ACh, acetylcholine. mAChR, muscarinic acetylcholine receptor. Figure made in Inkscape using information from [126, 228, 234].

4.4 Knockdown of *Kuz* in neurons induced lethality in *Drosophila*

Neuronal knockdown of *Kuz*, the *Drosophila* orthologue of *ADAM10*, caused developmental lethality. This is likely due to reduced proteolytic processing of *Notch*, as *Notch* cleavage by *Kuz* is required to form functional *Notch* protein for lateral inhibition during *Drosophila* neurogenesis [235]. Therefore, disrupted neurogenesis is likely to have caused the developmental lethality in *Elav>Kuz-RNAi* flies. This is currently being investigated by another member of the lab using immunostaining for *Elav* in *Elav/+* and *Elav>Kuz-RNAi* larvae to count the number of neuroblasts, as a decrease in *Notch* cleavage is expected to decrease the number of neuroblasts in the developing larval nervous system. Interestingly, *Kuz* knockdown did not cause a change in the shape or arrangement of photoreceptors, despite a previous study of *RNAi*-mediated *Kuz* knockdown reducing the number of photoreceptors in the *Drosophila* eye [236]. In humans, *ADAM10* and the γ-secretase complex are involved in *Notch* cleavage to promote neurogenesis [237], demonstrating that *Kuz* and *ADAM10* share conserved targets in *Drosophila* and humans. Knockdown of *Kuz* in glia in *Drosophila* caused a decrease in climbing performance in the negative geotaxis assay and had a minor negative effect on lifespan. *Kuz* is highly expressed in *Drosophila* glia in addition to other clusters, so impaired gliogenesis may impede maintenance of neurons and axon guidance during development [238], altering circuitry involved in locomotor behaviour [167]. Additionally, knockdown of *Kuz* in the mushroom body caused a small decrease in performance in the olfactory shock assay, although this was non-significant and requires repeats with *Kuz-RNAi/+* flies

and sensory controls. However, a study of *dAPPL* and *Kuz* involvement in *Drosophila* memory found that overexpression of *Kuz* exacerbated the memory deficit in flies with partial loss of *dAPPL* but had no effect on memory alone [86]. This indicates that variation in *Kuz* expression in either direction may affect memory, but particularly in combination with a change in *dAPPL* expression. To confirm this, the memory of flies with knockdown of *Kuz* and either knockdown or overexpression of Appl should be assessed. Based on phenotypes observed upon *Kuz* knockdown in this project, *Kuz* in *Drosophila* appears to have a conserved role in neurogenesis and APP/*dAPPL* cleavage with human *ADAM10*, meriting further investigation. In humans, early genetic and epigenetic changes at the *ADAM10* locus may affect neurogenesis via *NOTCH* signalling, as well as decreasing non-amyloidogenic processing of *APP* throughout life, predisposing individuals to AD.

4.5 Expression of *Ppt2 RNAi* induced premature death in *Drosophila*

Pan-neuronal expression of *RNAi* for *Ppt2*, the *Drosophila* orthologue of human *PPT2*, caused a large decrease in lifespan. However, repeats with a *Ppt2-RNAi*/+ control and RT-qPCR are required to confirm that the decrease in lifespan was due to *Ppt2* knockdown and not due to random insertion of *Ppt2-RNAi* into a longevity-related gene. *Ppt2* is a lysosomal thioesterase that hydrolyse thioesterase bonds in long chain fatty acyl-CoAs [131], part of a conserved degradation process in *Drosophila* and humans, disruption of which in *PPT1* or *PPT2* knockout mice leads to a lysosomal storage disorder, neurodegeneration and increased mortality [129, 130]. The cause of premature death in *elav>Ppt2-RNAi* flies is therefore likely related to accumulation of fatty-acid modified proteins in the lysosome, causing neuronal toxicity. *Elav>Ppt2-RNAi* flies did not show seizure-like activity or a change in locomotor behaviour, despite spasticity observed in *PPT2* deficient mice [130]. This may be due to a lower level of *RNAi*-mediated *Ppt2* knockdown meaning the level of Ppt2 mRNA may have been sufficiently high to maintain climbing ability. According to SCope analysis, *Drosophila Ppt2* is has comparatively high expression in peptidergic neurons and most glial subtypes. *Drosophila* neuropeptides are involved in modulation of a range of behaviours including hunger, satiety, sleep and memory [161]. The lifespan of flies with peptidergic neuron specific *Ppt2* knockdown should

be assessed, to identify whether these neurons are responsible for the decrease in lifespan.

A SNP at *PPT2* was identified in a GWAS of a Chinese and European population to be associated with an increase in docosapentaenoic acid, an omega-6 polyunsaturated acid [239], which may be due to a change in *PPT2* hydrolysis of acyl-CoAs involved in its metabolism. Interestingly, a high linoleic acid diet in aged APOE4 mice increased brain docosapentaenoic acid, and direct administration by gavage of docosapentaenoic acid reduced the brain levels of pro-inflammatory cytokines, attenuated microgliosis and correlated with an increase in neurotrophins and synaptic markers [240]. Whilst this study did not assess behaviour or cognition of these animals, it suggests that this fatty acid may be protective in AD. However, a SNP at *PPT2* resulted in an increase in docosapentaenoic acid which appears to be neuroprotective, whereas hypermethylation at the *PPT2* DMP was detected in the EWAS meta-analysis [59] used in this project suggesting that *PPT2* is downregulated in AD. This is supported by the decrease in lifespan in *Elav>Ppt2-RNAi* flies and neuronal ceroid lipofuscinosis observed in *PPT2* deficient mice [130]. Therefore, the *PPT2* SNP detected in the polyunsaturated fatty acid GWAS may have been a gain-of-function mutation which resulted in an increase in docosapentaenoic acid cleavage from associated proteins, but this requires further investigation to confirm. Further characterisation could involve assessment of the behavioural phenotypes and lifespan of *Elav>Ppt2-RNAi* flies, or *PPT2* knockout mouse, with linoleic acid (Table 9).

4.6 Expression of *Frl-RNAi* and *MTA1-like-RNAi* induced a locomotor defect in *Drosophila*

Knockdown of *Frl*, the *Drosophila* orthologue of *FMNL1*, caused a decrease in climbing performance in the negative geotaxis assay when knocked down in neurons and glia. Knockdown of *Frl* in neurons was validated using RT-qPCR. *Frl* was most highly expressed in peptidergic neurons and subperineural, chiasm and cortex glia according to SCope analysis, and participates in axonal growth and cell polarity during neurogenesis via modulation of actin polymerisation [241, 242]. Similarly, human *FMNL1* is expressed in the brain and mediates actin polymerisation [106]. A

change in axon guidance and therefore locomotor circuit connectivity may underlie the decrease in climbing performance in *Elav>Frl-RNAi* flies. However, *FMNL1* is also involved in podosome extension and immune cell migration, as *FMNL1* deficiency in mice caused reduced the number of podosome-extending macrophages and reduced macrophage migration [243], although this appeared to be independent of actin barbed end binding. Additionally, deletion of *FMNL1* was lethal in mice [243]. *FMNL1* function has not been investigated in human, rodent or *Drosophila* glial cells, but its role in macrophages indicates it may be also involved in microglial migration, which may share similar properties to macrophage migration due to derivement of microglia from pre-macrophage migration to the CNS [244]. If this role is conserved across species, a reduction in glial migration during development and after injury may be responsible for the climbing defect in *Repo>Frl-RNAi* flies, due to a reduction in their function as neural support cells in the dopaminergic neurons and mushroom body Kenyon cells involved in the startle response [167]. The memory of *OK107>Frl-RNAi* flies was not tested in this project due to an equipment break, but *Frl* is involved in mushroom body development [241], so knockdown of *Frl* in the mushroom body is expected to cause a memory deficit in the olfactory shock assay. Further characterisation should involve confocal microscopy on *OK107>GFP*, *Frl-RNAi* flies to determine the effect of *Frl* knockdown on mushroom body morphology and neurodegeneration.

Expression of *RNAi* for *MTA1-like*, the *Drosophila* orthologue of *MTA3*, in both neurons and glia caused a significant reduction in climbing performance in the negative geotaxis assay. These flies appeared to exhibit seizure-like activity which prevented an appropriate startle response. Whilst RT-qPCR experiments did not detect *MTA1-like* knockdown, the significant reduction in climbing performance suggests that the *RNAi* was successfully reducing *MTA1-like RNAi*, but further repeats with a second *RNAi* line are required to confirm that this was not due to an off-target effect on a different, motor-associated gene. According to SCope analysis, in *Drosophila*, *MTA1-like* is highly expressed in the subperineural glia, peptidergic neurons, clock neurons, and dFB compared to other clusters. It constitutes part of the *Drosophila* NuRD complex which participates in chromatin remodelling and histone deacetylation [113]. Therefore, it is likely to have large-scale effects on gene expression which may have caused the observed phenotype in *Elav>MTA1-like-*

RNAi flies, potentially through a change in expression of ion channels recruited in the startle response or involved in seizure activity. This may also underlie the climbing deficit in Repo>*MTA1-like-RNAi* flies, as a change in expression of glial supportive genes such as those involved astrocyte calcium signalling in neuron-glia interaction [245] may reduce motor circuit function. Like *Drosophila*, *MTA3* in humans also acts as a component of the NuRD complex involved in chromatin remodelling, which binds to the majority of gene enhancers and promotors in embryonic stem cells [246], indicating an important developmental role for *MTA3*. The NuRD complex also involved in both the transcriptional activation and repression of PER within the molecular circadian clock [246], suggesting a potential role in the dampening of circadian rhythms in AD patients [5, 185]. However, no change in sleep or circadian rhythms was detected when *MTA1-like* was knocked down in clock cells in this project. Hypermethylation of a loci downstream of the transcription start site of *MTA3* has been observed in Alzheimer's disease [59], and *MTA1-like RNAi* expression in flies caused AD-associated phenotypes, supporting the hypothesis that decreased *MTA3* expression in AD patients may contribute to AD pathogenesis. Given its role in chromatin remodelling, this may be due to a genome-wide effect on gene expression through altered NuRD complex function. However, further characterisation of *MTA3*/*MTA1-like* in *Drosophila* and rodents is required to understand its role in AD pathology.

4.7 Expression of *Kdm2-RNAi* caused hyperactivity in *Drosophila*

Expression of *Kdm2-RNAi* in all neurons caused no change in lifespan, but in glia, *Kdm2RNAi* expression caused a decrease in lifespan. However, this change was very small and not verified with a Kdm2-*RNAi*/+ control, so may be an effect of genetic background or random *UAS* insertion into a longevity-related gene. RT-qPCR is required to validate this. Overexpression of *Kdm2*in *Drosophila* in a previous study caused a climbing defect in a negative geotaxis assay [247], but did not affect climbing when knocked down in neurons or glia in this project, suggesting that an increase in *Kdm2* function rather than knockdown impairs the startle response, although the mechanism involved is not known.

Expression of *Kdm2-RNAi* in clock cells caused decreased total sleep and increased total activity counts at night, indicating that these flies are hyperactive at night. Hyperactivity, confusion and agitation at night is part of the 'sundowning' phenotype observed in AD patients [5], indicating that this phenotype may be influenced by downregulation of *KDM2B* in humans. *Kdm2* is a histone demethylase specific to H3K4me3 in *Drosophila* [115]. Human *KDM2B* also specifically demethylates H3K4me3 [248]. Histone methylation mark H3K4me3, present at promotors, is generally associated with active transcription [249], therefore a reduction in *KDM2B* is likely to result in increased active transcription. There are likely to be many genes associated with this methylation event, some of which may be involved in circadian rhythms. In *Drosophila*, *Kdm2*-null mutants had shortened circadian periods, but no change in CLK and PER levels [116], suggesting that *Kdm2* may demethylate H3K4me3 at promotors of circadian output genes rather than core clock genes. Additionally, the hyperactivity in *Tim>Kdm2-RNAi* flies may be related to their high climbing performance in the negative geotaxis assay, particularly as *Kdm2*-overexpressing flies exhibited a climbing defect in a previous study [247].

Due to time constraints, RT-qPCR was not performed to confirm *Kdm2* knockdown but should be used as a next step to validate the phenotypes observed in this project. Memory in *OK107>Kdm2-RNAi* flies was also not assessed. However, the circadian phenotype similar to the human AD-associated 'sundowning' phenomenon indicates that *Kdm2* may be a promising candidate for further characterisation in the context of AD pathogenesis.

Table 10: Summary of candidate genes suggested for further study based on this project.

The phenotypes observed, possible functional links to AD pathogenesis pathways and suggested further experiments are also included.

Human/ *Drosophila* gene	**AD-associated phenotypes observed in this project**	**Possible link to AD pathogenesis**	**Suggested validation/further experiments in *Drosophila***

SLC44A2 / Ctl2	Knockdown in neurons, glia and clock cells induced developmental lethality. Knockdown in the mushroom body caused a memory defect. Neuronal knockdown during adulthood caused premature death.	Choline availability [125]	Overexpressor line, rescue experiments with Aβ and tau. Courtship/chaining assay to assess hearing of *JO>Ctl2-RNAi* flies. Climbing assessment of *TH>Ctl2-RNAi* flies.
ADAM10 / Kuz	Neuronal knockdown caused developmental lethality. Glial knockdown reduced climbing ability.	*APP* processing (amyloidogenic) [97]	Overexpressor line, rescue experiments with Aβ and tau. RT-qPCR repeats. *GAL80ts-elav>Kuz-RNAi* assessment of lifespan and climbing ability.
PPT2 / Ppt2	Neuronal *RNAi* expression caused premature death.	Lysosomal storage [129]	RT-qPCR, *Ppt2/+* controls. Overexpressor line, rescue experiments with Aβ and tau. Assess lifespan of Elav>Ppt2-*RNAi*, Elav>Aβ42 and Elav>Tau flies supplemented with linoleic acid.
FMNL1 / Frl	Neuronal and glial knockdown reduced climbing ability. Clock cell knock-down caused arrhythmicity.	Cytoskeletal dynamics [107], impaired immune response and axon guidance	Overexpressor line, rescue experiments with Aβ and tau. Confocal microscopy inn *OK107>GFP*, *Frl-RNAi* flies to identify effect of Frl knockdown on mushroom body morphology. Assess

			memory of *OK107>Frl-RNAi* flies.
MTA3 / MTA1-like	Neuronal and glial *RNAi* expression reduced climbing ability.	Chromatin remodelling [246], aberrant gene expression	RT-qPCR with different primer. Overexpressor line, rescue experiments with Aβ and tau. Single cell RNAseq in elav>*MTA1-like-RNAi* flies to identify differentially expressed genes.
KDM2B / Kdm2	Clock cell *RNAi* expression caused hyperactivity.	Histone demethylation [114], aberrant gene expression	RT-qPCR, *Kdm2/+* controls (climbing and longevity). Overexpressor line, rescue experiments with Aβ and tau. Single cell RNAseq in elav>*Kdm2-RNAi* flies to identify differentially expressed genes.

4.8 Future perspectives

Genes that caused significant AD-associated phenotypes and their suggested further experiments are summarised in Table 9. *Drosophila* genes that did not cause major AD-associated phenotypes when *RNAi* targeted to them was expressed include *CG6984, Scr, AdamTS-A, Klp31E* and *cv-c*. STRING analysis (Figure 9) revealed no interactions between either human or fly orthologues these genes and hallmark AD proteins, despite their human orthologues having AD relevant functions (Table 1), including fatty acid metabolism (*CG6984/ECHDC3*) and disintegrin and metallopeptidase activity (*AdamTS-A/ADAMTS1*). This may be due to inactive *RNAi* lines used for these genes, that the pathway involved is not conserved in *Drosophila*, or that the candidate gene has a minor role or no role in AD pathogenesis. As inactive *RNAi* lines are common, RT-qPCR is needed to confirm a reduction in

mRNA in fly lines where an AD-associated phenotype has been detected. However, for future screening assays in *Drosophila*, it would also be valuable to run RT-qPCR on all *UAS-RNAi* lines before starting other assays to confirm their activity, or on fly lines not showing a phenotype to determine whether this was due to an inactive *RNAi* line (if no decrease in corresponding mRNA is detected) and therefore worth pursuing using a different *RNAi* line. For instance, *elav>CG6984-RNAi* flies had increased mRNA, indicating that non-specific amplification occurred, requiring repeats of the RT-qPCR with different primers to assess whether the *RNAi* line was inactive, and therefore whether a different *RNAi* line should be used to screen *CG6984* for AD-relevant phenotypes. Additionally, future AD screens should utilise two separate *UAS-RNAi* lines for each gene to increase confidence in any phenotypes observed.

Additionally, apart from in assays where the *GAL80ts, Elav-GAL4* driver was used, expression of candidate gene *RNAi* occurred throughout development as well as adulthood. Therefore, phenotypes observed are likely to be partially due to a developmental effect. This is relevant to AD in cases where a SNP is inherited, but most of the genes screened in this project were identified in an EWAS meta-analysis, meaning that the hypermethylation more likely occurred after development as a result of aging, the most important AD risk factor [11], and environmental or lifestyle factors [250]. As a result, the assays used in this project should be repeated with *GAL80ts* drivers to eliminate developmental effects. In relation to this, the memory and sleep and circadian rhythm assays tested young flies, which is less relevant to AD in humans because onset of symptoms occurs much later in life, at approximately 65 years in LOAD patients [9]. Therefore, testing older flies in these behavioural assays may have identified further phenotypes in candidate genes screened, and should be used in future experiments. Furthermore, DNA hypermethylation detected in the EWAS meta-analysis was considered to cause a decrease in gene expression, providing the rationale for using *RNAi* lines. However, DNA methylation can have varied effects on gene expression depending on the location, for example within a gene silencer [52]. Therefore, the effect of hypermethylation at some of the candidate gene loci may have been an increase in expression, meaning overexpressor lines for those candidate genes would have been appropriate for this project.

Following on from this project, further characterisation of candidate genes and validation of their phenotypes in *Drosophila* is necessary, and advances in genetic tools such as CRISPR-Cas9 editing are likely to be useful for this. CRISPR-Cas9 technology is becoming more accessible, and may benefit screening in *Drosophila* due to the ability to induce tissue-specific mutations by taking advantage of the *GAL4-UAS* system to deliver Cas9 and guide RNA [251]. Moreover, the *T2A-GAL4* system which takes advantage of viral 2A-like peptides to link *GAL4* expression to a gene of interest can be used to express a transgene in the cells that express a protein of interest [252]. This system could also be employed to express human genes in the same pattern as their *Drosophila* orthologue, allowing investigation into conserved functions.

4.9 Conclusion

During this project, I have used *Drosophila* as a model organism to screen for AD-associated phenotypes arising due to expression of candidate gene *RNAi*, taking advantage of its genetic tractability, short lifespan, and relatively simple physiology. I have also replicated AD-associated phenotypes observed in Aβ and tau-overexpressing flies and adapted a simple courtship assay to assess hearing ability. However, limitations in the use of flies as a model organism include low protein identity between humans and *Drosophila*, inability to model complex behaviour, and significant proportion of inactive *RNAi* lines, meaning that stringent controls and further characterisation in more complex models is necessary. Nonetheless, six *Drosophila* orthologues of GWAS and EWAS-identified risk genes induced AD-relevant phenotypes in one or more assays due to *RNAi* expression, including locomotor ability, lifespan, memory, sleep, and circadian rhythms. *SLC44A2/Ctl2*, *ADAM10/Kuz*, *PPT2/Ppt2*, *FMNL1/Frl*, *MTA3*/*MTA1-like* and *KDM2B/Kdm2* merit further investigation in the context of Alzheimer's disease using *Drosophila* and rodent models. These genes have a broad range of functions, and may influence AD pathology via cholinergic transport, *APP* processing, fatty acid metabolism, cytoskeletal dynamics, and epigenetic modifications. *Drosophila* bridge the gap between genetic association studies and rodent models for investigation of complex diseases like AD.

Appendix

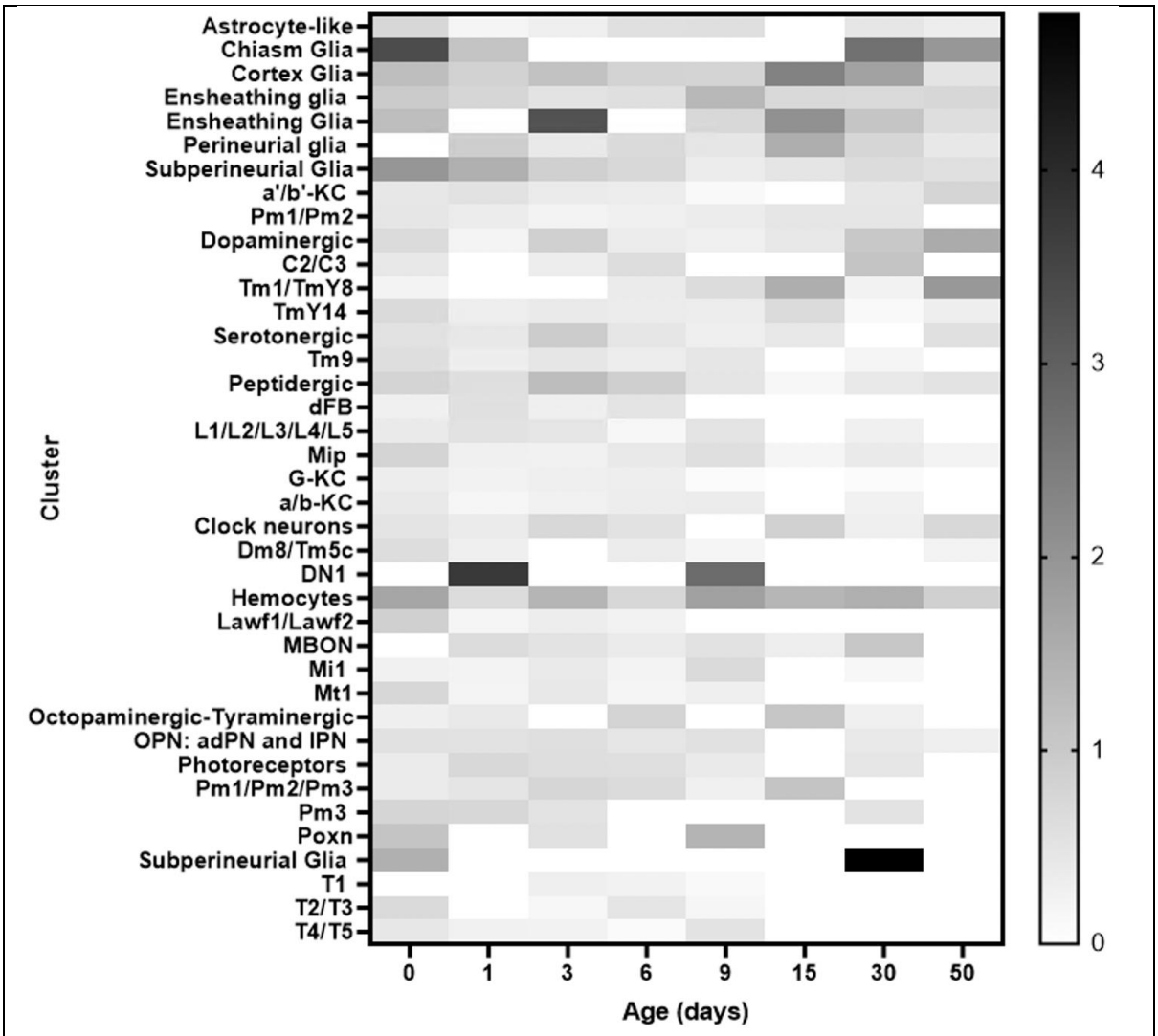

Figure 1: Gene expression heatmap for *Ctl2* over age in days. CPM by cluster calculated using single cell RNAseq data from the Aerts_Fly_AdultBrain_Filtered_57k database on SCope.com.

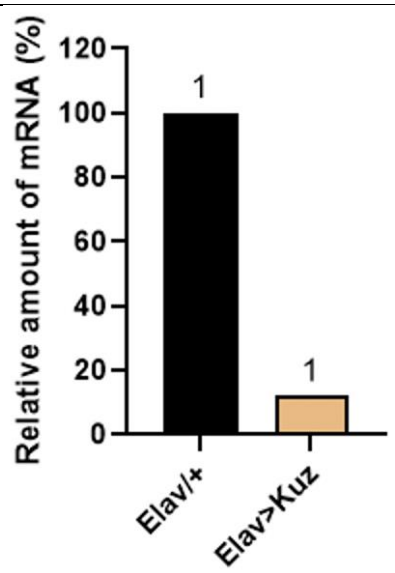

Figure 2: Relative amount of *Kuz* mRNA in E*lav>Kuz* flies compared to *Elav/+.* The Elav-*GAL4* driver was used to express candidate gene *RNAi* in neurons from development. RT-qPCR was used to measure mRNA (%) relative to Elav/+ control. The number above bars indicates the number of biological replicates (one biological replicate is one RNA extraction from 20-30 *Drosophila* heads). Relative amount of mRNA compared to *Elav/*+ control (100%). No statistical analysis performed due to N=1.

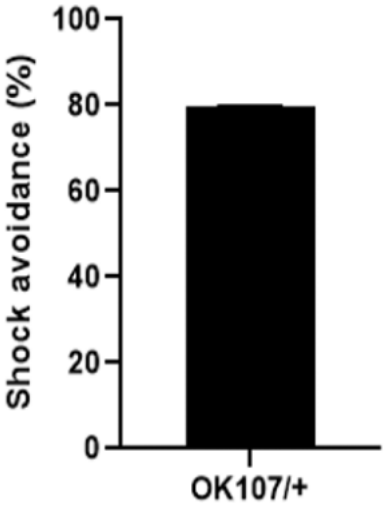

Figure 3: Shock avoidance (%) of *OK107/+* flies. Error bar is mean ± SEM. N=2 experiments, 20-60 flies per experiment.

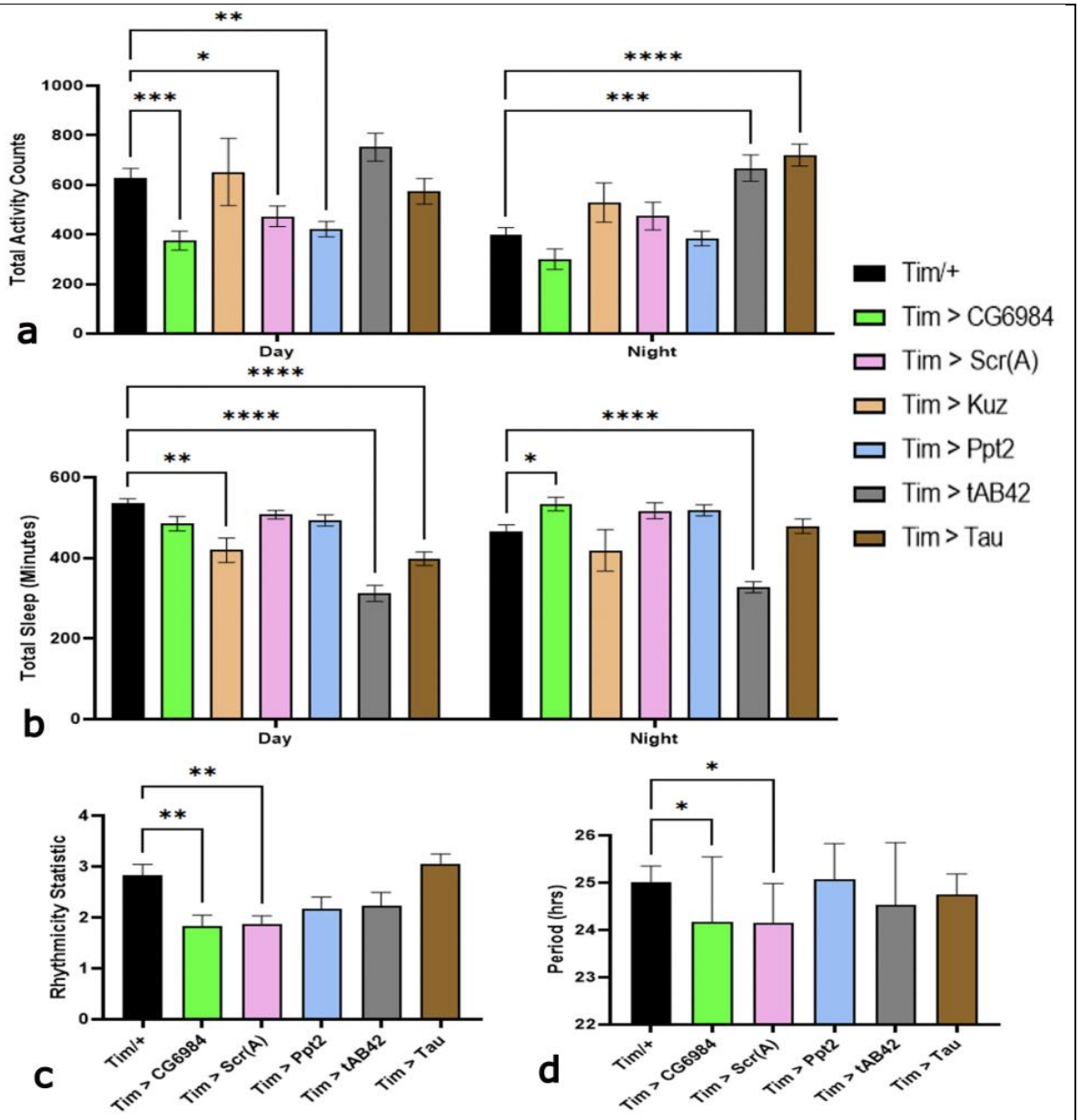

Figure 4: Effect of candidate gene knockdown on sleep and circadian rhythms of flies using a non-cantonised *Tim-GAL4* driver. *Tim-GAL4* was used to express candidate gene *RNAi* in clock cells. (a) Total activity counts (beam crosses) during the day (first 12-hr bin) and night (second 12-hr bin). (b) Total sleep duration in the day and night. (c) Circadian period length in hours. (d) Rhythmicity statistic, flies with <1.5 are considered arrhythmic. Total activity counts and total sleep duration were analysed in a two-way ANOVA, with Dunnett's post hoc for multiple comparisons. Period length and rhythmicity statistic were analysed in a one-way ANOVA with Dunnett's post hoc for multiple comparisons. All error bars are mean ± SEM. N=16 flies per genotype. *P<0.05, **P<0.01, ***P<0.001, ****P<0.0001.

References

1. *2022 Alzheimer's disease facts and figures.* Alzheimers Dement, 2022. **18**(4): p. 700-789.
2. Long, J.M. and D.M. Holtzman, *Alzheimer Disease: An Update on Pathobiology and Treatment Strategies.* Cell, 2019. **179**(2): p. 312-339.
3. Zhao, Q.F., et al., *The prevalence of neuropsychiatric symptoms in Alzheimer's disease: Systematic review and meta-analysis.* J Affect Disord, 2016. **190**: p. 264-271.
4. Moran, M., et al., *Sleep disturbance in mild to moderate Alzheimer's disease.* Sleep Med, 2005. **6**(4): p. 347-52.
5. Volicer, L., et al., *Sundowning and circadian rhythms in Alzheimer's disease.* Am J Psychiatry, 2001. **158**(5): p. 704-11.
6. Aggarwal, N.T., et al., *Motor dysfunction in mild cognitive impairment and the risk of incident Alzheimer disease.* Arch Neurol, 2006. **63**(12): p. 1763-9.
7. Albers, M.W., et al., *At the interface of sensory and motor dysfunctions and Alzheimer's disease.* Alzheimers Dement, 2015. **11**(1): p. 70-98.
8. Todd, S., et al., *Survival in dementia and predictors of mortality: a review.* Int J Geriatr Psychiatry, 2013. **28**(11): p. 1109-24.
9. Lane, C.A., J. Hardy, and J.M. Schott, *Alzheimer's disease.* Eur J Neurol, 2018. **25**(1): p. 59-70.
10. Bekris, L.M., et al., *Genetics of Alzheimer disease.* J Geriatr Psychiatry Neurol, 2010. **23**(4): p. 213-27.
11. *2021 Alzheimer's disease facts and figures.* Alzheimers Dement, 2021. **17**(3): p. 327-406.
12. Nasreddine, Z.S., et al., *The Montreal Cognitive Assessment, MoCA: a brief screening tool for mild cognitive impairment.* J Am Geriatr Soc, 2005. **53**(4): p. 695-9.
13. Cipriani, G., et al., *Alzheimer and his disease: a brief history.* Neurological Sciences, 2011. **32**(2): p. 275-279.
14. Kang, J., et al., *The precursor of Alzheimer's disease amyloid A4 protein resembles a cell-surface receptor.* Nature, 1987. **325**(6106): p. 733-6.
15. Kametani, F. and M. Hasegawa, *Reconsideration of Amyloid Hypothesis and Tau Hypothesis in Alzheimer's Disease.* Front Neurosci, 2018. **12**: p. 25.
16. Lammich, S., et al., *Constitutive and regulated alpha-secretase cleavage of Alzheimer's amyloid precursor protein by a disintegrin metalloprotease.* Proc Natl Acad Sci U S A, 1999. **96**(7): p. 3922-7.
17. Baratchi, S., et al., *Secreted amyloid precursor proteins promote proliferation and glial differentiation of adult hippocampal neural progenitor cells.* Hippocampus, 2012. **22**(7): p. 1517-27.
18. Yankner, B.A., L.K. Duffy, and D.A. Kirschner, *Neurotrophic and neurotoxic effects of amyloid beta protein: reversal by tachykinin neuropeptides.* Science, 1990. **250**(4978): p. 279-82.
19. Hardy, J. and D. Allsop, *Amyloid deposition as the central event in the aetiology of Alzheimer's disease.* Trends Pharmacol Sci, 1991. **12**(10): p. 383-8.
20. Goedert, M., et al., *Multiple isoforms of human microtubule-associated protein tau: sequences and localization in neurofibrillary tangles of Alzheimer's disease.* Neuron, 1989. **3**(4): p. 519-26.

21. Iqbal, K., et al., *Tau in Alzheimer disease and related tauopathies.* Curr Alzheimer Res, 2010. **7**(8): p. 656-64.
22. Weingarten, M.D., et al., *A protein factor essential for microtubule assembly.* Proc Natl Acad Sci U S A, 1975. **72**(5): p. 1858-62.
23. Köpke, E., et al., *Microtubule-associated protein tau. Abnormal phosphorylation of a non-paired helical filament pool in Alzheimer disease.* J Biol Chem, 1993. **268**(32): p. 24374-84.
24. Grundke-Iqbal, I., et al., *Abnormal phosphorylation of the microtubule-associated protein tau (tau) in Alzheimer cytoskeletal pathology.* Proc Natl Acad Sci U S A, 1986. **83**(13): p. 4913-7.
25. Kopeikina, K.J., B.T. Hyman, and T.L. Spires-Jones, *Soluble forms of tau are toxic in Alzheimer's disease.* Transl Neurosci, 2012. **3**(3): p. 223-233.
26. Gómez-Ramos, A., et al., *Extracellular tau is toxic to neuronal cells.* FEBS Lett, 2006. **580**(20): p. 4842-50.
27. Gandy, S., et al., *Days to criterion as an indicator of toxicity associated with human Alzheimer amyloid-beta oligomers.* Ann Neurol, 2010. **68**(2): p. 220-30.
28. Meyer-Luehmann, M., et al., *Rapid appearance and local toxicity of amyloid-beta plaques in a mouse model of Alzheimer's disease.* Nature, 2008. **451**(7179): p. 720-4.
29. Octave, J.N., et al., *From synaptic spines to nuclear signaling: nuclear and synaptic actions of the amyloid precursor protein.* J Neurochem, 2013. **126**(2): p. 183-90.
30. Walsh, D.M., et al., *Naturally secreted oligomers of amyloid beta protein potently inhibit hippocampal long-term potentiation in vivo.* Nature, 2002. **416**(6880): p. 535-9.
31. Shipton, O.A., et al., *Tau protein is required for amyloid {beta}-induced impairment of hippocampal long-term potentiation.* J Neurosci, 2011. **31**(5): p. 1688-92.
32. Vossel, K.A., et al., *Tau reduction prevents Abeta-induced defects in axonal transport.* Science, 2010. **330**(6001): p. 198.
33. Leroy, K., et al., *Lack of tau proteins rescues neuronal cell death and decreases amyloidogenic processing of APP in APP/PS1 mice.* Am J Pathol, 2012. **181**(6): p. 1928-40.
34. Bloom, G.S., *Amyloid-β and tau: the trigger and bullet in Alzheimer disease pathogenesis.* JAMA Neurol, 2014. **71**(4): p. 505-8.
35. Vaz, M. and S. Silvestre, *Alzheimer's disease: Recent treatment strategies.* Eur J Pharmacol, 2020. **887**: p. 173554.
36. Cole, S.L. and R. Vassar, *The Alzheimer's disease β-secretase enzyme, BACE1.* Molecular Neurodegeneration, 2007. **2**(1): p. 22.
37. Kellar, D. and S. Craft, *Brain insulin resistance in Alzheimer's disease and related disorders: mechanisms and therapeutic approaches.* Lancet Neurol, 2020. **19**(9): p. 758-766.
38. Sato, N. and R. Morishita, *The roles of lipid and glucose metabolism in modulation of β-amyloid, tau, and neurodegeneration in the pathogenesis of Alzheimer disease.* Front Aging Neurosci, 2015. **7**: p. 199.
39. Ong, W.Y., et al., *Slow excitotoxicity in Alzheimer's disease.* J Alzheimers Dis, 2013. **35**(4): p. 643-68.
40. Leng, F. and P. Edison, *Neuroinflammation and microglial activation in Alzheimer disease: where do we go from here?* Nat Rev Neurol, 2021. **17**(3): p. 157-172.

41. Stewart, C.R., et al., *CD36 ligands promote sterile inflammation through assembly of a Toll-like receptor 4 and 6 heterodimer.* Nat Immunol, 2010. **11**(2): p. 155-61.
42. Bamberger, M.E., et al., *A cell surface receptor complex for fibrillar beta-amyloid mediates microglial activation.* J Neurosci, 2003. **23**(7): p. 2665-74.
43. Nimmerjahn, A., F. Kirchhoff, and F. Helmchen, *Resting microglial cells are highly dynamic surveillants of brain parenchyma in vivo.* Science, 2005. **308**(5726): p. 1314-8.
44. Koenigsknecht, J. and G. Landreth, *Microglial phagocytosis of fibrillar beta-amyloid through a beta1 integrin-dependent mechanism.* J Neurosci, 2004. **24**(44): p. 9838-46.
45. Heneka, M.T., et al., *Neuroinflammation in Alzheimer's disease.* The Lancet Neurology, 2015. **14**(4): p. 388-405.
46. Perry, V.H. and C. Holmes, *Microglial priming in neurodegenerative disease.* Nature Reviews Neurology, 2014. **10**(4): p. 217-224.
47. Liddelow, S.A., et al., *Neurotoxic reactive astrocytes are induced by activated microglia.* Nature, 2017. **541**(7638): p. 481-487.
48. Liu, C.C., et al., *Apolipoprotein E and Alzheimer disease: risk, mechanisms and therapy.* Nat Rev Neurol, 2013. **9**(2): p. 106-18.
49. Mucke, L., *Alzheimer's disease.* Nature, 2009. **461**(7266): p. 895-897.
50. Frazer, K.A., et al., *Human genetic variation and its contribution to complex traits.* Nature Reviews Genetics, 2009. **10**(4): p. 241-251.
51. Boyle, E.A., Y.I. Li, and J.K. Pritchard, *An Expanded View of Complex Traits: From Polygenic to Omnigenic.* Cell, 2017. **169**(7): p. 1177-1186.
52. Ehrlich, M., *DNA hypermethylation in disease: mechanisms and clinical relevance.* Epigenetics, 2019. **14**(12): p. 1141-1163.
53. MacDonald, V.E. and L.J. Howe, *Histone acetylation: where to go and how to get there.* Epigenetics, 2009. **4**(3): p. 139-43.
54. Fenoglio, C., et al., *Role of Genetics and Epigenetics in the Pathogenesis of Alzheimer's Disease and Frontotemporal Dementia.* J Alzheimers Dis, 2018. **62**(3): p. 913-932.
55. Frost, B., et al., *Tau promotes neurodegeneration through global chromatin relaxation.* Nat Neurosci, 2014. **17**(3): p. 357-66.
56. Feil, R. and M.F. Fraga, *Epigenetics and the environment: emerging patterns and implications.* Nature Reviews Genetics, 2012. **13**(2): p. 97-109.
57. Uffelmann, E., et al., *Genome-wide association studies.* Nature Reviews Methods Primers, 2021. **1**(1): p. 59.
58. Bush, W.S. and J.H. Moore, *Chapter 11: Genome-wide association studies.* PLoS Comput Biol, 2012. **8**(12): p. e1002822.
59. Smith, R.G., et al., *A meta-analysis of epigenome-wide association studies in Alzheimer's disease highlights novel differentially methylated loci across cortex.* Nat Commun, 2021. **12**(1): p. 3517.
60. Kunkle, B.W., et al., *Genetic meta-analysis of diagnosed Alzheimer's disease identifies new risk loci and implicates Aβ, tau, immunity and lipid processing.* Nat Genet, 2019. **51**(3): p. 414-430.
61. Pidsley, R., et al., *A data-driven approach to preprocessing Illumina 450K methylation array data.* BMC Genomics, 2013. **14**: p. 293.

62. Lunnon, K., et al., *Methylomic profiling implicates cortical deregulation of ANK1 in Alzheimer's disease.* Nat Neurosci, 2014. **17**(9): p. 1164-70.
63. Zeggini, E. and J.P. Ioannidis, *Meta-analysis in genome-wide association studies.* Pharmacogenomics, 2009. **10**(2): p. 191-201.
64. Battram, T., et al., *A comparison of the genes and genesets identified by GWAS and EWAS of fifteen complex traits.* Nature Communications, 2022. **13**(1): p. 7816.
65. Michels, K.B., et al., *Recommendations for the design and analysis of epigenome-wide association studies.* Nature Methods, 2013. **10**(10): p. 949-955.
66. Andrews, S.J., B. Fulton-Howard, and A. Goate, *Interpretation of risk loci from genome-wide association studies of Alzheimer's disease.* Lancet Neurol, 2020. **19**(4): p. 326-335.
67. Buhl, E., et al., *Effects of Eph/ephrin signalling and human Alzheimer's disease-associated EphA1 on Drosophila behaviour and neurophysiology.* Neurobiology of Disease, 2022. **170**: p. 105752.
68. Higham, J.P., et al., *Alzheimer's Disease Associated Genes Ankyrin and Tau Cause Shortened Lifespan and Memory Loss in Drosophila.* Front Cell Neurosci, 2019. **13**: p. 260.
69. Lambert, E., et al., *The Alzheimer susceptibility gene BIN1 induces isoform-dependent neurotoxicity through early endosome defects.* Acta Neuropathol Commun, 2022. **10**(1): p. 4.
70. Fernandez-Funez, P., L. de Mena, and D.E. Rincon-Limas, *Modeling the complex pathology of Alzheimer's disease in Drosophila.* Exp Neurol, 2015. **274**(Pt A): p. 58-71.
71. Caygill, E.E. and A.H. Brand, *The GAL4 System: A Versatile System for the Manipulation and Analysis of Gene Expression.* Methods Mol Biol, 2016. **1478**: p. 33-52.
72. Prüßing, K., A. Voigt, and J.B. Schulz, *Drosophila melanogaster as a model organism for Alzheimer's disease.* Molecular Neurodegeneration, 2013. **8**(1): p. 35.
73. Chakraborty, R., et al., *Characterization of a Drosophila Alzheimer's disease model: pharmacological rescue of cognitive defects.* PLoS One, 2011. **6**(6): p. e20799.
74. Ogienko, A.A., et al., *Drosophila as a Model Organism to Study Basic Mechanisms of Longevity.* Int J Mol Sci, 2022. **23**(19).
75. Malik, B.R. and J.J. Hodge, *Drosophila adult olfactory shock learning.* J Vis Exp, 2014(90): p. e50107.
76. Chiu, J.C., et al., *Assaying locomotor activity to study circadian rhythms and sleep parameters in Drosophila.* J Vis Exp, 2010(43).
77. Greeve, I., et al., *Age-dependent neurodegeneration and Alzheimer-amyloid plaque formation in transgenic Drosophila.* J Neurosci, 2004. **24**(16): p. 3899-906.
78. Iijima, K., et al., *Dissecting the pathological effects of human Abeta40 and Abeta42 in Drosophila: a potential model for Alzheimer's disease.* Proc Natl Acad Sci U S A, 2004. **101**(17): p. 6623-8.
79. Buhl, E., J.P. Higham, and J.J.L. Hodge, *Alzheimer's disease-associated tau alters Drosophila circadian activity, sleep and clock neuron electrophysiology.* Neurobiol Dis, 2019. **130**: p. 104507.
80. Folwell, J., et al., *Abeta exacerbates the neuronal dysfunction caused by human tau expression in a Drosophila model of Alzheimer's disease.* Exp Neurol, 2010. **223**(2): p. 401-9.

81. Miguel, L., et al., *Moderate Overexpression of Tau in Drosophila Exacerbates Amyloid-β-Induced Neuronal Phenotypes and Correlates with Tau Oligomerization.* J Alzheimers Dis, 2020. **74**(2): p. 637-647.
82. Luo, L.Q., L.E. Martin-Morris, and K. White, *Identification, secretion, and neural expression of APPL, a Drosophila protein similar to human amyloid protein precursor.* J Neurosci, 1990. **10**(12): p. 3849-61.
83. Heidary, G. and M.E. Fortini, *Identification and characterization of the Drosophila tau homolog.* Mech Dev, 2001. **108**(1-2): p. 171-8.
84. Carmine-Simmen, K., et al., *Neurotoxic effects induced by the Drosophila amyloid-beta peptide suggest a conserved toxic function.* Neurobiol Dis, 2009. **33**(2): p. 274-81.
85. Bilen, J. and N.M. Bonini, *Drosophila as a model for human neurodegenerative disease.* Annu Rev Genet, 2005. **39**: p. 153-71.
86. Bourdet, I., T. Preat, and V. Goguel, *The full-length form of the Drosophila amyloid precursor protein is involved in memory formation.* J Neurosci, 2015. **35**(3): p. 1043-51.
87. Wentzell, J.S., et al., *Amyloid precursor proteins are protective in Drosophila models of progressive neurodegeneration.* Neurobiol Dis, 2012. **46**(1): p. 78-87.
88. McBride, S.M., et al., *Pharmacological and genetic reversal of age-dependent cognitive deficits attributable to decreased presenilin function.* J Neurosci, 2010. **30**(28): p. 9510-22.
89. Rieche, F., et al., *Drosophila Full-Length Amyloid Precursor Protein Is Required for Visual Working Memory and Prevents Age-Related Memory Impairment.* Current Biology, 2018. **28**(5): p. 817-823.e3.
90. Poeck, B., R. Strauss, and D. Kretzschmar, *Analysis of amyloid precursor protein function in Drosophilamelanogaster.* Experimental Brain Research, 2012. **217**(3): p. 413-421.
91. Jeon, Y., et al., *Genetic Dissection of Alzheimer's Disease Using Drosophila Models.* Int J Mol Sci, 2020. **21**(3).
92. Butterfield, D.A., et al., *Evidence of oxidative damage in Alzheimer's disease brain: central role for amyloid beta-peptide.* Trends Mol Med, 2001. **7**(12): p. 548-54.
93. Rival, T., et al., *Fenton chemistry and oxidative stress mediate the toxicity of the beta-amyloid peptide in a Drosophila model of Alzheimer's disease.* Eur J Neurosci, 2009. **29**(7): p. 1335-47.
94. Dias-Santagata, D., et al., *Oxidative stress mediates tau-induced neurodegeneration in Drosophila.* J Clin Invest, 2007. **117**(1): p. 236-45.
95. Panchal, K. and A.K. Tiwari, *Miro, a Rho GTPase genetically interacts with Alzheimer's disease-associated genes (Tau, Aβ(42) and Appl) in Drosophila melanogaster.* Biol Open, 2020. **9**(9).
96. Garrido-Maraver, J., S.H.Y. Loh, and L.M. Martins, *Forcing contacts between mitochondria and the endoplasmic reticulum extends lifespan in a Drosophila model of Alzheimer's disease.* Biol Open, 2020. **9**(1).
97. Kuhn, P.H., et al., *ADAM10 is the physiologically relevant, constitutive alpha-secretase of the amyloid precursor protein in primary neurons.* Embo j, 2010. **29**(17): p. 3020-32.
98. Yuan, X.Z., et al., *The Role of ADAM10 in Alzheimer's Disease.* J Alzheimers Dis, 2017. **58**(2): p. 303-322.

99. Miguel, R.F., A. Pollak, and G. Lubec, *Metalloproteinase ADAMTS-1 but not ADAMTS-5 is manifold overexpressed in neurodegenerative disorders as Down syndrome, Alzheimer's and Pick's disease.* Brain Res Mol Brain Res, 2005. **133**(1): p. 1-5.
100. Iruela-Arispe, M.L., D. Carpizo, and A. Luque, *ADAMTS1: a matrix metalloprotease with angioinhibitory properties.* Ann N Y Acad Sci, 2003. **995**: p. 183-90.
101. Bharadwaj, T., et al., *ADAMTS1, MPDZ, MVD, and SEZ6: candidate genes for autosomal recessive nonsyndromic hearing impairment.* Eur J Hum Genet, 2022. **30**(1): p. 22-33.
102. Griffiths, T.D., et al., *How Can Hearing Loss Cause Dementia?* Neuron, 2020. **108**(3): p. 401-412.
103. Rodríguez-Baena, F.J., et al., *ADAMTS1 protease is required for a balanced immune cell repertoire and tumour inflammatory response.* Scientific Reports, 2018. **8**(1): p. 13103.
104. Skeath, J.B., et al., *The extracellular metalloprotease AdamTS-A anchors neural lineages in place within and preserves the architecture of the central nervous system.* Development, 2017. **144**(17): p. 3102-3113.
105. Bai, S.W., et al., *Identification and characterization of a set of conserved and new regulators of cytoskeletal organization, cell morphology and migration.* BMC Biol, 2011. **9**: p. 54.
106. Young, K.G. and J.W. Copeland, *Formins in cell signaling.* Biochimica et Biophysica Acta (BBA) - Molecular Cell Research, 2010. **1803**(2): p. 183-190.
107. Calvo, V. and M. Izquierdo, *Role of Actin Cytoskeleton Reorganization in Polarized Secretory Traffic at the Immunological Synapse.* Front Cell Dev Biol, 2021. **9**: p. 629097.
108. Labat-de-Hoz, L. and M.A. Alonso, *Formins in Human Disease.* Cells, 2021. **10**(10).
109. Dehapiot, B., et al., *Assembly of a persistent apical actin network by the formin Frl/Fmnl tunes epithelial cell deformability.* Nat Cell Biol, 2020. **22**(7): p. 791-802.
110. Fulga, T.A., et al., *Abnormal bundling and accumulation of F-actin mediates tau-induced neuronal degeneration in vivo.* Nat Cell Biol, 2007. **9**(2): p. 139-48.
111. Xue, Y., et al., *NURD, a novel complex with both ATP-dependent chromatin-remodeling and histone deacetylase activities.* Mol Cell, 1998. **2**(6): p. 851-61.
112. Sen, N., B. Gui, and R. Kumar, *Physiological functions of MTA family of proteins.* Cancer Metastasis Rev, 2014. **33**(4): p. 869-77.
113. Demirdizen, E., et al., *Localization of Drosophila CENP-A to non-centromeric sites depends on the NuRD complex.* Nucleic Acids Res, 2019. **47**(22): p. 11589-11608.
114. Vacík, T., D. Lađinović, and I. Raška, *KDM2A/B lysine demethylases and their alternative isoforms in development and disease.* Nucleus, 2018. **9**(1): p. 431-441.
115. Kavi, H.H. and J.A. Birchler, *Drosophila KDM2 is a H3K4me3 demethylase regulating nucleolar organization.* BMC Res Notes, 2009. **2**: p. 217.
116. Zheng, Y., et al., *The Lysine Demethylase dKDM2 Is Non-essential for Viability, but Regulates Circadian Rhythms in Drosophila.* Front Genet, 2018. **9**: p. 354.
117. Duarte, M.K., et al., *The relationship of the oleic acid level and ECHDC3 mRNA expression with the extent of coronary lesion.* Lipids Health Dis, 2016. **15**(1): p. 144.
118. Eicher, J.D., et al., *Characterization of the platelet transcriptome by RNA sequencing in patients with acute myocardial infarction.* Platelets, 2016. **27**(3): p. 230-9.

119. Yin, J., et al., *Association analysis of polymorphisms in STARD6 and near ECHDC3 in Alzheimer's disease patients carrying the APOE ε4 Allele.* Neuropsychiatr Dis Treat, 2019. **15**: p. 213-218.
120. Tan, M.S., et al., *Associations of Alzheimer's disease risk variants with gene expression, amyloidosis, tauopathy, and neurodegeneration.* Alzheimers Res Ther, 2021. **13**(1): p. 15.
121. Chen, H.L., et al., *Reduced Function of the Glutathione S-Transferase S1 Suppresses Behavioral Hyperexcitability in Drosophila Expressing Mutant Voltage-Gated Sodium Channels.* G3 (Bethesda), 2020. **10**(4): p. 1327-1340.
122. Kommareddi, P.K., et al., *Autoantibodies to recombinant human CTL2 in autoimmune hearing loss.* Laryngoscope, 2009. **119**(5): p. 924-32.
123. Nalls, M.A., et al., *Identification of novel risk loci, causal insights, and heritable risk for Parkinson's disease: a meta-analysis of genome-wide association studies.* Lancet Neurol, 2019. **18**(12): p. 1091-1102.
124. Kommareddi, P.K., et al., *Isoforms, expression, glycosylation, and tissue distribution of CTL2/SLC44A2.* Protein J, 2010. **29**(6): p. 417-26.
125. Iwao, B., et al., *Functional expression of choline transporter like-protein 1 (CTL1) and CTL2 in human brain microvascular endothelial cells.* Neurochem Int, 2016. **93**: p. 40-50.
126. Inazu, M., *Functional Expression of Choline Transporters in the Blood-Brain Barrier.* Nutrients, 2019. **11**(10).
127. Duan, Y., et al., *Choline transporter-like protein 2 interacts with chitin synthase 1 and is involved in insect cuticle development.* Insect Biochem Mol Biol, 2022. **141**: p. 103718.
128. Calero, G., et al., *The crystal structure of palmitoyl protein thioesterase-2 (PPT2) reveals the basis for divergent substrate specificities of the two lysosomal thioesterases, PPT1 and PPT2.* J Biol Chem, 2003. **278**(39): p. 37957-64.
129. Gupta, P., et al., *Disruption of PPT1 or PPT2 causes neuronal ceroid lipofuscinosis in knockout mice.* Proc Natl Acad Sci U S A, 2001. **98**(24): p. 13566-71.
130. Gupta, P., et al., *Disruption of PPT2 in mice causes an unusual lysosomal storage disorder with neurovisceral features.* Proc Natl Acad Sci U S A, 2003. **100**(21): p. 12325-30.
131. Bannan, B.A., et al., *The Drosophila protein palmitoylome: characterizing palmitoyl-thioesterases and DHHC palmitoyl-transferases.* Fly (Austin), 2008. **2**(4): p. 198-214.
132. Hickey, A.J., et al., *Palmitoyl-protein thioesterase 1 deficiency in Drosophila melanogaster causes accumulation of abnormal storage material and reduced life span.* Genetics, 2006. **172**(4): p. 2379-90.
133. Braun, A.C. and M.A. Olayioye, *Rho regulation: DLC proteins in space and time.* Cell Signal, 2015. **27**(8): p. 1643-51.
134. Nagaraja, G.M. and R.P. Kandpal, *Chromosome 13q12 encoded Rho GTPase activating protein suppresses growth of breast carcinoma cells, and yeast two-hybrid screen shows its interaction with several proteins.* Biochemical and Biophysical Research Communications, 2004. **313**(3): p. 654-665.
135. Li, X., et al., *STARD13-correlated ceRNA network inhibits EMT and metastasis of breast cancer.* Oncotarget, 2016. **7**(17): p. 23197-211.
136. El-Sitt, S., et al., *DLC2/StarD13 plays a role of a tumor suppressor in astrocytoma.* Oncol Rep, 2012. **28**(2): p. 511-8.

137. Sato, D., et al., *Crossveinless-c, the Drosophila homolog of tumor suppressor DLC1, regulates directional elongation of dendritic branches via down-regulating Rho1 activity.* Genes Cells, 2010. **15**(5): p. 485-500.
138. Donlea, J.M., D. Pimentel, and G. Miesenböck, *Neuronal machinery of sleep homeostasis in Drosophila.* Neuron, 2014. **81**(4): p. 860-72.
139. Jeannotte, L., F. Gotti, and K. Landry-Truchon, *Hoxa5: A Key Player in Development and Disease.* J Dev Biol, 2016. **4**(2).
140. Lizen, B., et al., *Conditional Loss of Hoxa5 Function Early after Birth Impacts on Expression of Genes with Synaptic Function.* Front Mol Neurosci, 2017. **10**: p. 369.
141. Fan, F., et al., *HOXA5: A crucial transcriptional factor in cancer and a potential therapeutic target.* Biomed Pharmacother, 2022. **155**: p. 113800.
142. Lewis, E.B., *A gene complex controlling segmentation in Drosophila.* Nature, 1978. **276**(5688): p. 565-570.
143. Struhl, G., *Genes controlling segmental specification in the Drosophila thorax.* Proc Natl Acad Sci U S A, 1982. **79**(23): p. 7380-4.
144. van Riel, W.E., et al., *Kinesin-4 KIF21B is a potent microtubule pausing factor.* Elife, 2017. **6**.
145. Ghiretti, A.E., et al., *Activity-Dependent Regulation of Distinct Transport and Cytoskeletal Remodeling Functions of the Dendritic Kinesin KIF21B.* Neuron, 2016. **92**(4): p. 857-872.
146. Muhia, M., et al., *The Kinesin KIF21B Regulates Microtubule Dynamics and Is Essential for Neuronal Morphology, Synapse Function, and Learning and Memory.* Cell Rep, 2016. **15**(5): p. 968-977.
147. *Comprehensive follow-up of the first genome-wide association study of multiple sclerosis identifies KIF21B and TMEM39A as susceptibility loci.* Hum Mol Genet, 2010. **19**(5): p. 953-62.
148. Walkinshaw, E., et al., *Identification of Genes That Promote or Inhibit Olfactory Memory Formation in Drosophila.* Genetics, 2015. **199**(4): p. 1173-1182.
149. Hodge, J.J. and R. Stanewsky, *Function of the Shaw potassium channel within the Drosophila circadian clock.* PLoS One, 2008. **3**(5): p. e2274.
150. Speretta, E., et al., *Expression in drosophila of tandem amyloid β peptides provides insights into links between aggregation and neurotoxicity.* J Biol Chem, 2012. **287**(24): p. 20748-54.
151. Wittmann, C.W., et al., *Tauopathy in Drosophila: neurodegeneration without neurofibrillary tangles.* Science, 2001. **293**(5530): p. 711-4.
152. Nichols, C.D., J. Becnel, and U.B. Pandey, *Methods to assay Drosophila behavior.* J Vis Exp, 2012(61).
153. Hu, Y., et al., *An integrative approach to ortholog prediction for disease-focused and other functional studies.* BMC Bioinformatics, 2011. **12**(1): p. 357.
154. Bai, Z., et al., *AlzBase: an Integrative Database for Gene Dysregulation in Alzheimer's Disease.* Mol Neurobiol, 2016. **53**(1): p. 310-319.
155. Moore, L.D., T. Le, and G. Fan, *DNA Methylation and Its Basic Function.* Neuropsychopharmacology, 2013. **38**(1): p. 23-38.
156. Szklarczyk, D., et al., *STRING v11: protein-protein association networks with increased coverage, supporting functional discovery in genome-wide experimental datasets.* Nucleic Acids Res, 2019. **47**(D1): p. D607-d613.

157. Satir, T.M., et al., *Accelerated neuronal and synaptic maturation by BrainPhys medium increases Aβ secretion and alters Aβ peptide ratios from iPSC-derived cortical neurons.* Scientific Reports, 2020. **10**(1): p. 601.
158. Wang, X. and G. Pei, *Visualization of Alzheimer's Disease Related α-/β-/γ-Secretase Ternary Complex by Bimolecular Fluorescence Complementation Based Fluorescence Resonance Energy Transfer.* Front Mol Neurosci, 2018. **11**: p. 431.
159. Fagerberg, L., et al., *Analysis of the human tissue-specific expression by genome-wide integration of transcriptomics and antibody-based proteomics.* Mol Cell Proteomics, 2014. **13**(2): p. 397-406.
160. Davie, K., et al., *A Single-Cell Transcriptome Atlas of the Aging Drosophila Brain.* Cell, 2018. **174**(4): p. 982-998.e20.
161. Nässel, D.R. and Å.M.E. Winther, *Drosophila neuropeptides in regulation of physiology and behavior.* Progress in Neurobiology, 2010. **92**(1): p. 42-104.
162. Johnson, R.I., *Hexagonal patterning of the Drosophila eye.* Dev Biol, 2021. **478**: p. 173-182.
163. Cagan, R., *Principles of Drosophila eye differentiation.* Curr Top Dev Biol, 2009. **89**: p. 115-35.
164. Treisman, J.E., *Retinal differentiation in Drosophila.* Wiley Interdiscip Rev Dev Biol, 2013. **2**(4): p. 545-57.
165. Katz, B. and B. Minke, *Drosophila photoreceptors and signaling mechanisms.* Front Cell Neurosci, 2009. **3**: p. 2.
166. Mishra, M. and E. Knust, *Analysis of the Drosophila compound eye with light and electron microscopy.* Methods Mol Biol, 2013. **935**: p. 161-82.
167. Sun, J., et al., *Neural Control of Startle-Induced Locomotion by the Mushroom Bodies and Associated Neurons in Drosophila.* Front Syst Neurosci, 2018. **12**: p. 6.
168. Keller, L.C., et al., *Glial-derived prodegenerative signaling in the Drosophila neuromuscular system.* Neuron, 2011. **72**(5): p. 760-75.
169. Jessen, K.R., *Glial cells.* The International Journal of Biochemistry & Cell Biology, 2004. **36**(10): p. 1861-1867.
170. Yildirim, K., et al., *Drosophila glia: Few cell types and many conserved functions.* Glia, 2019. **67**(1): p. 5-26.
171. Zwaan, B.J., R. Bijlsma, and R.F. Hoekstra, *On the developmental theory of ageing. II. The effect of developmental temperature on longevity in relation to adult body size in D. melanogaster.* Heredity, 1992. **68**(2): p. 123-130.
172. Crowther, D.C., et al., *Intraneuronal Abeta, non-amyloid aggregates and neurodegeneration in a Drosophila model of Alzheimer's disease.* Neuroscience, 2005. **132**(1): p. 123-35.
173. Pereanu, W., D. Shy, and V. Hartenstein, *Morphogenesis and proliferation of the larval brain glia in Drosophila.* Dev Biol, 2005. **283**(1): p. 191-203.
174. Doherty, J., et al., *Ensheathing glia function as phagocytes in the adult Drosophila brain.* J Neurosci, 2009. **29**(15): p. 4768-81.
175. Ray, A., S.D. Speese, and M.A. Logan, *Glial Draper Rescues Aβ Toxicity in a Drosophila Model of Alzheimer's Disease.* J Neurosci, 2017. **37**(49): p. 11881-11893.
176. Jahn, H., *Memory loss in Alzheimer's disease.* Dialogues Clin Neurosci, 2013. **15**(4): p. 445-54.
177. Tully, T. and W.G. Quinn, *Classical conditioning and retention in normal and mutant Drosophila melanogaster.* J Comp Physiol A, 1985. **157**(2): p. 263-77.

178. Malik, B.R., J.M. Gillespie, and J.J. Hodge, *CASK and CaMKII function in the mushroom body α'/β' neurons during Drosophila memory formation.* Front Neural Circuits, 2013. **7**: p. 52.
179. Perisse, E., et al., *Shocking revelations and saccharin sweetness in the study of Drosophila olfactory memory.* Curr Biol, 2013. **23**(17): p. R752-63.
180. Isabel, G., A. Pascual, and T. Preat, *Exclusive consolidated memory phases in Drosophila.* Science, 2004. **304**(5673): p. 1024-7.
181. Tonoki, A. and R.L. Davis, *Aging impairs intermediate-term behavioral memory by disrupting the dorsal paired medial neuron memory trace.* Proc Natl Acad Sci U S A, 2012. **109**(16): p. 6319-24.
182. Tamura, T., et al., *Aging specifically impairs amnesiac-dependent memory in Drosophila.* Neuron, 2003. **40**(5): p. 1003-11.
183. Heisenberg, M., *Mushroom body memoir: from maps to models.* Nature Reviews Neuroscience, 2003. **4**(4): p. 266-275.
184. Hennawy, M., et al., *Sleep and Attention in Alzheimer's Disease.* Yale J Biol Med, 2019. **92**(1): p. 53-61.
185. van Someren, E.J., et al., *Circadian rest-activity rhythm disturbances in Alzheimer's disease.* Biol Psychiatry, 1996. **40**(4): p. 259-70.
186. Videnovic, A., et al., *'The clocks that time us'--circadian rhythms in neurodegenerative disorders.* Nat Rev Neurol, 2014. **10**(12): p. 683-93.
187. De Nobrega, A.K. and L.C. Lyons, *Aging and the clock: Perspective from flies to humans.* Eur J Neurosci, 2020. **51**(1): p. 454-481.
188. Gerstner, J.R., et al., *Amyloid-β induces sleep fragmentation that is rescued by fatty acid binding proteins in Drosophila.* J Neurosci Res, 2017. **95**(8): p. 1548-1564.
189. Dissel, S., et al., *The logic of circadian organization in Drosophila.* Curr Biol, 2014. **24**(19): p. 2257-66.
190. Guo, F., et al., *Circadian neuron feedback controls the Drosophila sleep--activity profile.* Nature, 2016. **536**(7616): p. 292-7.
191. Renn, S.C., et al., *A pdf neuropeptide gene mutation and ablation of PDF neurons each cause severe abnormalities of behavioral circadian rhythms in Drosophila.* Cell, 1999. **99**(7): p. 791-802.
192. Ueno, T., et al., *Identification of a dopamine pathway that regulates sleep and arousal in Drosophila.* Nat Neurosci, 2012. **15**(11): p. 1516-23.
193. Boekhoff-Falk, G. and D.F. Eberl, *The Drosophila auditory system.* Wiley Interdiscip Rev Dev Biol, 2014. **3**(2): p. 179-91.
194. Coen, P., et al., *Dynamic sensory cues shape song structure in Drosophila.* Nature, 2014. **507**(7491): p. 233-237.
195. Sweeney, S.T., et al., *Targeted expression of tetanus toxin light chain in Drosophila specifically eliminates synaptic transmission and causes behavioral defects.* Neuron, 1995. **14**(2): p. 341-51.
196. Asher, S. and R. Priefer, *Alzheimer's disease failed clinical trials.* Life Sciences, 2022. **306**: p. 120861.
197. Heigwer, F., F. Port, and M. Boutros, *RNA Interference (RNAi) Screening in Drosophila.* Genetics, 2018. **208**(3): p. 853-874.
198. Parsons, T., *Reducing the expression of Lap or Zydeco in Drosophila causes phenotypes similar to Alzheimer's disease*, in *School of Physiology, Pharmacology and Neuroscience*. 2022, University of Bristol: Bristol.

199. Matsumoto, K., A. Toh-e, and Y. Oshima, *Genetic control of galactokinase synthesis in Saccharomyces cerevisiae: evidence for constitutive expression of the positive regulatory gene gal4.* J Bacteriol, 1978. **134**(2): p. 446-57.
200. McGuire, S.E., et al., *Spatiotemporal rescue of memory dysfunction in Drosophila.* Science, 2003. **302**(5651): p. 1765-8.
201. Madabattula, S.T., et al., *Quantitative Analysis of Climbing Defects in a Drosophila Model of Neurodegenerative Disorders.* J Vis Exp, 2015(100): p. e52741.
202. Taylor, M.J. and R.I. Tuxworth, *Continuous tracking of startled Drosophila as an alternative to the negative geotaxis climbing assay.* J Neurogenet, 2019. **33**(3): p. 190-198.
203. Stone, B., et al., *A low-cost method for analyzing seizure-like activity and movement in Drosophila.* J Vis Exp, 2014(84): p. e51460.
204. Hoffman, J.M., et al., *Sex, mating and repeatability of Drosophila melanogaster longevity.* R Soc Open Sci, 2021. **8**(8): p. 210273.
205. David, J.R., *Temperature*, in *Drosophila as a Model Organism for Ageing Studies*, F.A. Lints and M.H. Soliman, Editors. 1988, Springer US: Boston, MA. p. 33-45.
206. Vermeulen, C.J. and R. Bijlsma, *Changes in mortality patterns and temperature dependence of lifespan in Drosophila melanogaster caused by inbreeding.* Heredity, 2004. **92**(4): p. 275-281.
207. Zhu, B., et al., *DYRK1a Inhibitor Mediated Rescue of Drosophila Models of Alzheimer's Disease-Down Syndrome Phenotypes.* Front Pharmacol, 2022. **13**: p. 881385.
208. Anholt, R.R., R.F. Lyman, and T.F. Mackay, *Effects of single P-element insertions on olfactory behavior in Drosophila melanogaster.* Genetics, 1996. **143**(1): p. 293-301.
209. Driscoll, M.E., C. Hyland, and D. Sitaraman, *Measurement of Sleep and Arousal in Drosophila.* Bio Protoc, 2019. **9**(12).
210. Zimmerman, J.E., et al., *Genetic background has a major impact on differences in sleep resulting from environmental influences in Drosophila.* Sleep, 2012. **35**(4): p. 545-57.
211. Qian, Y., et al., *Sleep homeostasis regulated by 5HT2b receptor in a small subset of neurons in the dorsal fan-shaped body of drosophila.* Elife, 2017. **6**.
212. Joiner, W.J., et al., *Sleep in Drosophila is regulated by adult mushroom bodies.* Nature, 2006. **441**(7094): p. 757-760.
213. Iijima-Ando, K., et al., *Overexpression of neprilysin reduces alzheimer amyloid-beta42 (Abeta42)-induced neuron loss and intraneuronal Abeta42 deposits but causes a reduction in cAMP-responsive element-binding protein-mediated transcription, age-dependent axon pathology, and premature death in Drosophila.* J Biol Chem, 2008. **283**(27): p. 19066-76.
214. Iijima, K., et al., *Abeta42 mutants with different aggregation profiles induce distinct pathologies in Drosophila.* PLoS One, 2008. **3**(2): p. e1703.
215. Greenspan, R.J. and J.F. Ferveur, *Courtship in Drosophila.* Annu Rev Genet, 2000. **34**: p. 205-232.
216. Tompkins, L., J.C. Hall, and L.M. Hall, *Courtship-stimulating volatile compounds from normal and mutant Drosophila.* Journal of Insect Physiology, 1980. **26**(10): p. 689-697.
217. Kulkarni, S.J. and J.C. Hall, *Behavioral and cytogenetic analysis of the cacophony courtship song mutant and interacting genetic variants in Drosophila melanogaster.* Genetics, 1987. **115**(3): p. 461-75.

218. Grossfield, J., *Geographic distribution and light-dependent behavior in Drosophila.* Proc Natl Acad Sci U S A, 1971. **68**(11): p. 2669-73.
219. Inagaki, H.K., A. Kamikouchi, and K. Ito, *Protocol for quantifying sound-sensing ability of Drosophila melanogaster.* Nat Protoc, 2010. **5**(1): p. 26-30.
220. Eberl, D.F., G.M. Duyk, and N. Perrimon, *A genetic screen for mutations that disrupt an auditory response in Drosophila melanogaster.* Proc Natl Acad Sci U S A, 1997. **94**(26): p. 14837-42.
221. Wang, L., et al., *Epidermal growth factor receptor is a preferred target for treating amyloid-β-induced memory loss.* Proc Natl Acad Sci U S A, 2012. **109**(41): p. 16743-8.
222. Zhu, B., et al., *DYRK1A antagonists rescue degeneration and behavioural deficits of in vivo models based on amyloid-β, Tau and DYRK1A neurotoxicity.* Scientific Reports, 2022. **12**(1): p. 15847.
223. Papanikolopoulou, K., et al., *Drosophila Tau Negatively Regulates Translation and Olfactory Long-Term Memory, But Facilitates Footshock Habituation and Cytoskeletal Homeostasis.* J Neurosci, 2019. **39**(42): p. 8315-8329.
224. Limmer, S., et al., *The Drosophila blood-brain barrier: development and function of a glial endothelium.* Front Neurosci, 2014. **8**: p. 365.
225. Newton, V.M.P.S., *Choline, sleep disturbances, and Alzheimer's disease.* JARLIFE, 2018. **7**: p. 91-99.
226. McGleenon, B.M., K.B. Dynan, and A.P. Passmore, *Acetylcholinesterase inhibitors in Alzheimer's disease.* Br J Clin Pharmacol, 1999. **48**(4): p. 471-80.
227. Giacobini, E., *Cholinergic function and Alzheimer's disease.* Int J Geriatr Psychiatry, 2003. **18**(Suppl 1): p. S1-5.
228. Haam, J. and J.L. Yakel, *Cholinergic modulation of the hippocampal region and memory function.* J Neurochem, 2017. **142 Suppl 2**(Suppl 2): p. 111-121.
229. Igarashi, M., et al., *Disturbed choline plasmalogen and phospholipid fatty acid concentrations in Alzheimer's disease prefrontal cortex.* J Alzheimers Dis, 2011. **24**(3): p. 507-17.
230. Barnstedt, O., et al., *Memory-Relevant Mushroom Body Output Synapses Are Cholinergic.* Neuron, 2016. **89**(6): p. 1237-1247.
231. Krishnan, N., et al., *Loss of circadian clock accelerates aging in neurodegeneration-prone mutants.* Neurobiol Dis, 2012. **45**(3): p. 1129-35.
232. Barber, A.F., et al., *Drosophila clock cells use multiple mechanisms to transmit time-of-day signals in the brain.* Proc Natl Acad Sci U S A, 2021. **118**(10).
233. Hamid, R., et al., *Drosophila Choline transporter non-canonically regulates pupal eclosion and NMJ integrity through a neuronal subset of mushroom body.* Dev Biol, 2019. **446**(1): p. 80-93.
234. Picciotto, M.R., M.J. Higley, and Y.S. Mineur, *Acetylcholine as a neuromodulator: cholinergic signaling shapes nervous system function and behavior.* Neuron, 2012. **76**(1): p. 116-29.
235. Pan, D. and G.M. Rubin, *Kuzbanian controls proteolytic processing of Notch and mediates lateral inhibition during Drosophila and vertebrate neurogenesis.* Cell, 1997. **90**(2): p. 271-80.
236. Liu, Z., Y. Chen, and Y. Rao, *An RNAi screen for secreted factors and cell-surface players in coordinating neuron and glia development in Drosophila.* Mol Brain, 2020. **13**(1): p. 1.

237. Bray, S.J., *Notch signalling: a simple pathway becomes complex.* Nature Reviews Molecular Cell Biology, 2006. **7**(9): p. 678-689.
238. Hartenstein, V., *Morphological diversity and development of glia in Drosophila.* Glia, 2011. **59**(9): p. 1237-52.
239. Hu, Y., et al., *Genome-wide meta-analyses identify novel loci associated with n-3 and n-6 polyunsaturated fatty acid levels in Chinese and European-ancestry populations.* Hum Mol Genet, 2016. **25**(6): p. 1215-24.
240. Ma, Q.L., et al., *The Novel Omega-6 Fatty Acid Docosapentaenoic Acid Positively Modulates Brain Innate Immune Response for Resolving Neuroinflammation at Early and Late Stages of Humanized APOE-Based Alzheimer's Disease Models.* Front Immunol, 2020. **11**: p. 558036.
241. Dollar, G., et al., *Unique and Overlapping Functions of Formins Frl and DAAM During Ommatidial Rotation and Neuronal Development in Drosophila.* Genetics, 2016. **202**(3): p. 1135-51.
242. Földi, I., et al., *Molecular Dissection of DAAM Function during Axon Growth in Drosophila Embryonic Neurons.* Cells, 2022. **11**(9).
243. Miller, M.R., E.W. Miller, and S.D. Blystone, *Non-canonical activity of the podosomal formin FMNL1γ supports immune cell migration.* J Cell Sci, 2017. **130**(10): p. 1730-1739.
244. Li, Q. and B.A. Barres, *Microglia and macrophages in brain homeostasis and disease.* Nat Rev Immunol, 2018. **18**(4): p. 225-242.
245. Ma, Z., et al., *Neuromodulators signal through astrocytes to alter neural circuit activity and behaviour.* Nature, 2016. **539**(7629): p. 428-432.
246. Hoffmann, A. and D. Spengler, *Chromatin Remodeling Complex NuRD in Neurodevelopment and Neurodevelopmental Disorders.* Front Genet, 2019. **10**: p. 682.
247. Park, S.Y., J. Seo, and Y.S. Chun, *Targeted Downregulation of kdm4a Ameliorates Tau-engendered Defects in Drosophila melanogaster.* J Korean Med Sci, 2019. **34**(33): p. e225.
248. Frescas, D., et al., *JHDM1B/FBXL10 is a nucleolar protein that represses transcription of ribosomal RNA genes.* Nature, 2007. **450**(7167): p. 309-13.
249. Kooistra, S.M. and K. Helin, *Molecular mechanisms and potential functions of histone demethylases.* Nature Reviews Molecular Cell Biology, 2012. **13**(5): p. 297-311.
250. Alegría-Torres, J.A., A. Baccarelli, and V. Bollati, *Epigenetics and lifestyle.* Epigenomics, 2011. **3**(3): p. 267-77.
251. Meltzer, H., et al., *Tissue-specific (ts)CRISPR as an efficient strategy for in vivo screening in Drosophila.* Nature Communications, 2019. **10**(1): p. 2113.
252. Diao, F. and B.H. White, *A Novel Approach for Directing Transgene Expression in Drosophila: T2A-Gal4 In-Frame Fusion.* Genetics, 2012. **190**(3): p. 1139-1144.